



JPTM

Journal of Pathology
and Translational Medicine

May 2020
Vol. 54 / No.3
jpatholm.org
pISSN: 2383-7837
eISSN: 2383-7845



*A Scoring System
for the Diagnosis
of NASH*

Aims & Scope

The *Journal of Pathology and Translational Medicine* is an open venue for the rapid publication of major achievements in various fields of pathology, cytopathology, and biomedical and translational research. The Journal aims to share new insights into the molecular and cellular mechanisms of human diseases and to report major advances in both experimental and clinical medicine, with a particular emphasis on translational research. The investigations of human cells and tissues using high-dimensional biology techniques such as genomics and proteomics will be given a high priority. Articles on stem cell biology are also welcome. The categories of manuscript include original articles, review and perspective articles, case studies, brief case reports, and letters to the editor.

Subscription Information

To subscribe to this journal, please contact the Korean Society of Pathologists/the Korean Society for Cytopathology. Full text PDF files are also available at the official website (<http://jpathol.tnm.org>). *Journal of Pathology and Translational Medicine* is indexed by Emerging Sources Citation Index (ESCI), PubMed, PubMed Central, Scopus, KoreaMed, KoMCI, WPRIM, Directory of Open Access Journals (DOAJ), and CrossRef. Circulation number per issue is 50.

Editors-in-Chief

Jung, Chan Kwon, MD (*The Catholic University of Korea, Korea*) <https://orcid.org/0000-0001-6843-3708>
Park, So Yeon, MD (*Seoul National University, Korea*) <https://orcid.org/0000-0002-0299-7268>

Senior Editors

Hong, Soon Won, MD (*Yonsei University, Korea*) <https://orcid.org/0000-0002-0324-2414>
Kim, Chong Jai, MD (*University of Ulsan, Korea*) <https://orcid.org/0000-0002-2844-9446>

Associate Editors

Shin, Eunah, MD (*Yongin Severance Hospital, Yonsei University, Korea*) <https://orcid.org/0000-0001-5961-3563>
Kim, Haeryoung, MD (*Seoul National University, Korea*) <https://orcid.org/0000-0002-4205-9081>

Editorial Board

Avila-Casado, Maria del Carmen, MD (*University of Toronto, Toronto General Hospital UHN, Canada*)

Bae, Yeong Kyung, MD (*Seungnam University, Korea*)

Bongiovanni, Massimo, MD (*Lausanne University Hospital, Switzerland*)

Bychkov, Andrey, MD (*Chulalongkorn University, Thailand Kamada Medical Center, Japan Nagasaki University Hospital, Japan*)

Choi, Yeong-Jin, MD (*The Catholic University of Korea, Korea*)

Chong, Yo Sep, MD (*The Catholic University of Korea, Korea*)

Chung, Jin-Haeng, MD (*Seoul National University, Korea*)

Fadda, Guido, MD (*Catholic University of Rome-Foundation Agostino Gemelli University Hospital, Italy*)

Gong, Gyungyub, MD (*University of Ulsan, Korea*)

Ha, Seung Yeon, MD (*Gachon University, Korea*)

Han, Jee Young, MD (*Inha University, Korea*)

Jain, Deepali, MD (*All India Institute of Medical Sciences, India*)

Jang, Se Jin, MD (*University of Ulsan, Korea*)

Jeong, Jin Sook, MD (*Dong-A University, Korea*)

Jun, Sun-Young, MD (*The Catholic University of Korea, Korea*)

Kang, Gyeong Hoon, MD (*Seoul National University, Korea*)

Kim, Aeree, MD (*Korea University, Korea*)

Kim, Jang-Hee, MD (*Ajou University, Korea*)

Kim, Jung Ho, MD (*Seoul National University, Korea*)

Kim, Kyu Rae, MD (*University of Ulsan, Korea*)

Kim, Se Hoon, MD (*Yonsei University, Korea*)

Kim, Woo Ho, MD (*Seoul National University, Korea*)

Ko, Young Hye, MD (*Sungkyunkwan University, Korea*)

Koo, Ja Seung, MD (*Yonsei University, Korea*)

Lai, Chiung-Ru, MD (*Taipei Veterans General Hospital, Taiwan*)

Lee, C. Soon, MD (*University of Western Sydney, Australia*)

Lee, Hye Seung, MD (*Seoul National University, Korea*)

Liu, Zhiyan, MD (*Shandong University, China*)

Lkhagvadorj, Sayamaa, MD (*Mongolian National University of Medical Sciences, Mongolia*)

Moon, Woo Sung, MD (*Jeonbuk University, Korea*)

Paik, Jin Ho, MD (*Seoul National University, Korea*)

Park, Chan-Sik, MD (*University of Ulsan, Korea*)

Park, Young Nyun, MD (*Yonsei University, Korea*)

Shahid, Pervez, MD (*Aga Khan University, Pakistan*)

Song, Joon Seon, MD (*University of Ulsan, Korea*)

Sung, Chang Ohk, MD (*University of Ulsan, Korea*)

Tan, Puay Hoon, MD (*National University of Singapore, Singapore*)

Than, Nandor Gabor, MD (*Semmelweis University, Hungary*)

Tse, Gary M., MD (*The Chinese University of Hong Kong, Hong Kong*)

Yatabe, Yasushi, MD (*Aichi Cancer Center, Japan*)

Yoon, Sun Och, MD (*Yonsei University, Korea*)

Zhu, Yun, MD (*Jiangsu Institution of Nuclear Medicine, China*)

Consulting Editors

Huh, Sun, MD (*Hallym University, Korea*)

Kakudo, Kennichi, MD (*Kindai University, Japan*)

Ro, Jae Y., MD (*Cornell University, The Methodist Hospital, U.S.A.*)

Ethic Editor

Choi, In-Hong, MD (*Yonsei University, Korea*)

Statistics Editors

Kim, Dong Wook (*National Health Insurance Service Ilsan Hospital, Korea*)

Lee, Hye Sun (*Yonsei University, Korea*)

Manuscript Editor

Chang, Soo-Hee (*InfoLumi Co., Korea*)

Layout Editor

Kim, Haeja (*iMiS Company Co., Ltd., Korea*)

Website and JATS XML File Producers

Cho, Yoosang (*M2Community Co., Korea*)

Im, Jeonghee (*M2Community Co., Korea*)

Administrative Assistants

Jung, Ji Young (*The Korean Society of Pathologists*)

Jeon, Anmi (*The Korean Society for Cytopathology*)

Contact the Korean Society of Pathologists/the Korean Society for Cytopathology

Publishers: Choi, Chan, MD, Hong, Soon Won, MD

Editors-in-Chief: Jung, Chan Kwon, MD, Park, So Yeon, MD

Published by the Korean Society of Pathologists/the Korean Society for Cytopathology

Editorial Office

Room 1209 Gwanghwamun Officia, 92 Saemunan-ro, Jongno-gu, Seoul 03186, Korea
Tel: +82-2-795-3094 Fax: +82-2-790-6635 E-mail: office@jpathol.tnm.org

#1508 Renaissancetower, 14 Mallijae-ro, Mapo-gu, Seoul 04195, Korea
Tel: +82-2-593-6943 Fax: +82-2-593-6944 E-mail: office@jpathol.tnm.org

Printed by iMiS Company Co., Ltd. (JMC)

Jungang Bldg. 18-8 Wonhyo-ro 89-gil, Yongsan-gu, Seoul 04314, Korea
Tel: +82-2-717-5511 Fax: +82-2-717-5515 E-mail: ml@smileml.com

Manuscript Editing by InfoLumi Co.

210-202, 421 Pangyo-ro, Bundang-gu, Seongnam 13522, Korea
Tel: +82-70-8839-8800 E-mail: infolumi.chang@gmail.com

Front cover image: Representative pictures of 'not-NASH', 'borderline', and 'NASH' cases (Fig. 2). p231.

© Copyright 2020 by the Korean Society of Pathologists/the Korean Society for Cytopathology

© Journal of Pathology and Translational Medicine is an Open Access journal under the terms of the Creative Commons Attribution Non-Commercial License (<https://creativecommons.org/licenses/by-nc/4.0>).

© This paper meets the requirements of KS X ISO 9706, ISO 9706-1994 and ANSI/NISO Z.39.48-1992 (Permanence of Paper).

CONTENTS

EDITORIAL

- 197 New insights into classification and risk stratification of encapsulated thyroid tumors with a predominantly papillary architecture
Chan Kwon Jung, So Yeon Park, Jang-Hee Kim, Kennichi Kakudo

REVIEWS

- 204 Current status and future perspectives of liquid biopsy in non-small cell lung cancer
Sunhee Chang, Jae Young Hur, Yoon-La Choi, Chang Hun Lee, Wan Seop Kim
- 213 Clinical management of abnormal Pap tests: differences between US and Korean guidelines
Seyeon Won, Mi Kyoung Kim, Seok Ju Seong

ORIGINAL ARTICLES

- 220 Sarcoma metastasis to the pancreas: experience at a single institution
Miseon Lee, Joon Seon Song, Seung-Mo Hong, Se Jin Jang, Jihun Kim, Ki Byung Song, Jae Hoon Lee, Kyung-Ja Cho
- 228 A scoring system for the diagnosis of non-alcoholic steatohepatitis from liver biopsy
Kyoungbun Lee, Eun Sun Jung, Eunsil Yu, Yun Kyung Kang, Mee-Yon Cho, Joon Mee Kim, Woo Sung Moon, Jin Sook Jeong, Cheol Keun Park, Jae-Bok Park, Dae Young Kang, Jin Hee Sohn, So-Young Jin
- 237 Gene variant profiles and tumor metabolic activity as measured by *FOXM1* expression and glucose uptake in lung adenocarcinoma
Ashley Goodman, Waqas Mahmud, Lela Buckingham
- 246 Continuous quality improvement program and its results of Korean Society for Cytopathology
Yoo-Duk Choi, Hoon-Kyu Oh, Su-Jin Kim, Kyung-Hee Kim, Yun-Kyung Lee, Bo-Sung Kim, Eun-Jeong Jang, Yoon-Jung Choi, Eun-Kyung Han, Dong-Hoon Kim, Younghee Choi, Chan-Kwon Jung, Sung-Nam Kim, Kyueng-Whan Min, Seok-Jin Yoon, Hun-Kyung Lee, Kyung Un Choi, Hye Kyoung Yoon

CASE REPORTS

- 253 **Morphologic variant of follicular lymphoma reminiscent of hyaline-vascular Castleman disease**
Jiwon Koh, Yoon Kyung Jeon
- 258 **Gastric IgG4-related disease presenting as a mass lesion and masquerading as a gastrointestinal stromal tumor**
Banumathi Ramakrishna, Rohan Yewale, Kavita Vijayakumar, Patta Radhakrishna, Balakrishnan Siddartha Ramakrishna
- 263 **Noninvasive encapsulated papillary RAS-like thyroid tumor (NEPRAS) or encapsulated papillary thyroid carcinoma (PTC)**
Pedro Wesley Rosario

Instructions for Authors for *Journal of Pathology and Translational Medicine* are available at <http://jpatholm.org/authors/authors.php>

New insights into classification and risk stratification of encapsulated thyroid tumors with a predominantly papillary architecture

Chan Kwon Jung^{1,2}, So Yeon Park³, Jang-Hee Kim⁴, Kennichi Kakudo⁵

¹Department of Hospital Pathology, College of Medicine, The Catholic University of Korea, Seoul;

²Cancer Research Institute, College of Medicine, The Catholic University of Korea, Seoul;

³Department of Pathology, Seoul National University Bundang Hospital, Seoul National University College of Medicine, Seongnam;

⁴Department of Pathology, Ajou University School of Medicine, Suwon, Korea;

⁵Department of Pathology and Thyroid Disease Center, Izumi City General Hospital, Izumi, Japan

Three cases of noninvasive encapsulated papillary *RAS*-like (NEPRAS) thyroid tumor are reported in this issue [1]. The term “NEPRAS” was first used by Ohba et al. in 2019 [2] to designate a noninvasive thyroid tumor showing a complete fibrous capsule, a predominantly papillary architecture, and *RAS* mutation but with subtle nuclear features of papillary thyroid carcinoma (PTC) (Fig. 1). The tumor was considered a borderline thyroid tumor that showed a predominantly papillary structure. The name and concept of “NEPRAS” tumors were proposed as a counterpart of noninvasive follicular thyroid neoplasm with papillary-like nuclear features (NIFTP) having a predominantly follicular architecture. NEPRAS is different from follicular adenoma with papillary hyperplasia because of the appearance of nuclear features of PTC (Fig. 2). The distinction between NEPRAS and NIFTP is based on the presence of papillary structure in NEPRAS tumors (Table 1). NEPRAS tumors with *RAS* mutations or other *RAS*-like mutations are different from encapsulated classic PTCs in that classic PTCs typically harbor the *BRAF* V600E mutation. Therefore, in the diagnostic schema recommended by the World Health Organization (WHO) classification of thyroid tumors, pathologists might have variably classified these noninvasive encapsulated tumors as either benign follicular adenoma or encapsulated PTC depending on the subjective judgment of nuclear features.

The 2017 WHO classification newly adopted a borderline

tumor of the thyroid [3]. Encapsulated follicular-patterned thyroid tumors with borderline behavior include follicular tumor of uncertain malignant potential (FT-UMP), well-differentiated tumor of uncertain malignant potential (WDT-UMP), and NIFTP [3]. FT-UMP has round nuclei that lack PTC-type nuclear features, whereas WDT-UMP and NIFTP share the nuclear features of PTC, including a nuclear score of 2 or 3 on a three-point scoring scale [3]. Although encapsulated follicular-patterned lesions are well defined by the WHO classification, there is a lack of consensus on encapsulated papillary-patterned thyroid tumors that demonstrate subtle nuclear changes. Many diagnostically controversial cases exhibit subtle nuclear features, such as a nuclear score of 2, and therefore pose challenges for accurate diagnosis.

Pathologic diagnosis of a thyroid tumor is fundamentally dependent on pathologists’ knowledge and experience in interpreting microscopic findings [4-8]. Due to variable application of loose or strict criteria in assessing the nuclear features of PTC and its invasion of the tumor capsule and vessels, there is discrepancy in diagnosis of encapsulated/well-circumscribed thyroid tumors among pathologists [6-9]. Noninvasive encapsulated papillary-patterned thyroid tumor is diagnosed as encapsulated classic PTC if nuclear features of the tumor are interpreted as nuclear score of 3. However, diagnostic challenges may arise in cases with subtle nuclear changes. In Western practice, equivocal nuclear changes are more easily interpreted as PTC-type nuclear features, whereas most Asian pathologists agree that such nuclear features are insufficient for diagnosis of PTC [10]. As a result, the same tumor can be diagnosed as a follicular adenoma by certain pathologists who apply more stringent criteria for diag-

Received: April 23, 2020 Accepted: April 29, 2020

Corresponding Author: Chan Kwon Jung, MD, PhD

Department of Pathology, Seoul St. Mary’s Hospital, College of Medicine, The Catholic University of Korea, 222 Banpo-daero, Seocho-gu, Seoul 06591, Korea
 Tel: +82-2-2258-1622, Fax: +82-2-2258-1627, E-mail: ckjung@catholic.ac.kr

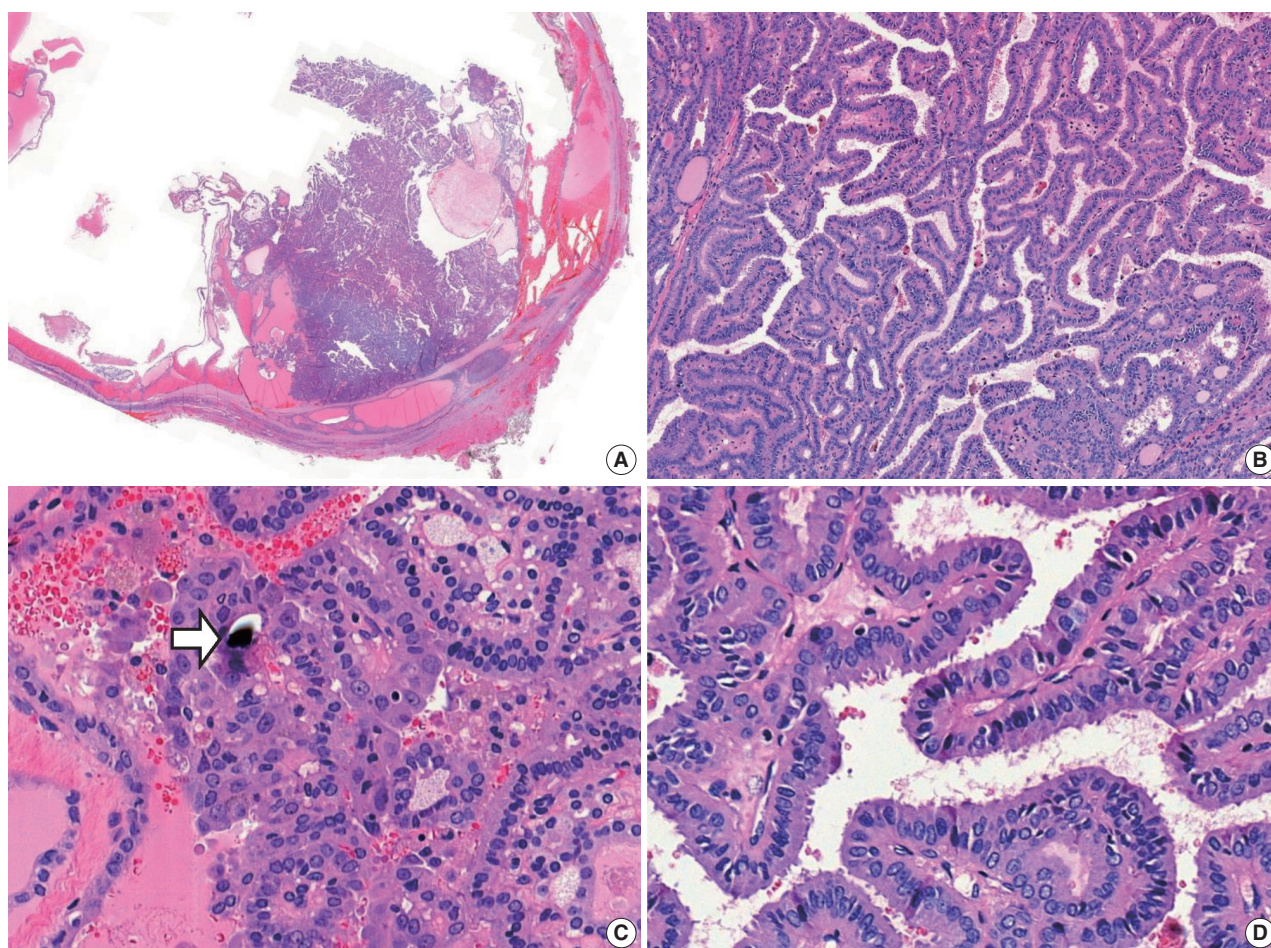


Fig. 1. Noninvasive encapsulated papillary *RAS*-like thyroid tumor. (A) The tumor has a thick fibrous capsule and shows cystic change. (B) The solid area is predominantly composed of papillary architecture lined by cuboidal to columnar follicular cells. (C) Psammoma bodies are occasionally seen (arrow). (D) Tumor cells show nuclear enlargement, overlapping, and elongation, with slightly irregular nuclear membranes and dark chromatin, and have no nuclear pseudo-inclusions. Molecular analysis revealed *KRAS* G12V mutation.

nosis of PTC.

RAS-mutated thyroid tumors demonstrate different histology and biological behavior than tumors with *BRAF* V600E mutation [11]. *RAS* or other *RAS*-like mutations are frequently found in follicular adenoma, NIFTP, and follicular carcinoma with a similarity in the possible spectrum of mutations [12-14]. In PTCs, two molecular subtypes, *BRAF* V600E-like and *RAS*-like types, were proposed by the Cancer Genome Atlas (TCGA) project [11]. Follicular-patterned PTCs typically carry *RAS*-like mutations, including *RAS* mutations, whereas PTCs with papillary architecture have *BRAF* V600E or other *BRAF*-like mutations. However, this rule does not apply in all cases. *RAS*-like mutations can be found in PTCs with papillary architecture. In the TCGA dataset [11], of 250 classic PTCs with molecular classification data, 43 (17.2%) had an *RAS*-like molecular signature, while 16 (6.3%) had *RAS* mutations. Noninvasive en-

capsulated papillary-patterned tumor can also demonstrate PTC-like nuclear features and *RAS* mutations. The tumor was previously classified either as encapsulated classic PTC if it had a nuclear score of 2–3 or as follicular adenoma with papillary hyperplasia if it had a nuclear score of 0 or 1 according to the WHO classification [3]. However, the new diagnostic term “NEPRAS” can reclassify a subset of noninvasive encapsulated papillary-patterned tumors as borderline tumors [2].

NEPRASs share common characteristics of NIFTP as a noninvasive encapsulated tumor, having *RAS*-like mutations, and demonstrating a PTC-type nuclear score of 2. However, NEPRAS lesions are papillary-patterned tumors and can have psammoma bodies (Fig. 1). Because the presence of true papillae and psammoma bodies suggest the probability of classic PTC, these findings are major exclusion criteria for the diagnosis of NIFTP. A nuclear score of 3 and the well-developed nu-

clear features of PTC are not exclusion criteria for NIFTP, but they indicate a higher probability of classic PTC and should serve as an indicator for a more thorough examination of the tu-

mor, including more grossing and immunostaining or molecular testing for *BRAF* V600E (Fig. 3) [15-18]. As encapsulated papillary-patterned tumors with nuclear scores of 3 are fre-

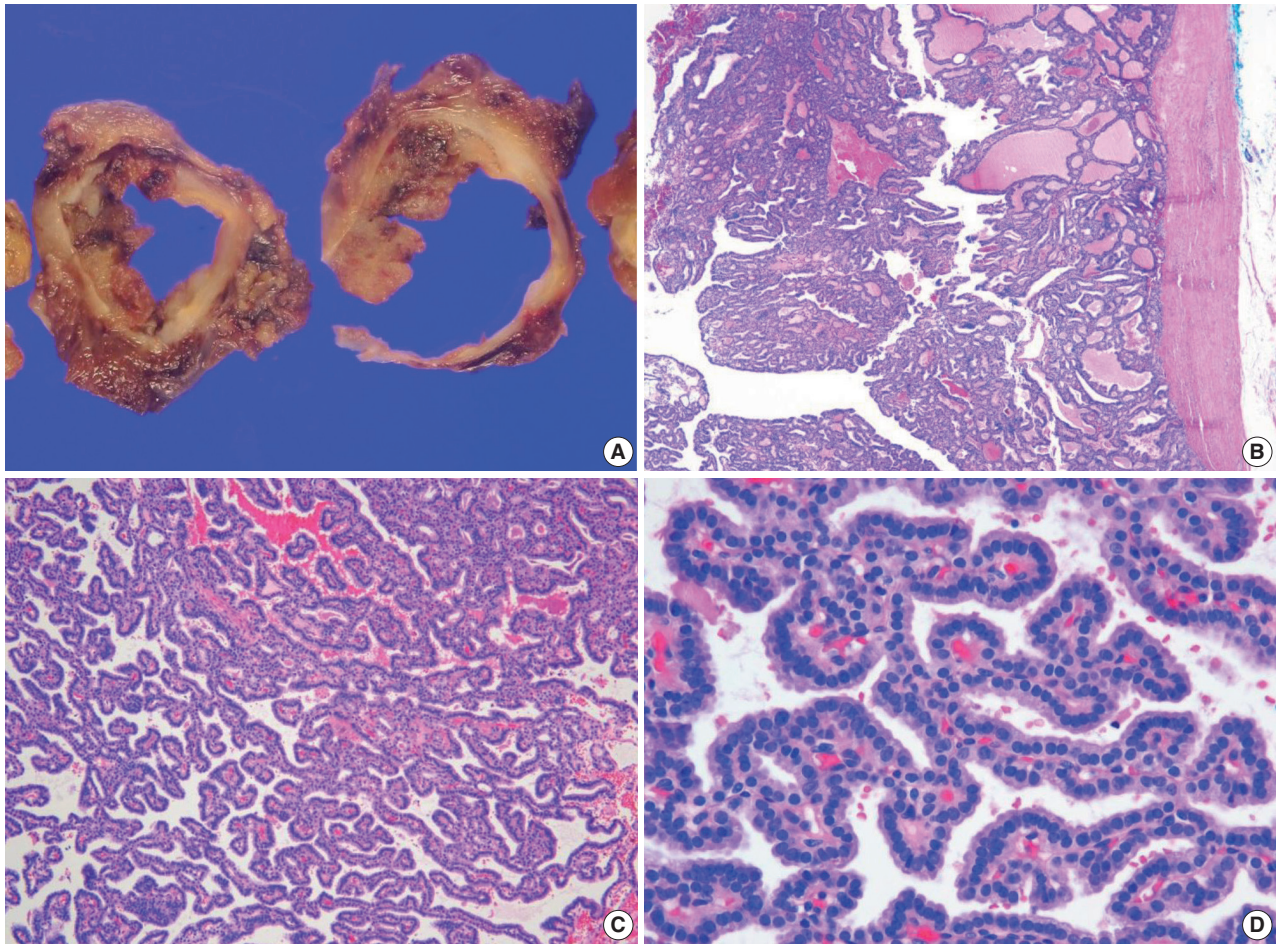


Fig. 2. Follicular adenoma with papillary hyperplasia. The tumor is cystic and has a thick complete capsule upon gross (A) and microscopic examination (B). (C) The tumor is composed of a predominantly papillary structure. (D) Tumor cells show basally located, small, and dark nuclei with round contours.

Table 1. Classification of encapsulated thyroid tumors with *RAS*-like mutations: a proposal for NEPRAS

Tumor behavior	Invasion	Nuclear score ^a	Papillary architecture	Predominantly follicular growth	
				Presence of true papillae	Absence of true papillae
Benign	Absent	0 to 1	Follicular adenoma with papillary hyperplasia	Follicular adenoma, conventional type	Follicular adenoma, conventional type
Borderline	Absent	2 (rarely 3)	NEPRAS	-	NIFTP
	Questionable	2 (rarely 3)	-	-	WDT-UMP
Malignant	Present	1 (rarely 0)	Follicular carcinoma	Follicular carcinoma	Follicular carcinoma
	Present	2 to 3	Papillary carcinoma, encapsulated classic variant	Papillary carcinoma, encapsulated classic variant with predominant follicular growth	Papillary carcinoma, invasive encapsulated follicular variant

NEPRAS, noninvasive encapsulated papillary *RAS*-like thyroid tumor; NIFTP, noninvasive follicular thyroid neoplasm with papillary-like nuclear features; WDT-UMP, well-differentiated tumor of uncertain malignant potential.

^aNuclear score is calculated as the sum of all categories of nuclear features of papillary carcinoma: (1) nuclear size and shape (nuclear enlargement, overlapping, crowding, and elongation), (2) nuclear membrane irregularities (irregular nuclear contours, grooves, and pseudoinclusions), (3) chromatin characteristics (chromatin clearing, margination of chromatin to the membrane, glassy nuclei) [14].

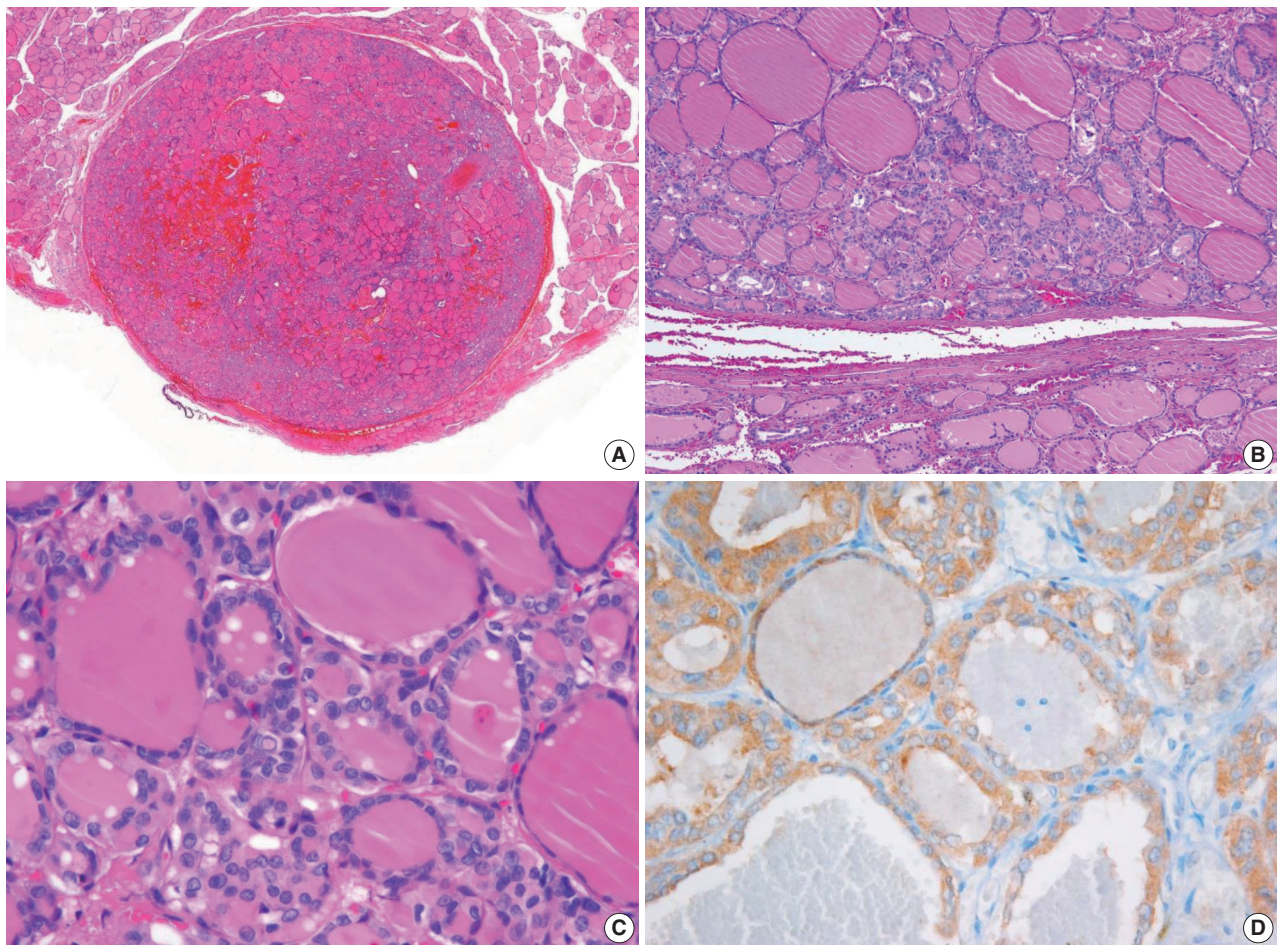


Fig. 3. Noninvasive encapsulated classic papillary thyroid carcinoma with predominant follicular growth and *BRAF* V600E. This tumor was initially misdiagnosed as noninvasive follicular thyroid neoplasm with papillary-like nuclear features (NIFTP). (A) The tumor is completely surrounded by a thin fibrotic capsule. (B) The encapsulated tumor is composed of follicular architecture. (C) The tumor cells have florid nuclear features of papillary carcinoma. Nuclear pseudoinclusions and grooves are frequently seen. (D) Immunostaining for *BRAF* V600E (VE1) is positive.

quently positive for the *BRAF* V600E mutation and therefore confidently diagnosed as PTC, a nuclear score of 3 is an exclusion criterion for diagnosis of NEPRAS. While NEPRAS remains a morphologic diagnosis like NIFTP, detection of *RAS*-like low-risk mutations (*RAS*, *BRAF* K601E, *EIF1AX*, *PPARG* fusion, *THADA* fusion, and so forth) further substantiates the diagnosis when molecular results are available. *BRAF*-like mutations (*BRAF* V600E, *ALK*, *RET/PTC*, *NTRK* fusions, etc.) and high-risk mutations (*TERT* promoter, *TP53*, *PIK3CA*, *CTNNB1*, etc.) are essentially exclusionary criteria for diagnosis of NEPRAS and NIFTP lesions. In our case series (Table 2), one NEPRAS tumor had a *KRAS* mutation. In addition, the *NRAS* mutation was found in one NEPRAS tumor showing minimal capsular invasion. Another case had no *RAS* mutations.

Most encapsulated thyroid tumors without invasion are very

indolent and behave like follicular adenoma despite their growth patterns. The management strategy for patients with NEPRAS tumors is similar to those with NIFTP lesions. Thyroid lobectomy is a sufficient treatment for NEPRAS and NIFTP tumors. No further surgery, completion thyroidectomy, or radioactive iodine treatment is required after surgical resection of the primary tumor. Thus, reclassification of a subset of encapsulated classic PTCs into borderline tumors would ultimately lead to more conservative treatment standard and improved quality of life for patients with these tumors.

NEPRAS tumors can progress to invasive cancer just as NIFTP has the potential to progress to an invasive encapsulated follicular variant of PTC (Fig. 4). When NIFTP and NEPRAS tumors develop capsular and/or vascular invasion, they are truly malignant and mostly labelled as PTCs based on the PTC-type nuclear features (Table 1). However, the same cases may be di-

Table 2. Cases of noninvasive encapsulated papillary *RAS*-like thyroid tumor and its malignant counterpart with invasion

Reference	Age (yr)	Sex	FNA category ^a	Size (cm)	Invasion	Nuclear score	Papillary component	Cystic change	Psammoma bodies	Molecular profile	Immunohistochemistry
Index case, Ohba et al. (2019) [2]	26	M	II, IV	2.3	Absent	2	Dominant	Present	Present	<i>KRAS</i> G12A; <i>BRAF</i> , <i>NRAS</i> , <i>HRAS</i> , and <i>TERT</i> promoter: wild type	Ki-67 index 1%–2%
Rosario (2020) [1]	35	F	IV	4.0	Absent	2	<1%	NA	NA	<i>BRAF</i> wild type	
	43	F	III	2.2	Absent	2	1%	NA	NA	<i>BRAF</i> wild type	
	48	M	IV	3.5	Absent	2	1%	NA	NA	<i>BRAF</i> wild type	
Case 1	9	M	V	3.7	Absent	2	Dominant	Present	Present	<i>KRAS</i> G12V; <i>BRAF</i> and <i>NRAS</i> : wild type	CK19, focal +; HBME1, focal +; CD56, focal loss; ALK, negative; Pan-Trk, negative
Case 2	38	M	III	1.2	Capsular	2	Dominant	Present	Absent	<i>NRAS</i> Q61R; <i>BRAF</i> , <i>HRAS</i> , <i>KRAS</i> , and <i>TERT</i> promoter: wild type	
Case 3	21	M	II	4.0	Capsular	2	Dominant	Present	Absent	<i>BRAF</i> , <i>NRAS</i> , <i>HRAS</i> , and <i>KRAS</i> : wild type	

FNA, fine-needle aspiration cytology; M, male; F, female; NA, not available.

^aBased on the categories of the Bethesda System for Reporting Thyroid Cytopathology.

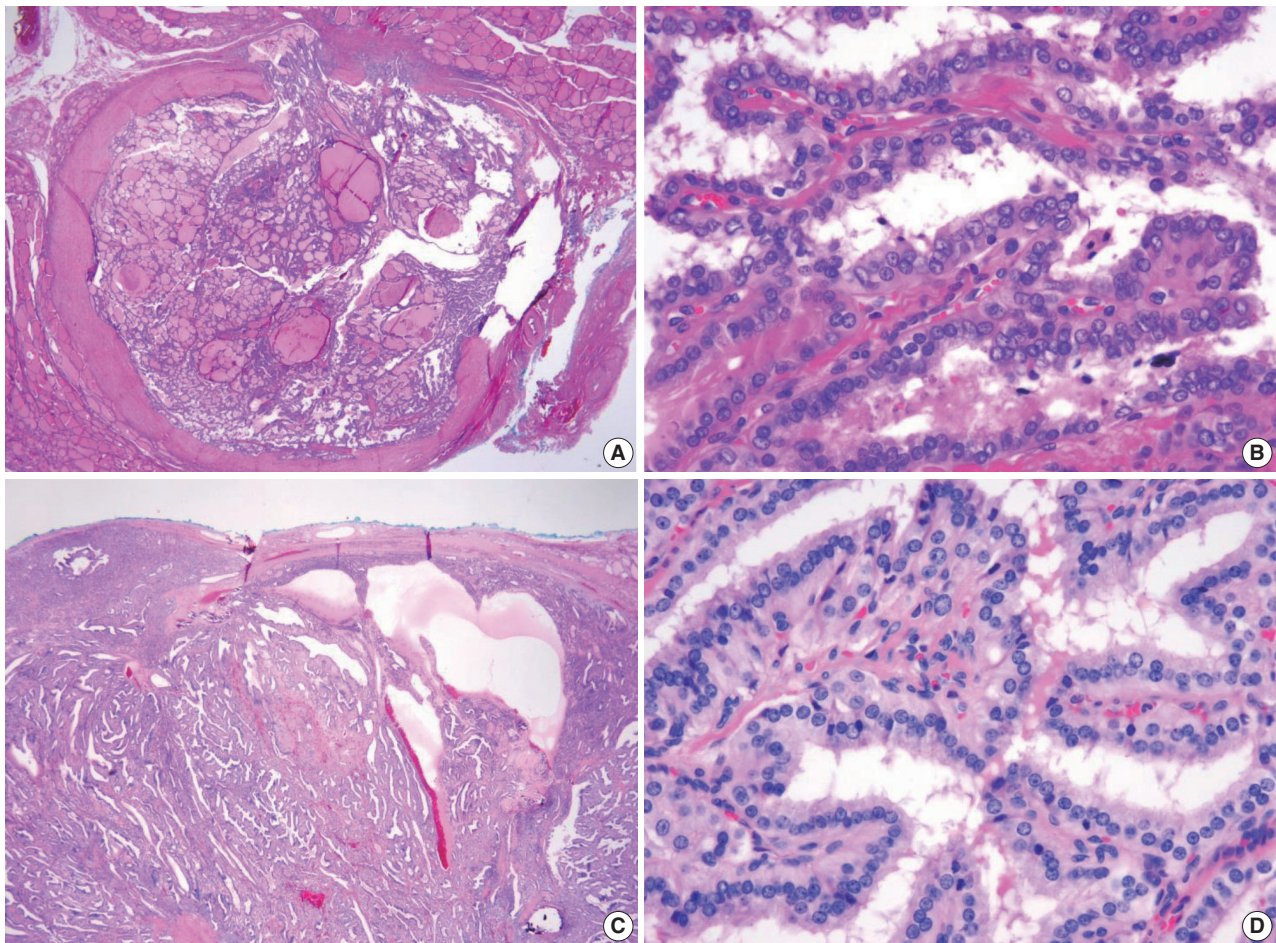


Fig. 4. Two cases of the invasive form of noninvasive encapsulated papillary *RAS*-like thyroid tumor. (A, B) A tumor with *NRAS* Q61R. (C, D) The other case without *BRAF* V600E or *RAS* mutations. Both tumors show capsular invasion (A, C). A high-power view of the tumors reveals enlarged round-to-ovoid, overlapping nuclei with few nuclear grooves and less chromatin clearing than seen in classic papillary carcinoma.

agnosed as follicular carcinoma if the nuclear features are interpreted as a nuclear score of 1. Fortunately, these tumors are low-risk cancers despite their name and do not require additional treatment after surgical resection if the tumor is only minimally invasive without angioinvasion. Table 2 summarizes the reported cases in the literature, including our cases.

Although long-term follow-up results of patients with NE-PRAS are not available, it is reasonable to expect an excellent outcome after surgical resection of the tumor. Even when late recurrences do occur, the disease can be successfully treated. While reclassification has important impacts in clinical practice, implementation of new diagnostic criteria and terminologies may provoke resistance in pathologists and clinicians at variable levels. However, these efforts by pathologists will contribute to reducing the incidence rates of overdiagnosis and overtreatment of thyroid cancer.

Ethics Statement

This study was approved by the Institutional Review Boards of Seoul St. Mary's Hospital (IRB No. KC20ZASI0282), Seoul National University Bundang Hospital (IRB No. B-2004-611-103), and Ajou University Hospital (IRB No. AJIRB-BMR-EXP-20-074) with a waiver of informed consent.

ORCID

Chan Kwon Jung: <http://orcid.org/0000-0001-6843-3708>

So Yeon Park: <http://orcid.org/0000-0002-0299-7268>

Jang-Hee Kim: <http://orcid.org/0000-0001-5825-1361>

Kennichi Kakudo: <http://orcid.org/0000-0002-0347-7264>

Author Contributions

Conceptualization: CKJ, KK.

Data curation: CKJ, SYP, JHK, KK.

Formal analysis: CKJ.

Funding acquisition: CKJ.

Investigation: CKJ.

Methodology: CKJ, SYP, JHK, KK.

Project administration: CKJ.

Resources: CKJ.

Supervision: CKJ.

Validation: CKJ, SYP, JHK, KK.

Visualization: CKJ, KK.

Writing—original draft: CKJ.

Writing—review & editing: CKJ, SYP, JHK, KK.

Conflicts of Interest

C.K.J. and S.Y.P. are the editors-in-chief of *Journal of Pathology and Translational Medicine*. J.H.K. and K.K. are editorial-board members of the journal.

Funding

This research was funded by a grant (2017R1D1A1B03029597) from the Basic Science Research Program through the National Research Foundation of Korea funded by the Ministry of Science and ICT.

REFERENCES

- Rosario PW. Noninvasive encapsulated papillary RAS-like thyroid tumor (NEPRAS) or encapsulated papillary thyroid carcinoma (PTC). *J Pathol Transl Med* 2020 Mar 4 [Epub]. <https://doi.org/10.4132/jptm.2020.02.05>.
- Ohba K, Mitsutake N, Matsuse M, et al. Encapsulated papillary thyroid tumor with delicate nuclear changes and a KRAS mutation as a possible novel subtype of borderline tumor. *J Pathol Transl Med* 2019; 53: 136-41.
- Lloyd RV, Osamura RY, Klöppel G, Rosai J. WHO classification of tumours of endocrine organs. 4th ed. Lyon: IARC Press, 2017; 65-91.
- Mete O, Asa SL. Thyroid tumor capsular invasion: the bottom line or much ado about nothing? *Endocr Pathol* 2020 Mar 24 [Epub]. <https://doi.org/10.1007/s12022-020-09621-6>.
- Jung CK, Kim C. Effect of lowering the diagnostic threshold for encapsulated follicular variant of papillary thyroid carcinoma on the prevalence of non-invasive follicular thyroid neoplasm with papillary-like nuclear features: a single-institution experience in Korea. *J Basic Clin Med* 2017; 6: 26-8.
- Hirokawa M, Carney JA, Goellner JR, et al. Observer variation of encapsulated follicular lesions of the thyroid gland. *Am J Surg Pathol* 2002; 26: 1508-14.
- Lloyd RV, Erickson LA, Casey MB, et al. Observer variation in the diagnosis of follicular variant of papillary thyroid carcinoma. *Am J Surg Pathol* 2004; 28: 1336-40.
- Zhu Y, Li Y, Jung CK, et al. Histopathologic assessment of capsular invasion in follicular thyroid neoplasms: an observer variation study. *Endocr Pathol* 2020 Mar 31 [Epub]. <https://doi.org/10.1007/s12022-020-09620-7>.
- Tallini G, Tuttle RM, Ghossein RA. The history of the follicular variant of papillary thyroid carcinoma. *J Clin Endocrinol Metab* 2017; 102: 15-22.
- Kakudo K, Bychkov A, Abelardo A, Keelawat S, Kumarasinghe P.

- Malpractice climate is a key difference in thyroid pathology practice between North America and the rest of the world. *Arch Pathol Lab Med* 2019; 143: 1171.
11. Cancer Genome Atlas Research Network. Integrated genomic characterization of papillary thyroid carcinoma. *Cell* 2014; 159: 676-90.
 12. Yoo SK, Lee S, Kim SJ, et al. Comprehensive analysis of the transcriptional and mutational landscape of follicular and papillary thyroid cancers. *PLoS Genet* 2016; 12: e1006239.
 13. Jung SH, Kim MS, Jung CK, et al. Mutational burdens and evolutionary ages of thyroid follicular adenoma are comparable to those of follicular carcinoma. *Oncotarget* 2016; 7: 69638-48.
 14. Nikiforov YE, Seethala RR, Tallini G, et al. Nomenclature revision for encapsulated follicular variant of papillary thyroid carcinoma: a paradigm shift to reduce overtreatment of indolent tumors. *JAMA Oncol* 2016; 2: 1023-9.
 15. Jeon S, Kim Y, Jeong YM, Bae JS, Jung CK. CCND1 splice variant as a novel diagnostic and predictive biomarker for thyroid cancer. *Cancers (Basel)* 2018; 10: E437.
 16. Cho U, Mete O, Kim MH, Bae JS, Jung CK. Molecular correlates and rate of lymph node metastasis of non-invasive follicular thyroid neoplasm with papillary-like nuclear features and invasive follicular variant papillary thyroid carcinoma: the impact of rigid criteria to distinguish non-invasive follicular thyroid neoplasm with papillary-like nuclear features. *Mod Pathol* 2017; 30: 810-25.
 17. Choden S, Keelawat S, Jung CK, Bychkov A. VE1 immunohistochemistry improves the limit of genotyping for detecting *BRAF(V600E)* mutation in papillary thyroid cancer. *Cancers (Basel)* 2020; 12: E596.
 18. Nikiforov YE, Baloch ZW, Hodak SP, et al. Change in diagnostic criteria for noninvasive follicular thyroid neoplasm with papillary-like nuclear features. *JAMA Oncol* 2018; 4: 1125-6.

Current status and future perspectives of liquid biopsy in non-small cell lung cancer

Sunhee Chang¹, Jae Young Hur², Yoon-La Choi³, Chang Hun Lee⁴, Wan Seop Kim²

¹Department of Pathology, Inje University Ilsan Paik Hospital, Goyang;

²Department of Pathology, Konkuk University Medical Center, Konkuk University School of Medicine, Seoul;

³Department of Pathology and Translational Genomics, Samsung Medical Center, Sungkyunkwan University School of Medicine, Seoul;

⁴Department of Pathology, Pusan National University Hospital, Pusan National University School of Medicine, Busan, Korea

With advances in target therapy, molecular analysis of tumors is routinely required for treatment decisions in patients with advanced non-small cell lung cancer (NSCLC). Liquid biopsy refers to the sampling and analysis of circulating cell-free tumor DNA (ctDNA) in various body fluids, primarily blood. Because the technique is minimally invasive, liquid biopsies are the future in cancer management. Epidermal growth factor receptor (*EGFR*) ctDNA tests have been performed in routine clinical practice in advanced NSCLC patients to guide tyrosine kinase inhibitor treatment. In the near future, liquid biopsy will be a crucial prognostic, predictive, and diagnostic method in NSCLC. Here we present the current status and future perspectives of liquid biopsy in NSCLC.

Key Words: Carcinoma, non-small cell lung cancer; Liquid biopsy; Circulating tumor DNA; Epidermal growth factor receptor; Biomarkers

Received: November 29, 2019 **Revised:** January 29, 2020 **Accepted:** February 27, 2020

Corresponding Author: Wan Seop Kim, MD, Department of Pathology, Konkuk University Medical Center, Konkuk University School of Medicine, 120-1 Neungdong-ro, Gwangjin-gu, Seoul 05030, Korea

Tel: +82-2-2030-5642, Fax: +82-2-2030-5629, E-mail: wskim@kuh.ac.kr

Molecular analysis is traditionally performed on tumor tissue. Although the number of mandatory tests for treatment decisions increases in patients with advanced non-small cell lung cancer (NSCLC), it is difficult to secure adequate tumor tissue for this purpose [1]. Small biopsy specimens, cell blocks, or aspirates are often the only available samples in patients with advanced NSCLC [2,3]. It is difficult to repeat tissue biopsies because they are invasive. Liquid biopsy could be an alternative or a complementary minimally invasive method for detecting molecular changes in NSCLC [1,2,4,5].

The clinical use of liquid biopsy to select patients with advanced NSCLC who are candidates for third-generation epidermal growth factor receptor (*EGFR*) tyrosine kinase inhibitor (TKI) therapy has been demonstrated in many clinical trials [6-10]. The United States Food and Drug Administration (FDA) approved Cobas *EGFR* Mutation Test v2 (Roche, Indianapolis, IN, USA) in 2018 as a companion diagnostic for third-generation *EGFR* TKI based on these results [11]. The Korea National Health Insurance Service (NHIS) has covered circulating cell-free tumor

DNA (ctDNA) tests for *EGFR* mutations in advanced NSCLC since 2018. In this review, we present the current status and future perspectives of liquid biopsy in patients with NSCLC.

BIOLOGY OF CIRCULATING TUMOR DNA

Liquid biopsy refers to the collection and analysis of analytes from various body fluids such as blood, urine, sputum, and pleural fluid [12-14]. Different analytes can be present in a liquid biopsy including circulating tumor cells (CTCs), circulating cell-free DNAs (cfDNAs), circulating tumor RNAs (ctRNAs), circulating exosomes, tumor-educated platelets, proteins, and metabolites [15,16]. CTCs are intact, viable tumor cells circulating in the blood [12]. Cancer releases single or clusters of CTCs into the bloodstream during the course of hematogenous spread. cfDNA refers to all circulating DNA in body fluids. cfDNA can be derived from neoplastic as well as non-neoplastic cells [15,16]. cfDNA can be detected in other body fluids, including urine, saliva, or cerebrospinal fluid. ctDNA refers to a subgroup

of cell-free DNA originating from tumor cells.

Circulating DNA fragments have a fragmentation pattern similar to a nucleosomal fragmentation pattern resulting from activation of nucleases in apoptotic cells [17,18]. Apoptosis (and necrosis) of the tumor is thought to be the major source of ctDNA [19-21]. As the tumor grows, apoptosis/necrosis increases as a result of rapid cell turnover. This leads to more release of tumor DNA into the circulation [14]. Macrophages may play a role in tumor cell release by phagocytosis of necrotic tumor cells. CTCs and active secretion from tumor cells may also be a source of ctDNA [21,22]. Circulating DNA is rapidly cleared via the kidney, liver, and spleen [23,24]. The load of ctDNA is highly correlated with total tumor burden and both volume and number of metastatic sites, suggesting that ctDNA may potentially have diagnostic and prognostic value [1,25-27]. Abbosh et al. [25] monitored clonal changes in NSCLC cells from initial diagnosis to death in the TRACER \times trial (TRACKing non-small cell lung cancer evolution through therapy R[x]) and suggested that ctDNA release is dependent on proliferation rate, apoptotic potential, and genomic instability. The amount of ctDNA before treatment highly correlated with the metabolic tumor volume on positron emission tomography-computed tomography. However, some patients with metastases have an unexpectedly low fraction of ctDNA [17,28,29]. Further investigation is required to understand the release and removal of ctDNA.

LIQUID BIOPSY VERSUS TISSUE BIOPSY

Liquid biopsy is a minimally invasive procedure [30], it avoids the complications of surgical biopsies and can be used for serial monitoring. Liquid biopsy allows for storage of tissue for further analyses such as immunohistochemistry related to immuno-oncology or participation in clinical trials. Tumors generally consist of different subclones (tumor heterogeneity). The outgrowth of some subclones under selection pressures such as therapeutic stress, particularly by targeted drugs, and micro-environmental changes can lead to disease progression and metastasis [14,30,31]. This clonal evolution can dynamically modify the genomic landscape of tumors. Tissue-based molecular analysis provides only a snapshot of tumor heterogeneity when and where the tumor was biopsied. Liquid biopsy can analyze complete and real-time molecular profiling of the tumor because blood samples contain ctDNA constantly released into the circulation from multiple regions of primary and metastatic tumors [14].

Despite these advantages, liquid biopsy has several limita-

tions in its widespread use. ctDNA detection requires more sensitive techniques than traditional approaches such as Sanger sequencing or pyrosequencing because of low fraction and high fragmentation of ctDNA [17,18,21,30]. Highly sensitive and highly specific tests, which are not available in all laboratories, are needed for ctDNA analysis. Liquid biopsy has an unfamiliar preanalytical variable associated with special processing and handling [11,32]. It does not yield information concerning histological tumor type, morphologic changes such as small cell lung cancer transformation that is one of the acquired resistance mechanisms to *EGFR* TKIs, and the tumor microenvironment in a liquid biopsy [16,33].

CURRENT TECHNOLOGIES FOR CIRCULATING TUMOR DNA DETECTION

Current tools for ctDNA analysis include real-time polymerase chain reaction (RT-PCR), digital PCR (dPCR), and next-generation sequencing (NGS) [15,21,30,34]. RT-PCR and dPCR are targeted methods that only allow screening of specific mutations. NGS allows targeted sequencing and whole exome sequencing. RT-PCR detects allele frequency (AF) and the ratio of variant alleles to wild type (WT) alleles down to 0.1% [8,15,35]. NGS and dPCR have detection thresholds approximately 0.01% or lower [36]. NGS and dPCR allow more precise quantification of the amount of ctDNA harboring target mutations than RT-PCR. dPCR can determine the absolute concentration of a gene of interest in a sample using the ratio of positive partitions with a targeted PCR product and an associated fluorescence signal over the total number [37]. RT-PCR uses a fluorescence readout to measure the amount of PCR product after each amplification and calculates the relative ratio of the target and reference genes for each sample (Semi-Quantitative Index).

The clinical use of various ctDNA tests for detecting *EGFR* mutations in plasma from patients with advanced NSCLC has been validated [6-9,38]. A meta-analysis showed that the sensitivity of ctDNA testing for the *EGFR* mutation was 66.4% (95% confidence interval [CI], 62.7% to 69.9%) and specificity was 95.6% (95% CI, 83.3% to 99.0%) in lung adenocarcinoma [39].

The Cobas *EGFR* Mutation Test v2 is the first ctDNA test to be approved by the US FDA to select patients who may benefit from TKI treatment. The Cobas *EGFR* Mutation Test v2 (Cobas) and PANAMutyper R *EGFR* (PANAMutyper; Panagene, Daejeon, Korea) were approved by the Korea FDA. A cross-platform comparison study showed comparable sensitivity between Cobas and PANAMutyper [40]. Commercially available ctD-

NA tests for detecting *EGFR* mutations in plasma are summarized in Table 1 [11,14,40–42].

Cobas can detect 42 mutations in exons 18–21 including L858R, exon 19 deletions, L861Q, and T790M in tissue and plasma [40]. The Cobas DNA Sample Preparation Kit (Roche, Indianapolis, IN, USA) was simultaneously developed for extracting ctDNA from plasma. PANAMutyper is a combination of peptide nucleic acid (PNA)-mediated clamping and melting curve analysis [40]. PNAclamp is a technology that selectively amplifies only the desired mutant sequences by combining the PNA clamping probe complementary to the WT sequences [40]. The PNA probe has a unique melting temperature according to the base sequence, separating from the DNA of the target sequence at a given temperature and reducing the fluorescence signal. The genotype of the target DNA can be determined by analyzing the temperature at which the signal decreases. The Therascreen *EGFR* Plasma RGQ PCR Kit (Qiagen, Manchester, UK) can detect *EGFR* mutations with amplification-refractory mutation system PCR and scorpion primers.

Droplet digital PCR (ddPCR; Bio-Rad, Hercules, CA, USA) and OncoBEAM (beads, emulsion, amplification, and magnetics; Sysmex Inostics, Hamburg, Germany) are dPCR-based techniques.

In dPCR, the sample is distributed into many reaction compartments containing one or no DNA copies and associated PCR reagents [4,12,40]. After amplification, the individual compartments are analyzed by a binary (presence or absence of amplification product) system. The number of compartments with amplification product corresponds directly to the number of copies of target mutation in the sample. In ddPCR, emulsion droplets are analyzed by fluorescence signal detection after target DNA is amplified within water-in-oil emulsion droplets. OncoBEAM combines emulsion PCR with magnetic beads and flow cytometry. After amplification, beads are coated with thousands of copies of single DNA molecules and each bead enters the water droplets

[43]. Flow cytometry analyzes the beads. A prospective study revealed that the positive predictive value is 100% for detection of *EGFR* L858R and 19del and 79% for T790M [27].

Because there is an increasing number of mutations to be analyzed, NGS panels are an attractive approach for ctDNA analysis [15]. NGS panels offer advantages of higher throughput, higher sensitivity, more efficient use of limited tissue, and lower cost per analysis than PCR-based methods [15,44,45]. FoundationOne CDx (Foundation Medicine, Cambridge, MA, USA) is an FDA-approved targeted NGS panel and detects mutations in 324 genes. Another FDA-approved panel, OncoPrint Dx Target Test (ThermoFisher Scientific, Waltham, MA, USA) is designed to detect 368 variants in 23 genes associated with NSCLC including *EGFR*, *ROS1*, and *BRAF*. The overall concordance rate of gene panel testing for tissue and ctDNA was 70.3% for *EGFR* mutation [46]. Cancer personalized profiling by deep sequencing combines optimized library preparation methods for low DNA input with a specialized bioinformatics approach to design a “selector” consisting of biotinylated DNA oligonucleotides that target recurrently mutated genomic regions in the cancer of interest [26,47].

CURRENT USE OF CIRCULATING TUMOR DNA TESTING IN LUNG CANCER

The clinical use of ctDNA testing for *EGFR* mutation using plasma specimens has been demonstrated by the AURA trials, which evaluated the dose, safety, and efficacy of osimertinib in patients with NSCLC who progressed following *EGFR* TKIs. The sensitivity of Cobas, OncoBEAM, ddPCR, and Therascreen for plasma T790M was up to 93%, 81%, 71%, and 29%, respectively (Table 2) [6–10]. The specificity of Cobas, OncoBEAM, ddPCR, and Therascreen for plasma T790M was 100%, 69%, 83%, and 100%, respectively. The concordance rate of T790M testing in plasma and tissue was up to 74%. Patients with T790M

Table 1. Summary of commercially available ctDNA tests for *EGFR* mutation

Trade name	Cobas	Therascreen	PANAMutyper	ddPCR	OncoBEAM
Kit	Cobas <i>EGFR</i> mutation test version 2	Therascreen <i>EGFR</i> plasma RGQ PCR version 2	PANAMutyper R <i>EGFR</i> kit	QX200 ddPCR Dx system	oncoBEAM- <i>EGFR</i> assay
Company	Roche	Qiagen	Panagene	Bio-Rad	Sysmex Inostics
Method	RT-PCR	Scorpion ARMS	PNA clamp	Water-emulsion droplet technology	Emulsion PCR
Gene coverage	42 Mutations	29 Mutations	47 Mutations	15 Mutations	10 Mutations
Result	Semi-quantitative	Semi-quantitative	Semi-quantitative	Absolute quantitative	Absolute quantitative

ctDNA, circulating cell-free tumor DNA; *EGFR*, epidermal growth factor receptor; ddPCR, droplet digital polymerase chain reaction; BEAM, beads, emulsion, amplification, magnetics; RT-PCR, real-time polymerase chain reaction; ARMS, amplification-refractory mutation system; PNA, peptide nucleic acid; PCR, polymerase chain reaction.

mutation in tissues or plasma had similar outcomes of osimertinib treatment [6,7,10]. Aura 17 showed that outcomes for patients with T790M mutations were comparable across the three plasma tests (56%–64%) [10]. Patients with T790M-positive plasma/T790M-negative tissue had unfavorable outcomes [6]. Patients with T790M-positive tissue/T790M-negative plasma status had better outcomes than patients who were tissue- and plasma-positive [8].

Currently, plasma ctDNA tests are recommended to detect *EGFR* mutations in patients with advanced NSCLC [11,15,16,39].

Korea NHIS covers up to three uses of ctDNA testing to select NSCLC patients for *EGFR* TKI when a tissue biopsy specimen is unavailable or insufficient for molecular testing. Liquid samples other than plasma have not been approved. Cobas and

PANAMutyper are ctDNA tests for *EGFR* mutation covered by Korea NHIS.

CURRENT STATUS OF LIQUID BIOPSY IN KOREA BASED ON EXTERNAL QUALITY ASSURANCE RESULTS

Proficiency testing for *EGFR* mutation analysis using liquid biopsy specimens has been performed annually by The Korean Society for Pathologists since 2018. Twenty-six laboratories participated in the proficiency test in 2018. The cfDNA Reference Standard (Horizon Discovery, Cambridge, UK) was used as reference material, which contained mutant AFs of 1% and 0% T790M, E19del, L858R, L861Q, G719S, S768I, and E20ins. Laboratories were requested to report the following: (1) time to sample processing, (2) tube type, (3) methods for plasma storage, (4) methods for ctDNA extraction, (5) methods for ctDNA analysis, and (6) results. All participating laboratories showed excellent performance with 100% accuracy for *EGFR* E19del, L858R, and T790M mutations (Table 3). There were no false-positive results for L861Q, G719S, S768I, or E20ins. In 2019, 24 laboratories participated in the proficiency test. The Korea Research Institute of Standards and Science produced reference materials comprising AFs of 1.9% for E19del, 1.5% for L858R, and 2.5% for T790M. All participating laboratories had excellent performance with 100% accuracy for *EGFR* E19del, L858R, and T790M mutations (Table 3). The 2017 European External Quality Assessments (EQA) scheme for ctDNA analysis that involved 32 laboratories from 16 countries showed an overall error rate of 42% for 1% of T790M/L858R and 7% for 5% of T790M/L858R [48]. One false-positive result was observed. Compared with these results, the results of Korean EQA over the past 2 years support the notion that good quality ctDNA analyses for *EGFR* mutation are performed in Korean pathology laboratories.

PANAMutyper was the most commonly used test in 2018. Twenty-four of 26 laboratories (92%) used PANAMutyper for ctDNA analysis. One used Cobas and another used ddPCR. For ctDNA extraction, 12 of 26 laboratories (45%) used Cobas, nine (33%) used TANBead (Taiwan Advanced Nanotech, Taoyuan,

Table 2. Detection of T790M using ctDNA in third-generation TKI clinical trials

Platform	Sample size (n)	Sensitivity (%)	Specificity (%)	Concordance (%)
Aura 1				
Preliminary assessment [7]				
Cobas ^a	38	41	100	57
Therascreen ^a	38	29	100	48
ddPCR ^a	38	71	83	74
BEAMing ^a	38	71	67	70
Subsequent assessment [7]				
Cobas	72	73 ^c	67 ^c	90 ^b
BEAMing	72	81 ^c	58 ^c	
Escalation and expansion cohorts [6]				
BEAMing ^a	216	70	69	-
AURA extension and AURA2 [8]				
Cobas ^a	551	61	79	65
Cobas ^d	562	93	92	92
Aura17 [9]				
Cobas ^a	240	42	83	-
AmoyDx SuperARMS ^a	249	49	78	-
ddPCR (in-house) ^a	249	56	73	-

ctDNA, circulating cell-free tumor DNA; TKI, tyrosine kinase inhibitor; ddPCR, droplet digital PCR; BEAM, beads, emulsion, amplification, magnetics; RT-PCR, real-time polymerase chain reaction; ARMS, amplification-refractory mutation system.

^aThe reference value is the result of the Cobas test with tissue; ^bThe concordance rate is between Cobas and BEAMing with plasma; ^cThe reference value is the result of the Cobas test with tissue; ^dThe reference value is the result of next-generation sequencing with plasma.

Table 3. Results of proficiency test

	Wild type	E19del	L858R	T790M	L861Q	G719S	S768I	E20ins
2018	26 ^a /26 ^b	26/26	26/26	26/26	25/26	20/26	22/26	21/26
2019	24/24	24/24	24/24	24/24	-	-	-	-

^aNumber of laboratory with correct results; ^bNumber of participating laboratory.

Taiwan), three (11%) used Maxwell RSC ccfDNA Plasma Kit (Promega, Madison, WI, USA), 2 (7%) used QIAamp circulating nucleic acid kit (Qiagen), and one (4%) used LIBEX (Tianlong Science and Technology, Xian, China). Plasma volume used for ctDNA extraction was 2 mL in 17 (63%), 1 mL in 4 (15%), and 0.6 mL in six of the laboratories (22%). The volume of DNA used for mutation testing was 100 μ L (n = 11, 41%) or 50 μ L (n = 11, 41%). The purity of DNA was assessed by NanoDrop (ThermoFisher Scientific) in 16 (76%) of the laboratories. Qubit (Invitrogen, Carlsbad, CA, USA), Bioanalyzer (Agilent Technologies, Santa Clara, CA, USA), Quantus (Promega), and TapeStation (Agilent Technologies) were also used in two, one, one, and one laboratories, respectively. Ethylenediaminetetraacetic acid (EDTA) tubes were used in 21 laboratories (78%). Seventeen laboratories (63%) kept blood samples refrigerated. Samples were processed within 2 hours in 13 (48%) and between 2 and 4 hours in 11 of the laboratories (41%). Plasma was stored in a freezer in 22 of the laboratories (82%) and immediately used in three laboratories.

Compared with 2018, there were decreases in sample processing time, decreases in volumes of plasma and DNA used, and increases in the use of TANBead for ctDNA extraction in 2019. All but one lab used PANAMutyper for ctDNA analysis. Twelve of 24 laboratories (50%) used TANBead for ctDNA extraction. The use of Cobas decreased (n = 6, 25%). Maxwell (n = 3, 13%), QIAamp (n = 1, 4%), and LIBEX (n = 2, 13%) were used. The number of laboratories using 2 mL of plasma for ctDNA extraction decreased to nine (38%), and those using 1 mL and 0.6 mL increased to seven (29%) and eight (33%), respectively. Some laboratories reduced the volume of DNA used for mutation testing to 50 μ L (n = 18, 75%). Five laboratories (21%) used 100 μ L. There was no change in DNA QC method. EDTA tubes were used in 21 laboratories (96%). Blood samples were kept refrigerated in 17 laboratories (71%). Twenty-one of the laboratories (88%) processed samples within 2 hours. The rest of the laboratories processed samples within 4 hours. The number of laboratories that immediately used plasma samples increased to six (25%). The rest stored plasma samples in a freezer. In the European EQA scheme, NGS (39%) is the most commonly used ctDNA test, followed by Cobas (26%) and ddPCR (23%) [48]. Fifty-five percent of the laboratories used QIAamp and 25% used Cobas for ctDNA extraction.

FUTURE PERSPECTIVES ON CIRCULATING TUMOR DNA TESTING IN LUNG CANCER

Other targetable mutations including *ALK*, *BRAF*, *ROS1*, *MEK*, and *HER2* have been detected in plasma from patients with NSCLC, although the sensitivity for detecting these mutations is lower than that for *EGFR* mutant detection [15,49-52]. The NGS-based approaches will facilitate detection of various rare genetic mutations that could be targeted. Highly fragmented ctDNA could result in insufficient mappable sequences to identify fusion events [51]. New technologies have been developed for detection of *ALK* fusion in ctDNA or ctRNA [15,49-52]. Recently developed, hybrid capture-based NGS can retrieve large genomic fragments to whole genomes with high sequencing coverage and accurate detection of genomic alterations, including genomic re-arrangements and short variants at low AFs and copy number amplifications. The clinical value of rare targetable mutations has not been demonstrated in NSCLC. The clinical use of ctDNA testing for *BRAF* V600E mutation was reported in metastatic melanoma and similar clinical trials are in progress in NSCLC [53].

Sputum, pleural fluid, and urine could also be used for molecular analysis [15,39]. T790M mutation was detected in urine and relevant tumor tissue from patients with NSCLC undergoing TKI therapy [24]. Using extracellular vesicle-derived DNA and ctDNA from pleural fluid supernatants yielded significant improvement in *EGFR* mutation analysis compared to the use of cell blocks or smears [54]. Kawahara et al. [55] also detected *EGFR* mutations in four of 18 cytologically negative groups using pleural fluid supernatant ctDNA. Further trials using these body fluids are needed for use in real practice.

In the near future, ctDNA testing is expected to play a significant role in identifying prognostic, predictive, and diagnostic biomarkers in patients with NSCLC patients. Tracking of ctDNA levels by an absolute quantitative method could be a minimally invasive tool for monitoring therapeutic effects and tumor recurrence [2,15,16]. Clinical trials showed that serial ctDNA tests using BEAMing can be used to monitor tumor response during treatment. Median progression-free survival (PFS) was shortened and objective response rate decreased in patients with persistent detection of plasma T790M for six weeks after initiation of osimertinib treatment [56]. Changes in plasma *EGFR* mutation load predicted response in 93% and progression in 89% of patients with lung adenocarcinoma in advance of radiologic evaluation [57].

PFS was significantly longer for patients without ctDNA de-

tection compared to those with ctDNA detection (295 vs. 55 days) during treatment [58]. However, the lack of consensus evaluation criteria and standard methodology are major limitations to expanding the use of ctDNA to monitor treatment efficacy and relapse [2].

Immunohistochemical programmed death-ligand 1 (PD-L1) assays are a companion or complementary diagnostic test for checkpoint inhibitor immune therapy. But, there are many challenges to the effective use of the PD-L1 test [59]. Tumor mutation burden (TMB), which is the total number of non-synonymous somatic mutations in the tumor genome, has recently been proposed as a predictive biomarker for immunotherapy in various tumors [58]. Liquid biopsy using the NGS-based approach is an emerging tool to assess TMB [2]. The OAK and POPLAR trials, which evaluated the efficacy of atezolizumab, showed a relationship between PFS and TMB of plasma ctDNA with FoundationOne CDx [60,61]. Giroux Leprieur et al. [62] also showed that TMB of ctDNA determined by an NCS gene panel approach can predict the efficacy of nivolumab in patients with advanced NSCLC. Patients with a ctDNA increase > 9% from baseline to the first tumor evaluation at 2 months had no long-term clinical benefit with nivolumab with a sensitivity of 71.4% and specificity of 100%. Because tumor-induced leukocyte infiltration may increase tumor volume or result in the development of new lesions, it may be difficult to radiographically assess the response to immunotherapy. Serial assessment of TMB using ctDNA testing will be beneficial for monitoring efficacy of immunotherapy. Goldberg et al. [63] showed that > 50% decrease in ctDNA was associated with improved PFS and OS. Median time to initial ctDNA response was 24.5 days, while the median time to initial radiographic partial response was 72.5 days. The use of ctDNA with imaging will allow a more comprehensive assessment of the response to immunotherapy.

The use of liquid biopsy has been studied in the assessment of minimal residual disease (MRD) after surgical resection in localized NSCLC [2,15]. Persistent detection of ctDNA after surgery in patients with NSCLC is highly correlated with tumor relapse [5,25,64]. Abbosh et al. [25] showed that the median interval between postoperative detection of ctDNA detection and tumor relapse confirmed on computed tomography (CT) imaging was 70 days in NSCLC patients. Chaudhuri et al. [64] also showed the utility of postoperative ctDNA detection using an NGS-based approach for MRD detection. The MRD detection rate was 94% by tracking all known mutations while 58% on average by tracking a single mutation. Postoperative ctDNA detection was earlier than imaging in 72% of patients with a median

of 5.2 months. Patients without postoperative ctDNA detection had a better outcome than those with ctDNA detection, while radiographic response assessment by CT at four months was not prognostic. Prospective clinical trials are needed to establish the clinical utility of MRD assessment using ctDNA.

Low-dose CT scans play a significant role in reducing lung cancer mortality. However, the overall false-positive rate is 96.4% because of many indeterminate pulmonary nodules [65]. Conventional sputum cytology is a simple, rapid, and specific screening tool, but less sensitive for lung cancer. Epigenetic changes such as hypermethylation were detected in the sputum of patients with lung cancer years preceding clinical diagnosis [1,66,67]. Combining the detection of epigenetic changes in sputum and CT scanning could facilitate a reduction in false-positive results and improve early diagnosis of lung cancer. Low sensitivity is the major limitation for detection of hypermethylation because a relative excess of background WT DNAs can mask epigenetic changes. Panels of methylated promoter genes and ultrasensitive detection methods should be developed for lung cancer screening.

CONCLUSION

Although the mechanism of ctDNA release and removal is not clearly understood, *EGFR* mutation detection in liquid biopsy specimens can be used to guide *EGFR* TKI treatment when a tissue biopsy cannot be obtained. Liquid biopsy will play a significant role as a prognostic, predictive, and diagnostic tool for various tumors. Pathologists should be able to integrate the results of molecular tests from the liquid biopsy and the morphological characteristics of relevant tissue, understand the preanalytical variables and different assay performance, and participate in a multidisciplinary team approach for optimal management of cancer patients.

ORCID

Sunhee Chang: <https://orcid.org/0000-0002-7775-4711>
 Jae Young Hur: <https://orcid.org/0000-0001-6105-9899>
 Yoon-La Choi: <http://orcid.org/0000-0002-5788-5140>
 Chang Hun Lee: <http://orcid.org/0000-0003-4216-2836>
 Wan Seop Kim: <http://orcid.org/0000-0001-7704-5942>

Author Contributions

Conceptualization: SC, WSK, CHL.
 Data curation: SC, JYH, YLC, WSK.
 Formal analysis: SC, JYH, YLC, WSK.

Investigation: SC, JYH, YLC, WSK.
 Methodology: YLC, WSK.
 Project administration: WSK, CHL.
 Supervision: WSK, CHL.
 Writing—original draft: SC.
 Writing—review & editing: SC, WSK.

Conflicts of Interest

The authors declare that they have no potential conflicts of interest.

Funding

No funding to declare.

REFERENCES

- Santarpia M, Liguori A, D'Aveni A, et al. Liquid biopsy for lung cancer early detection. *J Thorac Dis* 2018; 10(Suppl 7): S882-97.
- Herbreteau G, Vallée A, Charpentier S, Normanno N, Hofman P, Denis MG. Circulating free tumor DNA in non-small cell lung cancer (NSCLC): clinical application and future perspectives. *J Thorac Dis* 2019; 11(Suppl 1): S113-26.
- Diaz LA Jr, Bardelli A. Liquid biopsies: genotyping circulating tumor DNA. *J Clin Oncol* 2014; 32: 579-86.
- Cheung AH, Chow C, To KF. Latest development of liquid biopsy. *J Thorac Dis* 2018; 10(Suppl 14): S1645-51.
- Liang H, Huang J, Wang B, Liu Z, He J, Liang W. The role of liquid biopsy in predicting post-operative recurrence of non-small cell lung cancer. *J Thorac Dis* 2018; 10(Suppl 7): S838-45.
- Oxnard GR, Thress KS, Alden RS, et al. Association between plasma genotyping and outcomes of treatment with osimertinib (AZD9291) in advanced non-small-cell lung cancer. *J Clin Oncol* 2016; 34: 3375-82.
- Thress KS, Brant R, Carr TH, et al. *EGFR* mutation detection in ctDNA from NSCLC patient plasma: a cross-platform comparison of leading technologies to support the clinical development of AZD9291. *Lung Cancer* 2015; 90: 509-15.
- Jenkins S, Yang JC, Ramalingam SS, et al. Plasma ctDNA analysis for detection of the *EGFR* T790M mutation in patients with advanced non-small cell lung cancer. *J Thorac Oncol* 2017; 12: 1061-70.
- Zhou C, Wang M, Cheng Y, et al. Detection of *EGFR* T790M in Asia-Pacific patients (pts) with *EGFR* mutation-positive advanced non-small cell lung cancer (NSCLC): circulating tumour (ct) DNA analysis across 3 platforms. *Ann Oncol* 2017; 28(Suppl 5): v460-96.
- Zhou C, Cheng Y, Lu Y, et al. CNS response to osimertinib in Asian-Pacific patients (pts) with T790M-positive advanced NSCLC: data from an open-label Phase II trial (AURA17). *Ann Oncol* 2017; 28(Suppl 5): v460-96.
- Shin DH, Shim HS, Kim TJ, et al. Provisional guideline recommendation for *EGFR* gene mutation testing in liquid samples of lung cancer patients: a proposal by the Korean Cardiopulmonary Pathology Study Group. *J Pathol Transl Med* 2019; 53: 153-8.
- Heitzer E, Haque IS, Roberts CE, Speicher MR. Current and future perspectives of liquid biopsies in genomics-driven oncology. *Nat Rev Genet* 2019; 20: 71-88.
- Wan JC, Massie C, Garcia-Corbacho J, et al. Liquid biopsies come of age: towards implementation of circulating tumour DNA. *Nat Rev Cancer* 2017; 17: 223-38.
- Siravegna G, Marsoni S, Siena S, Bardelli A. Integrating liquid biopsies into the management of cancer. *Nat Rev Clin Oncol* 2017; 14: 531-48.
- Rolfo C, Mack PC, Scagliotti GV, et al. Liquid biopsy for advanced non-small cell lung cancer (NSCLC): a statement paper from the IASLC. *J Thorac Oncol* 2018; 13: 1248-68.
- Merker JD, Oxnard GR, Compton C, et al. Circulating tumor DNA analysis in patients with cancer: American Society of Clinical Oncology and College of American Pathologists Joint Review. *Arch Pathol Lab Med* 2018; 142: 1242-53.
- Heitzer E, Auer M, Hoffmann EM, et al. Establishment of tumor-specific copy number alterations from plasma DNA of patients with cancer. *Int J Cancer* 2013; 133: 346-56.
- Lo YM, Chan KC, Sun H, et al. Maternal plasma DNA sequencing reveals the genome-wide genetic and mutational profile of the fetus. *Sci Transl Med* 2010; 2: 61ra91.
- Sorber L, Zwaenepoel K, Deschoolmeester V, et al. Circulating cell-free nucleic acids and platelets as a liquid biopsy in the provision of personalized therapy for lung cancer patients. *Lung Cancer* 2017; 107: 100-7.
- Jahr S, Hentze H, Englisch S, et al. DNA fragments in the blood plasma of cancer patients: quantitations and evidence for their origin from apoptotic and necrotic cells. *Cancer Res* 2001; 61: 1659-65.
- Hench IB, Hench J, Tolnay M. Liquid biopsy in clinical management of breast, lung, and colorectal cancer. *Front Med (Lausanne)* 2018; 5: 9.
- Wang W, Kong P, Ma G, et al. Characterization of the release and biological significance of cell-free DNA from breast cancer cell lines. *Oncotarget* 2017; 8: 43180-91.
- Lo YM, Zhang J, Leung TN, Lau TK, Chang AM, Hjelm NM. Rapid clearance of fetal DNA from maternal plasma. *Am J Hum Genet* 1999; 64: 218-24.
- Husain H, Melnikova VO, Kosco K, et al. Monitoring daily dynamics of early tumor response to targeted therapy by detecting circulating tumor DNA in urine. *Clin Cancer Res* 2017; 23: 4716-23.

25. Abbosh C, Birkbak NJ, Wilson GA, et al. Phylogenetic ctDNA analysis depicts early-stage lung cancer evolution. *Nature* 2017; 545: 446-51.
26. Newman AM, Bratman SV, To J, et al. An ultrasensitive method for quantitating circulating tumor DNA with broad patient coverage. *Nat Med* 2014; 20: 548-54.
27. Sacher AG, Paweletz C, Dahlberg SE, et al. Prospective validation of rapid plasma genotyping for the detection of *EGFR* and *KRAS* mutations in advanced lung cancer. *JAMA Oncol* 2016; 2: 1014-22.
28. Bettgowda C, Sausen M, Leary RJ, et al. Detection of circulating tumor DNA in early- and late-stage human malignancies. *Sci Transl Med* 2014; 6: 224ra24.
29. Heidary M, Auer M, Ulz P, et al. The dynamic range of circulating tumor DNA in metastatic breast cancer. *Breast Cancer Res* 2014; 16: 421.
30. Heydt C, Michels S, Thress KS, Bergner S, Wolf J, Buettner R. Novel approaches against epidermal growth factor receptor tyrosine kinase inhibitor resistance. *Oncotarget* 2018; 9: 15418-34.
31. Sholl LM, Aisner DL, Allen TC, et al. Liquid biopsy in lung cancer: a perspective from members of the Pulmonary Pathology Society. *Arch Pathol Lab Med* 2016; 140: 825-9.
32. El Messaoudi S, Rolet F, Moulriere F, Thierry AR. Circulating cell free DNA: preanalytical considerations. *Clin Chim Acta* 2013; 424: 222-30.
33. Normanno N, Denis MG, Thress KS, Ratcliffe M, Reck M. Guide to detecting epidermal growth factor receptor (*EGFR*) mutations in ctDNA of patients with advanced non-small-cell lung cancer. *Oncotarget* 2017; 8: 12501-16.
34. Diehl F, Li M, Dressman D, et al. Detection and quantification of mutations in the plasma of patients with colorectal tumors. *Proc Natl Acad Sci U S A* 2005; 102: 16368-73.
35. Sorensen BS, Wu L, Wei W, et al. Monitoring of epidermal growth factor receptor tyrosine kinase inhibitor-sensitizing and resistance mutations in the plasma DNA of patients with advanced non-small cell lung cancer during treatment with erlotinib. *Cancer* 2014; 120: 3896-901.
36. Wang W, Song Z, Zhang Y. A Comparison of ddPCR and ARMS for detecting *EGFR* T790M status in ctDNA from advanced NSCLC patients with acquired *EGFR*-TKI resistance. *Cancer Med* 2017; 6: 154-62.
37. Quan PL, Sauzade M, Brouzes E. dPCR: a technology review. *Sensors (Basel)* 2018; 18: E1271.
38. Weber B, Meldgaard P, Hager H, et al. Detection of *EGFR* mutations in plasma and biopsies from non-small cell lung cancer patients by allele-specific PCR assays. *BMC Cancer* 2014; 14: 294.
39. Lindeman NI, Cagle PT, Aisner DL, et al. Updated molecular testing guideline for the selection of lung cancer patients for treatment with targeted tyrosine kinase inhibitors: guideline from the College of American Pathologists, the International Association for the Study of Lung Cancer, and the Association for Molecular Pathology. *Arch Pathol Lab Med* 2018; 142: 321-46.
40. Chen YL, Lin CC, Yang SC, et al. Five technologies for detecting the *EGFR* T790M mutation in the circulating cell-free DNA of patients with non-small cell lung cancer: a comparison. *Front Oncol* 2019; 9: 631.
41. Li X, Zhou C. Comparison of cross-platform technologies for *EGFR* T790M testing in patients with non-small cell lung cancer. *Oncotarget* 2017; 8: 100801-18.
42. Xu T, Kang X, You X, et al. Cross-platform comparison of four leading technologies for detecting *EGFR* mutations in circulating tumor DNA from non-small cell lung carcinoma patient plasma. *Theranostics* 2017; 7: 1437-46.
43. Buono G, Gerratana L, Bulfoni M, et al. Circulating tumor DNA analysis in breast cancer: is it ready for prime-time? *Cancer Treat Rev* 2019; 73: 73-83.
44. Blumenthal GM, Pazdur R. Approvals in 2017: gene therapies and site-agnostic indications. *Nat Rev Clin Oncol* 2018; 15: 127-8.
45. Yu T, Morrison C, Gold E, Tradonsky A, Layton A. MA 11.06 Retrospective analysis of NSCLC testing in low tumor content samples: single-gene tests, NGS, and the OncoPrint Dx Target Test. *J Thoracic Oncol* 2017; 12(Suppl 2): S1845.
46. Schwaederle M, Husain H, Fanta PT, et al. Use of liquid biopsies in clinical oncology: pilot experience in 168 patients. *Clin Cancer Res* 2016; 22: 5497-505.
47. Chen M, Zhao H. Next-generation sequencing in liquid biopsy: cancer screening and early detection. *Hum Genomics* 2019; 13: 34.
48. Keppens C, Dequeker EM, Patton SJ, et al. International pilot external quality assessment scheme for analysis and reporting of circulating tumour DNA. *BMC Cancer* 2018; 18: 804.
49. Tong Y, Zhao Z, Liu B, et al. 5'/3' imbalance strategy to detect *ALK* fusion genes in circulating tumor RNA from patients with non-small cell lung cancer. *J Exp Clin Cancer Res* 2018; 37: 68.
50. Yang Y, Shen X, Li R, et al. The detection and significance of *EGFR* and *BRAF* in cell-free DNA of peripheral blood in NSCLC. *Oncotarget* 2017; 8: 49773-82.
51. McCoach CE, Blakely CM, Banks KC, et al. Clinical utility of cell-free DNA for the detection of *ALK* fusions and genomic mechanisms of *ALK* inhibitor resistance in non-small cell lung cancer. *Clin Cancer Res* 2018; 24: 2758-70.
52. Bordi P, Tiseo M, Rofi E, et al. Detection of *ALK* and *KRAS* mutations in circulating tumor DNA of patients with advanced *ALK*-positive NSCLC with disease progression during crizotinib treat-

- ment. *Clin Lung Cancer* 2017; 18: 692-7.
53. Herbreteau G, Vallée A, Knol AC, et al. Circulating tumour DNA: analytical aspects and clinical applications for metastatic melanoma patients. *Ann Biol Clin (Paris)* 2017; 75: 619-30.
 54. Lee JS, Hur JY, Kim IA, et al. Liquid biopsy using the supernatant of a pleural effusion for *EGFR* genotyping in pulmonary adenocarcinoma patients: a comparison between cell-free DNA and extracellular vesicle-derived DNA. *BMC Cancer* 2018; 18: 1236.
 55. Kawahara A, Fukumitsu C, Azuma K, et al. A combined test using both cell sediment and supernatant cell-free DNA in pleural effusion shows increased sensitivity in detecting activating *EGFR* mutation in lung cancer patients. *Cytopathology* 2018; 29: 150-5.
 56. Thress KS, Markovets A, Barrett JC, et al. Complete clearance of plasma *EGFR* mutations as a predictor of outcome on osimertinib in the AURA trial. *J Clin Oncol* 2017; 35(15 Suppl): 9018.
 57. Taus A, Camacho L, Rocha P, et al. Dynamics of *EGFR* mutation load in plasma for prediction of treatment response and disease progression in patients with *EGFR*-mutant lung adenocarcinoma. *Clin Lung Cancer* 2018; 19: 387-94.
 58. Hellmann MD, Ciuleanu TE, Pluzanski A, et al. Nivolumab plus ipilimumab in lung cancer with a high tumor mutational burden. *N Engl J Med* 2018; 378: 2093-104.
 59. Kim H, Chung JH. PD-L1 testing in non-small cell lung cancer: past, present, and future. *J Pathol Transl Med* 2019; 53: 199-206.
 60. Gandara DR, Paul SM, Kowanetz M, et al. Blood-based tumor mutational burden as a predictor of clinical benefit in non-small-cell lung cancer patients treated with atezolizumab. *Nat Med* 2018; 24: 1441-8.
 61. Gandara DR, Kowanetz M, Mok TS, et al. Blood-based biomarkers for cancer immunotherapy: tumor mutational burden in blood (bTMB) is associated with improved atezolizumab (atezo) efficacy in 2L+ NSCLC (POPLAR and OAK). *Ann Oncol* 2017; 28(Suppl 5): v460-96.
 62. Giroux Leprieur E, Herbreteau G, Dumenil C, et al. Circulating tumor DNA evaluated by next-generation sequencing is predictive of tumor response and prolonged clinical benefit with nivolumab in advanced non-small cell lung cancer. *Oncoimmunology* 2018; 7: e1424675.
 63. Goldberg SB, Narayan A, Kole AJ, et al. Early assessment of lung cancer immunotherapy response via circulating tumor DNA. *Clin Cancer Res* 2018; 24: 1872-80.
 64. Chaudhuri AA, Chabon JJ, Lovejoy AF, et al. Early detection of molecular residual disease in localized lung cancer by circulating tumor DNA profiling. *Cancer Discov* 2017; 7: 1394-403.
 65. Tammemagi MC, Katki HA, Hocking WG, et al. Selection criteria for lung-cancer screening. *N Engl J Med* 2013; 368: 728-36.
 66. Tomasetti M, Amati M, Neuzil J, Santarelli L. Circulating epigenetic biomarkers in lung malignancies: From early diagnosis to therapy. *Lung Cancer* 2017; 107: 65-72.
 67. Hubers AJ, Heideman DA, Duin S, et al. DNA hypermethylation analysis in sputum of asymptomatic subjects at risk for lung cancer participating in the NELSON trial: argument for maximum screening interval of 2 years. *J Clin Pathol* 2017; 70: 250-4.

Clinical management of abnormal Pap tests: differences between US and Korean guidelines

Seyeon Won, Mi Kyoung Kim, Seok Ju Seong

Department of Obstetrics and Gynecology, CHA Gangnam Medical Center, CHA University College of Medicine, Seoul, Korea

Cervical cancer has been the most common gynecological cancer in Korea but has become a preventable disease with regular screening and proper vaccination. If regular screening is provided, cervical cancer does not progress to more than carcinoma in situ, due to its comparatively long precancerous duration (years to decades). In 2012, the American Society for Colposcopy and Cervical Pathology published guidelines to aid clinicians in managing women with abnormal Papanicolaou (Pap) tests, and they soon became the standard in the United States. Not long thereafter, the Korean Society of Gynecologic Oncology and the Korean Society for Cytopathology published practical guidelines to reflect the specific situation in Korea. The detailed screening guidelines and management options in the case of abnormal Pap test results are sometimes the same and sometimes different in the United States and Korean guidelines. In this article, we summarize the differences between the United States and Korean guidelines in order to facilitate physicians' proper management of abnormal Pap test results.

Key Words: Cervix uteri; Uterine cervical neoplasms; Screening; Papanicolaou test

Received: February 12, 2020 **Revised:** March 6, 2020 **Accepted:** March 11, 2020

Corresponding Author: Seok Ju Seong, MD, Department of Obstetrics and Gynecology, CHA Gangnam Medical Center, CHA University, 566 Nonhyeon-ro, Gangnam-gu, Seoul 06135, Korea

Tel: +82-2-3468-3673, Fax: +82-2-558-1112, E-mail: sjseongcheil@naver.com

Cervical cancer has been the most common gynecological cancer in Korea. Its incidence, however, has been consistently decreasing, from 18.9 per 100,000 females in 1999 to 13.9 in 2016 [1] due to increased interest in cervical cancer screening and the introduction of vaccination [2]. With regular screening and proper vaccination, cervical cancer has become a preventable disease. In fact, if regular screening is provided, cervical cancer does not progress to more than carcinoma in situ, due to its comparatively long precancerous duration (years to decades). In Korea, the promotion and provision of free screening tests for cervical cancer have steadily increased the rate of women undergoing screening [3]. In 2012, the American Society for Colposcopy and Cervical Pathology (ASCCP) published guidelines [4] to aid clinicians' management of women with abnormal cervical cytology and cervical intraepithelial neoplasia (CIN), and they soon became the US standard. Not long thereafter, the Korean Society of Gynecologic Oncology and the Korean Society for Cytopathology published practical guidelines for early detection of cervical cancer to reflect the high incidence of cervical cancer and

low medical costs in Korea [5]. The Papanicolaou (Pap) test is the primary screening method in both guidelines; however, in the case of abnormal Pap test results, the detailed screening guidelines and management options differ in some respects. In this article, we summarize the differences between the US and Korean guidelines in order to facilitate physicians' proper management of abnormal Pap test results.

SCREENING STRATEGIES

When to start screening?

According to the guidelines of the ASCCP [4], the Pap test is the standard screening method for cervical cancer and should be started at the age of 21. Women aged 20 and younger are not considered eligible for screening, regardless of sexual activity, owing to the rarity of cervical cancer cases among that cohort [6]. The ASCCP suggested that the Pap test screening interval for women in their 20s should be 3 years [4]. For such women, spontaneous regression occurs frequently, and the rate of progression

to invasive cancer is low, notwithstanding the high incidence of human papillomavirus (HPV) infection among that age group [7]. Therefore, HPV triage would be less efficient for those women [8]. In the case of women aged 30 years and older, the screening strategy changes. For them, the ASCCP guidelines call for both a Pap test and an HPV test (i.e., a co-test) every 5 years [4]. The US Preventive Services Task Force (USPSTF) stated that an HPV test alone every 5 years also is possible [9], as women aged 30 years and older are less likely to clear a new HPV infection and more likely to have HPV persistence [10]. Although the co-test may have financial and logistical limitations, it can both increase the detection of prevalent CIN 3 and enhance the detection of adenocarcinoma and adenocarcinoma in situ (AIS) [11].

The Korean guidelines [5] are somewhat different. All women aged 20 years and older who have commenced sexual activity should be screened with a Pap test annually. The co-test for women aged 30 years and older can be applicable. The interval can be extended to every 2 years for a woman who has negative results from both a Pap smear and an HPV test. In summary, the screening test interval is shorter in Korea than in the United States. This difference can be attributed to Korea's lower medical costs and higher cervical cancer incidence rate. Also, whereas in Korea, women aged 20 years and older who have not commenced sexual activity are excluded from screening, in the United States, women aged 21 years and older should be screened regardless of sexual activity.

When to terminate?

According to the ASCCP [4], screening can be terminated in women aged 65 years and older if three consecutive Pap tests within 10 years are negative or two consecutive co-tests are negative for women with no history of CIN 2 or 3. Women with a history of CIN 2 or 3 or AIS should be screened for 20 years from the date on which the cervical lesion was treated. Women who have had a total hysterectomy and who have a history of CIN 2 or 3 should be screened every 3 years for a total duration of 20 years from the date on which the cervical lesion was treated. Meanwhile, women who have had a total hysterectomy but lack any history of CIN 2 or 3 can be excluded from screening.

In Korea, screening terminates later than in the United States. Screening can be terminated in women aged 70 years and older if three consecutive Pap smears within 10 years are negative [5].

HPV test alone?

The HPV test was approved by the Food and Drug Administration (FDA) in 2014 for use in the United States. However,

the FDA does not include any specific guidelines for application of this test in cervical cancer screening [12]. The USPSTF stated that screening every 5 years with the HPV test alone can be performed for women aged 30 to 65 years [9]. Also a study of the USPSTF showed that HPV testing detected higher rates of CIN 3 or worse (CIN 3+) and that co-testing did not provide for increased CIN 3+ detection relative to the Pap test [13]. Although the HPV test shows high sensitivity, the efficacy and cost effectiveness of primary HPV screening vary in different medical environments [3]. Considering the Korean situation, which entails lower screening costs and easier access to healthcare, the Pap test, rather than the HPV test, is considered to be the primary screening modality. According to the Korean guidelines [5], the data on primary HPV screening is not yet sufficient to assess its utility for cervical cancer screening [14].

MANAGEMENT OF ABNORMAL PAP RESULTS

Negative cytology

We will summarize how to manage negative cytology according to only the ASCCP guidelines [4], as specific corresponding Korean guidelines do not exist. Negative cytology can be classified into three categories. The first is "unsatisfactory cytology" resulting mainly from an insufficiency of squamous cells [15], and its reporting rates are 1.1% or less [16]. Women with unsatisfactory cytology should undergo a repeat Pap test after 2–4 months. Immediate colposcopy is recommended for women aged 30 years and older who are HPV positive. Women with two consecutive unsatisfactory cytology results should undergo colposcopy. The second category of negative cytology is "negative but absent or insufficient endocervical/transformation component," which means that the squamocolumnar junction may not have been sufficiently collected. Women aged younger than 30 years or 30 years and older with HPV negativity can be returned to routine screening without any further evaluation. However, women aged 30 years and older who are HPV-unknown status should be screened by HPV testing. If women aged 30 years and older are HPV positive, it is recommended that they undergo both repeated Pap testing and HPV testing 12 months later or immediate genotyping of HPV. If HPV 16 or 18 shows positivity by genotyping, immediate colposcopy is recommended. The third category of negative cytology is "negative with a positive HPV test," which presents two options. The first option is repeated co-testing at 12 months, because most cases of HPV infection are cleared rapidly, two-thirds clearing by 12 months [17]. Among a group of women whose HPV infection

persisted for 1 year, only 21% progressed to CIN 2+ within 30 months [17]. If, according to the repeated test, HPV is positive or the cytology is atypical squamous cells of undetermined significance (ASC-US) or worse, immediate colposcopy is recommended. The second option for treatment of the “negative with a positive HPV test” category is HPV DNA typing. If HPV 16 or 18 is positive, immediate colposcopy is recommended. In Korea, the overall management does not differ from that in the United States, except for the follow-up interval and duration, which are determined at the clinician’s discretion.

Atypical squamous cell

ASC is a common status that is worse than reactive change but does not attain to the criteria of squamous intraepithelial lesion. ASC is classified into ASC-US and high-grade lesion (ASC-H), which runs a high risk of CIN 2+ [18].

ASC-US

The prevalence rate of ASC-US is 5%, which is relatively high, though the possibility of its becoming a high-grade lesion such as CIN 3+ is low. In the cases of one-third to two-thirds of women, their ASC-US is not related to HPV infection [8]. Therefore, proactive management, including screening, of women with ASC-US who have a high-grade lesion (e.g., CIN 2+) has proved to be problematic. There are three options for women with ASC-US: repeated Pap test, HPV test, or colposcopy. In the Korean guidelines, any of these options can be chosen, and the actual choice is made by the clinician’s personal preference. However, in the ASCCP guidelines, HPV testing is preferred over repeated Pap testing, though colposcopy is not an available option. The more specific guidelines are as follows.

Repeated Pap test

According to the ASCCP, repeated Pap testing at 12-month intervals can be chosen [4]. In the Korean guidelines [5], the interval of repeated Pap testing is shortened to 6 months. If the result of repeated Pap testing is ASC-US or worse, immediate colposcopy is recommended. If the result is negative, returning to the routine screening program is recommended in the United States, while one additional repeated Pap test (to be performed in 6 months’ time) is recommended in Korea. If two consecutive Pap tests show negativity, returning to routine screening is recommended. To sum up, one additional repeated Pap test is needed in Korea, whereas in the United States, the prescription is a return to routine screening.

HPV test

HPV testing is the preferred management for women with ASC-US in the United States. If HPV is detected, immediate colposcopy is recommended. If the HPV test is negative, a return to the routine screening program is recommended.

Colposcopy

Immediate colposcopy is an option only in Korea. If the result is confirmed as CIN 1 or less, Pap testing at 6 and 12 months or HPV testing at 12 months is recommended. If all of the these results are negative, returning to routine screening is possible. In the United States by contrast, immediate colposcopy, according to the ASCCP guidelines, is not recommended [4]. This may be explained by the significantly expensive medical costs in the United States. Actually, the cost of a colposcopy in the United States is over 230 US dollars, whereas in Korea, it is around a tenth of that (28,950 won), cheaper even than an HPV test (50,890 won) or a Pap test (55,000 won, or free once every two years).

ASC-US in special situations

The ASCCP guidelines are more subdivided for women aged 21–24 years than is the case in Korea [4], due to the fact that the cervical cancer risk remains low there for women aged under 25 years [6]. An inappreciable difference for women aged 21–24 years is the fact that repeated Pap testing is preferred over HPV testing. If the result of a repeated Pap test is ASC-US, low-grade squamous intraepithelial lesion (LSIL), or negative, again-repeated Pap testing in 12 months is recommended. If the result of a repeated Pap test is ASC-H, atypical glandular cells (AGC), or high-grade squamous intraepithelial lesion (HSIL), immediate colposcopy is recommended. After two consecutive Pap tests are negative, returning to routine screening is possible. If an HPV test is negative once, returning to routine screening is possible. In the Korean guidelines, however, adolescent woman with ASC-US are considered instead of women aged 21–24. For such women, only annual Pap testing is recommended. If the results of a Pap test at 12 months is HSIL or worse, immediate colposcopy should be done. If the results of a Pap test at 24 months are ASC-US or worse, immediate colposcopy should be done.

The management of pregnant women with ASC-US is the same as that of adult women with ASC-US, except for a colposcopy option [4,5]. It should be noted that even though colposcopy is permitted for pregnant women, deferring it until 6 weeks after delivery is also acceptable. However, endocervical curettage (ECC) is prohibited during pregnancy.

ASC-H

There are no differences in the management of ASC-H between the US and Korean guidelines [4,5]. Colposcopy should be conducted immediately, because the risk of CIN 3+ in women with ASC-H is several times higher than in women with ASC-US or LSIL [19,20]. ASC-H, therefore, should be managed in the same manner as HSIL. According to the literature [19], the 5-year cancer risk of women having ASC-H with HPV negativity is approximately 2%, which is too high for conservative observation without further evaluation or treatment. If the result of a colposcopy is not CIN 1, immediate repeated Pap testing and colposcopy can be considered, or, especially according to the Korean guidelines, they can be repeated after 6 months [5]. If two consecutive results of both Pap testing and colposcopy are negative, returning to routine screening is possible. HPV testing for such women is not recommended.

According to the ASCCP guidelines [4], if the result of a colposcopy is CIN 1, co-testing at 1 year is recommended.

ASC-H in special situations

According to the ASCCP guidelines, immediate colposcopy should be primarily considered for women aged 21–24 years with ASC-H. According to the Korean guidelines, immediate colposcopy should be done for adolescent women with ASC-H. There are no detailed recommendations for pregnant women with ASC-H in either the Korean or ASCCP guidelines.

LSIL

The natural history of LSIL is clinically equivalent to that of HPV-positive ASC-US [21]. CIN2+ has been found in 11.8% of woman with LSIL [22]. According to the ASCCP guidelines [4], colposcopy is preferred for women in whom there is LSIL with no HPV test result or in whom there is HPV positivity. For women in whom there is LSIL with HPV negativity, repeated co-testing at 12 months is preferred, or alternatively, colposcopy is acceptable. If the results of co-testing at 12 months is ASC-US or worse or positive for HPV, immediate colposcopy is recommended. If the results of co-testing at 12 months are negative, repeated co-testing at 36 months is recommended.

According to the Korean guidelines [5], immediate colposcopy is preferentially recommended [23] irrespective of HPV test results. ECC should be considered for women in whom cervical lesion is not identified or those for whom colposcopy proves unsatisfactory, except for pregnant women [24].

LSIL in special situations

For women aged 21–24 years with LSIL, only Pap testing in 12 months is recommended in the ASCCP guidelines [4]; neither colposcopy nor HPV should be considered. For adolescent women with LSIL according to the Korean guidelines [5], observation with Pap testing in 12 months is permitted. Immediate colposcopy is preferred for pregnant women with LSIL according to both the ASCCP and Korean guidelines [4,5]. Deferring of the colposcopy until 6 weeks after delivery is acceptable.

HSIL

There are no specific differences between the ASCCP [4] and Korean guidelines [5] for management of HSIL. The 5-year cancer risk is not statistically different between woman aged 30 to 64 with HPV-negative HSIL and those with HPV-positive HSIL (6.8 and 6.6%) [18]. Consideration of HPV testing, therefore, is not proper for women with HSIL. Because 40%–60% of women with HSIL turn out to be CIN 2+ by colposcopy [20,22], an immediate excisional procedure can be pursued; otherwise, colposcopy is acceptable. If the colposcopic findings are unsatisfactory, an excisional procedure should be done. If there is no lesion visible by colposcopy, ECC should be done. If the ECC results are negative, two consecutive Pap tests and colposcopy at 6 and 12 months should also be negative in order to return to routine screening. If the finding is CIN 2+ by colposcopy, an excisional procedure is called for. If the colposcopic findings are CIN 1, there are three options [5]: First, a diagnostic excisional procedure can be performed; second, both the Pap test and colposcopy results can be reviewed once again; and third, both colposcopy and Pap testing should be done at 6 and 12 months until two consecutive results are negative. If the Pap test shows HSIL again, an excisional procedure should be done.

HSIL in special situations

Only immediate colposcopy (not any excisional procedure) should be considered for adolescent women [5], or those aged 21–24 years (only applicable in United States [4]), with HSIL. Understandably too, only immediate colposcopy is recommended for pregnant women with HSIL as well. However, colposcopic biopsy should be conducted only in cases where high-grade lesion is suspected. Also, ECC is prohibited in pregnant women. If CIN 2 or 3 is found through colposcopic biopsy, an excisional procedure can be delayed until after the birth of the baby, because several studies have shown that high-grade lesion may regress postpartum [25,26].

Atypical glandular cells

AGC as detected on a Pap test may originate from a variety of locations [27]. Therefore, endometrial sampling or ECC might be needed in certain situations. In addition, AGC has not only been associated with benign disease but also with neoplasms of the endometrium, cervix, fallopian tube, and even ovary [28]. According to Katki et al. [18], CIN 3+ was found in 4.7% and cancer in 2.3% of woman aged 30 to 64 years with AGC. Basically, immediate colposcopy with ECC is recommended for women with AGC, due to the relatively high risk of CIN3+. Moreover, HPV testing in concert with colposcopy and ECC should be performed in Korea [5]. Given that endometrial cancer is not HPV associated, routine HPV test is not proper for identification of women who need less invasive management [4]. Endometrial sampling is also recommended in conjunction with colposcopy and ECC in women aged 35 years and older or who are at risk for endometrial cancer. According to the Korean guidelines [5], for women with CIN 1 and negative ECC, a Pap test can be performed at 6 and 12 months or an HPV test can be performed at 12 months. If ASC-US or worse is found in the ensuing Pap test, immediate colposcopy is recommended. Otherwise, a diagnostic excisional procedure is recommended. There are a few differences in the ASCCP guidelines [4]. For women with AGC in whom CIN 2+ is not found, co-testing at 12 and 24 months is recommended. If both co-tests are negative, co-testing 3 years later is recommended. If any abnormality is found

Table 1. Summary of the United States/Korea differences in screening strategies for cervical cancer

Screening strategy	United States	Korea
Screening age (yr)	21–65	20–70
Screening methods		
Pap test	Every 3 yr	Every year
HPV test	Every 5 yr at age 30 yr	Not recommended
Co-test	Every 5 yr at age 30 yr	Every 2 yr at age 30 yr

Pap test, Papanicolaou test; HPV, human papillomavirus; Co-test, Pap test + HPV test.

Table 2. Summary of the United States/Korea differences in management of abnormal Pap tests

Result	United States	Korea
ASC-US	HPV test ^a or Pap test (12 mo)	Pap test (6 mo) or HPV test or colposcopy
ASC-H	Colposcopy	Same as the United States
LSIL	Co-test ^a (12 mo, only for HPV-) or Colposcopy	Colposcopy
HSIL	Colposcopy or excisional procedure	Same as the United States
AGC	Colposcopy and ECC	Colposcopy, ECC and HPV test

All procedures should be performed immediately unless otherwise noted.

Pap, Papanicolaou test; ASC-US, atypical squamous cells of undetermined significance; HPV, human papillomavirus; ASC-H, ASC-US and high-grade lesion; LSIL, low-grade squamous intraepithelial lesion; Co-test, Pap test + HPV test; HPV-, women who are HPV negative; HSIL, high-grade squamous intraepithelial lesion; AGC, atypical glandular cells; ECC, endo-cervical curettage.

^aPreferred method.

in the subsequent co-test, immediate colposcopy is recommended. Diagnostic excisional procedure is recommended for women with AGC (favor neoplasia) or AIS, regardless of colposcopic results.

AGC in special situations

Only ASCCP guideline [4] is available. Women aged 21–24 years or those pregnant with AGC should be managed in the same manners as adult women with AGC. Again, ECC and endometrial biopsy are prohibited in pregnant women.

MANAGEMENT OF CIN 1, CIN 2, AND CIN 3

Abnormal results of Pap test should be managed as described above. Subsequently, once the lesion is revealed to be CIN 1, CIN 2, or CIN 3 by colposcopy or ECC, it should be treated by respective proper methods. CIN 1 has been considered as observable status and known to regress well, and it does not progress frequently to CIN 2+ [29,30]. For women with CIN 1, co-test at 1 year is recommended in the United States [4]. If the subsequent co-test is negative, an age-appropriate test at 3 years (Pap test for women younger than 30 years, co-test for women aged 30 years and older) is recommended. If the age-appropriate test is negative, returning to routine screening is possible. On the other hand, in Korea, Pap testing at 6 and 12 months or HPV testing at 1 year is recommended [5]. If two consecutive Pap tests or HPV tests are negative, returning to routine screening is possible.

CIN 2 and 3 have higher progression rates and lower regression rates than CIN 1. Basically, excisional or ablation therapy, therefore, is recommended for CIN 2 or 3 with adequate colposcopy. However, ablation therapy is not recommended for CIN 2 or 3 with inadequate colposcopy or ECC showing CIN 2, CIN 3, or ungraded CIN. If residual lesion remains at the resection margin after excisional therapy, Pap testing at 6 months or HPV testing at 1 year can be done in follow-up [5].

CONCLUSION

The overall tendency of the Korean strategy for abnormal Pap test results, relative to the US guidelines, is a shorter interval of follow-up and more invasive evaluation (e.g., immediate colposcopy) rather than following up with HPV or repeated Pap testing [4]. Summarized differences between the guidelines are shown in Tables 1 and 2. These differences reflect the inherent medical environment in Korea. First, the incidence rate of cervical cancer is still higher than in the United States or other developed countries. Second, there is good overall accessibility to medical service in Korea. Third, medical costs are low, and especially, colposcopy is cheaper than a Pap test or HPV test. Strengthening these national advantages and clearly understanding (and consistently following) the treatment guidelines may further reduce the incidence of cervical cancer in Korea.

ORCID

Seyeon Won: <https://orcid.org/0000-0002-2254-2703>

Mi Kyoung Kim: <https://orcid.org/0000-0002-9520-2339>

Seok Ju Seong: <https://orcid.org/0000-0003-3820-3412>

Author Contributions

Conceptualization: SJS.

Supervision: SJS.

Writing—original draft: SW.

Writing—review & editing: SW, MKK, SJS.

Conflicts of Interest

The authors declare that they have no potential conflicts of interest.

Funding

No funding to declare.

REFERENCES

1. Korea Central Cancer Registry, National Cancer Center. Annual report of cancer statistics in Korea in 2016. Sejong: Ministry of Health and Welfare, 2018.
2. Lim MC, Won YJ, Ko MJ, et al. Incidence of cervical, endometrial, and ovarian cancer in Korea during 1999-2015. *J Gynecol Oncol* 2019; 30: e38.
3. Lim SC, Yoo CW. Current status of and perspectives on cervical cancer screening in Korea. *J Pathol Transl Med* 2019; 53: 210-6.
4. Massad LS, Einstein MH, Huh WK, et al. 2012 Updated consensus guidelines for the management of abnormal cervical cancer screening tests and cancer precursors. *J Low Genit Tract Dis* 2013; 17(5 Suppl 1): S1-27.
5. Lee JK, Hong JH, Kang S, et al. Practice guidelines for the early detection of cervical cancer in Korea: Korean Society of Gynecologic Oncology and the Korean Society for Cytopathology 2012 edition. *J Gynecol Oncol* 2013; 24: 186-203.
6. Benard VB, Watson M, Castle PE, Saraiya M. Cervical carcinoma rates among young females in the United States. *Obstet Gynecol* 2012; 120: 1117-23.
7. Moscicki AB, Schiffman M, Burchell A, et al. Updating the natural history of human papillomavirus and anogenital cancers. *Vaccine* 2012; 30 Suppl 5: F24-33.
8. Katki HA, Schiffman M, Castle PE, et al. Five-year risks of CIN 3+ and cervical cancer among women with HPV testing of ASC-US Pap results. *J Low Genit Tract Dis* 2013; 17(5 Suppl 1): S36-42.
9. US Preventive Services Task Force, Curry SJ, Krist AH, et al. Screening for cervical cancer: US Preventive Services Task Force Recommendation Statement. *JAMA* 2018; 320: 674-86.
10. Lees BF, Erickson BK, Huh WK. Cervical cancer screening: evidence behind the guidelines. *Am J Obstet Gynecol* 2016; 214: 438-43.
11. Katki HA, Kinney WK, Fetterman B, et al. Cervical cancer risk for women undergoing concurrent testing for human papillomavirus and cervical cytology: a population-based study in routine clinical practice. *Lancet Oncol* 2011; 12: 663-72.
12. Huh WK, Ault KA, Chelmow D, et al. Use of primary high-risk human papillomavirus testing for cervical cancer screening: interim clinical guidance. *Obstet Gynecol* 2015; 125: 330-7.
13. Melnikow J, Henderson JT, Burda BU, Senger CA, Durbin S, Weyrich MS. Screening for cervical cancer with high-risk human papillomavirus testing: updated evidence report and systematic review for the US Preventive Services Task Force. *JAMA* 2018; 320: 687-705.
14. Min KJ, Lee YJ, Suh M, et al. The Korean guideline for cervical cancer screening. *J Gynecol Oncol* 2015; 26: 232-9.
15. Holton T, Smith D, Terry M, Madgwick A, Levine T. The effect of lubricant contamination on ThinPrep (Cytec) cervical cytology liquid-based preparations. *Cytopathology* 2008; 19: 236-43.
16. Moriarty AT, Clayton AC, Zaleski S, et al. Unsatisfactory reporting rates: 2006 practices of participants in the college of american pathologists interlaboratory comparison program in gynecologic cytology. *Arch Pathol Lab Med* 2009; 133: 1912-6.
17. Rodríguez AC, Schiffman M, Herrero R, et al. Rapid clearance of human papillomavirus and implications for clinical focus on per-

- sistent infections. *J Natl Cancer Inst* 2008; 100: 513-7.
18. Katki HA, Schiffman M, Castle PE, et al. Five-year risks of CIN 3+ and cervical cancer among women with HPV-positive and HPV-negative high-grade Pap results. *J Low Genit Tract Dis* 2013; 17(5 Suppl 1): S50-5.
 19. Katki HA, Gage JC, Schiffman M, et al. Follow-up testing after colposcopy: five-year risk of CIN 2+ after a colposcopic diagnosis of CIN 1 or less. *J Low Genit Tract Dis* 2013; 17(5 Suppl 1): S69-77.
 20. Massad LS, Collins YC, Meyer PM. Biopsy correlates of abnormal cervical cytology classified using the Bethesda system. *Gynecol Oncol* 2001; 82: 516-22.
 21. Cox JT, Schiffman M, Solomon D, Group A-LTS. Prospective follow-up suggests similar risk of subsequent cervical intraepithelial neoplasia grade 2 or 3 among women with cervical intraepithelial neoplasia grade 1 or negative colposcopy and directed biopsy. *Am J Obstet Gynecol* 2003; 188: 1406-12.
 22. Alvarez RD, Wright TC; Optical Detection Group. Effective cervical neoplasia detection with a novel optical detection system: a randomized trial. *Gynecol Oncol* 2007; 104: 281-9.
 23. ASCUS-LSIL Traige Study (ALTS) Group. A randomized trial on the management of low-grade squamous intraepithelial lesion cytology interpretations. *Am J Obstet Gynecol* 2003; 188: 1393-400.
 24. Partridge EE, Abu-Rustum NR, Campos SM, et al. Cervical cancer screening. *J Natl Compr Canc Netw* 2010; 8: 1358-86.
 25. Vlahos G, Rodolakis A, Diakomanolis E, et al. Conservative management of cervical intraepithelial neoplasia (CIN(2-3)) in pregnant women. *Gynecol Obstet Invest* 2002; 54: 78-81.
 26. Serati M, Uccella S, Laterza RM, et al. Natural history of cervical intraepithelial neoplasia during pregnancy. *Acta Obstet Gynecol Scand* 2008; 87: 1296-300.
 27. Schorge JO, Rauh-Hain JA. Atypical glandular cells. *Clin Obstet Gynecol* 2013; 56: 35-43.
 28. Zhao C, Florea A, Onisko A, Austin RM. Histologic follow-up results in 662 patients with Pap test findings of atypical glandular cells: results from a large academic womens hospital laboratory employing sensitive screening methods. *Gynecol Oncol* 2009; 114: 383-9.
 29. Trimble CL, Piantadosi S, Gravitt P, et al. Spontaneous regression of high-grade cervical dysplasia: effects of human papillomavirus type and HLA phenotype. *Clin Cancer Res* 2005; 11: 4717-23.
 30. Moscicki AB, Shiboski S, Hills NK, et al. Regression of low-grade squamous intra-epithelial lesions in young women. *Lancet* 2004; 364: 1678-83.

Sarcoma metastasis to the pancreas: experience at a single institution

Miseon Lee¹, Joon Seon Song¹, Seung-Mo Hong¹, Se Jin Jang¹, Jihun Kim¹, Ki Byung Song², Jae Hoon Lee², Kyung-Ja Cho¹

¹Department of Pathology, ²Division of Hepatobiliary and Pancreatic Surgery, Department of Surgery, Asan Medical Center, University of Ulsan College of Medicine, Seoul, Korea

Background: Reports of metastatic sarcoma to the pancreas are limited. We reviewed the clinicopathologic characteristics of such cases. **Methods:** We reviewed 124 cases of metastatic tumors to the pancreas diagnosed at Asan Medical Center between 2000 and 2017. **Results:** Metastatic tumors to the pancreas consisted of 111 carcinomas (89.5%), 12 sarcomas (9.6%), and one melanoma (0.8%). Primary sarcoma sites were bone (n=4); brain, lung, and soft tissue (n=2 for each); and the uterus and pulmonary vein (n=1 for each). Pathologically, the 12 sarcomas comprised 2 World Health Organization grade III solitary fibrous tumors/hemangiopericytomas, and one case each of synovial sarcoma, malignant solitary fibrous tumor, undifferentiated pleomorphic sarcoma, osteosarcoma, mesenchymal chondrosarcoma, intimal sarcoma, myxofibrosarcoma, myxoid liposarcoma, rhabdomyosarcoma, subtype uncertain, and high-grade spindle-cell sarcoma of uncertain type. The median interval between primary cancer diagnosis and pancreatic metastasis was 28.5 months. One case manifested as a solitary pancreatic osteosarcoma metastasis 15 months prior to detection of osteosarcoma in the femur and was initially misdiagnosed as sarcomatoid carcinoma of the pancreas. **Conclusions:** The metastatic sarcoma should remain a differential diagnosis when spindle-cell malignancy is found in the pancreas, even for solitary lesions or in patients without prior history.

Key Words: Pancreas; Metastasis; Sarcoma

Received: January 20, 2020 **Revised:** February 26, 2020 **Accepted:** March 4, 2020

Corresponding Author: Kyung-Ja Cho, MD, PhD, Department of Pathology, Asan Medical Center, University of Ulsan College of Medicine, 88 Olympic-ro 43-gil, Songpa-gu, Seoul 05505, Korea

Tel: +82-2-3010-4545, Fax: +82-2-472-7898, E-mail: kjc@amc.seoul.kr

Most pancreatic tumors are primary, and the majority are adenocarcinomas of ductal origin [1,2]. Although direct invasion of the pancreas by adjacent aggressive tumors is often observed, pancreatic metastasis from distant primary sites is very rare [1,3]. Metastatic pancreatic cancer accounts for less than 2% of all pancreatic malignancies [4,5]. Renal cell carcinoma is the most common primary tumor to metastasize to the pancreas [4,5]. Other common tumors are colorectal cancer, melanoma, breast cancer, lung cancer, and sarcoma [4]. Among these, cases of metastatic sarcoma to the pancreas are limited [4]. Metastatic sarcoma to the pancreas may present a diagnostic and therapeutic challenge due to its rarity and the difficulty in distinguishing between primary and metastatic tumors based on their radiologic features, especially for solitary mass [3,6]. Furthermore, tumors located in the body or tail of the pancreas often present with no symptoms [3,7]. Therapeutic approaches can vary greatly between primary pancreatic cancer and metastatic sarcoma [3,4,8-10]. With continued improvements in treatment and survival for sarcoma patients, the frequency of detection of

metastasis to unusual sites is increasing [11]. However, the index of suspicion for metastatic sarcoma in the pancreas is still very low, and a standard management regimen for metastatic pancreatic sarcoma has not been established. Prolonged survival after surgery for isolated or resectable pancreatic metastatic sarcoma has been reported [10,12-16].

In this paper, we present 12 cases of metastatic sarcoma to the pancreas and report their clinical and histologic features.

MATERIALS AND METHODS

One hundred twenty-four cases of metastasis to the pancreas diagnosed by biopsy (n = 49, 39.5%) or surgical resection (n = 75, 60.5%) at Asan Medical Center between 2000 and 2017 were reviewed. Only distant metastatic tumors to the pancreas were included; adjacent tumors directly extending to the pancreas were excluded. Patient medical records were retrospectively reviewed to evaluate clinical presentation, treatment, and patient status. Hematoxylin and eosin-stained slides of both

primary tumors and pancreatic metastases were reviewed by two pathologists (M.L. and K.J.C.).

Ethics statement

This study was approved by the appropriate institutional review board (2020-0048), and the informed consent was waived.

RESULTS

The primary tumors of 124 patients with pancreatic metastases included 111 carcinomas (89.5%), 12 sarcomas (9.6%), and one melanoma (0.8%). The metastatic carcinomas ($n = 111$) were mainly renal cell carcinomas ($n = 50$, 40.3%), followed by lung cancer ($n = 18$; eight small-cell carcinomas, five adenocarcinomas, three squamous cell carcinomas, and two sarcomatoid carcinomas), colorectal cancer ($n = 12$, all adenocarcinomas), gastric cancer ($n = 12$; six tubular adenocarcinomas, three poorly cohesive carcinomas, two mucinous adenocarcinomas, and one hepatoid adenocarcinoma), ovarian or fallopian tube cancers ($n = 7$; six serous carcinomas and one clear-cell carcinoma), hepatocellular carcinoma ($n = 4$), and other cancers ($n = 8$).

Of the 12 sarcoma patients, nine were female and three were male, with ages ranging from 20–70 years (Table 1). Among the primary lesions, the most common site was bone ($n = 4$); followed by brain, lung, soft tissue ($n = 2$ for each), uterus, and pulmonary vein ($n = 1$ each) (Table 1). Histologically, the sarcomas included two World Health Organization (WHO) grade III solitary fibrous tumors/hemangiopericytomas, and one case each of synovial sarcoma, malignant solitary fibrous tumor, undifferentiated pleomorphic sarcoma, osteosarcoma, mesenchymal chondrosarcoma, intimal sarcoma, myxofibrosarcoma, myxoid liposarcoma, rhabdomyosarcoma, subtype uncertain, and high-grade spindle-cell sarcoma of uncertain type (Table 1). In the case of synovial sarcoma, the presence of an SYT-SSX fusion product was confirmed by reverse transcription polymerase chain reaction.

The primary tumor of case no. 8 arose in the medullary cavity of the metaphysis of the distal femur. The tumor destroyed the cortex and extended into the adjacent soft tissue. Clinically, osteosarcoma was highly suspected, but neoplastic bone formation, which is the essential diagnostic feature of osteosarcoma, was not observed in either primary or metastatic tumor. Thus, we diagnosed it as a high-grade spindle-cell sarcoma of uncertain type.

The median interval between primary sarcoma diagnosis and detection of pancreatic metastasis was 28.5 months. In one exceptional case, a pancreatic metastasis of an osteosarcoma mani-

fested 15 months prior to detection of the osteosarcoma in the femur (Table 1). This patient first presented with abdominal pain, and abdominal computed tomography revealed a 2.5-cm mass-like lesion in the pancreatic tail. Other radiologic work-up, such as imaging of the extremities, was not performed at that time. A 2.7-cm, ovoid, solid mass was identified during distal pancreatectomy (Fig. 1A). Microscopy revealed proliferation of pleomorphic spindle cells, numerous giant cells with infiltrative margins (Fig. 1B), high mitotic activity, and focal osteoid and bone formation (Fig. 1C). Vascular invasion was also identified (Fig. 1D). The tumor was diagnosed as a sarcomatoid carcinoma of the pancreas. The patient was hospitalized with left leg pain 15 months after distal pancreatectomy. Magnetic resonance imaging revealed a 9-cm mass in the left femur with fracture and adjacent soft-tissue extension (Fig. 1E). A biopsy was performed, revealing histologic features similar to those of the pancreatic mass (Fig. 1F). We concluded that the osteosarcoma of the femur had metastasized to the pancreas, and the original diagnosis of sarcomatoid carcinoma of the pancreas was incorrect.

Metastatic tumors were located in the body or tail of the pancreas ($n = 8$), the head of the pancreas ($n = 3$), and throughout the entire pancreas ($n = 1$) (Table 1). Nine cases were single masses, and three cases showed multiple masses. Pancreatic tumor size ranged from 2.5–19 cm (median, 2.7 cm) (Table 1). Primary lesions and pancreatic metastatic lesions (Fig. 2) showed similar histologic features except in one case in which about 30% of the round-cell components were present in the primary myxoid liposarcoma but not in the metastasis.

Primary tumors from 12 patients had undergone surgical resection: two patients with distant metastasis synchronously received neoadjuvant chemotherapy, six received postoperative or preoperative radiation therapy, and four received adjuvant chemotherapy (Table 1). The chemotherapy regimens varied, and several combinations of methotrexate, ifosfamide, doxorubicin, cisplatin, and etoposide were used. In five patients, local recurrence of the primary lesions occurred prior to detection of pancreatic metastasis (Table 1).

After diagnosis of metastatic pancreatic lesions, nine of 12 patients underwent surgical resection with or without preoperative chemotherapy or radiation therapy. Five cases received postoperative radiation therapy or chemotherapy (Table 1). Lymph-node dissection was performed in eight cases, and none of the cases showed metastasis to the lymph nodes. After detection of pancreatic metastasis, eight patients died between 5–48 months, and four patients remained alive from 4–92 months (Table 1).

Table 1. Clinicopathologic characteristics of primary sarcoma and pancreatic metastasis in 12 patients

Case No.	Sex/age at pancreatic metastasis (yr)	Primary tumor			Pathologic diagnosis	Interval between primary tumor detection and pancreatic metastasis (mo)	Pancreatic metastasis			Survival after pancreatic metastasis (mo)				
		Location	Size (cm)	Treatment			Local recurrence	No. of pancreatic metastases	Size (largest, cm)	Treatment	Type of procedure	Associated metastases	Dead	Alive
1	F/62	Lung	7.5	OP	No	40	Body	Single	2.7	NeoCTx +OP	DP	No	-	92
2	M/45	Lung	7	OP	Yes	11	Tail	Single	2.6	OP+RTx and CTx	T	Umbilicus, adrenal gland	24	-
3	F/48	Brain	7.5	OP+RTx	Yes	64	Body, tail	Multiple	3.5	RTx+OP	DP	Bone (femur, tibia), breast, lung	31	-
4	F/70	Brain	NA	OP+RTx	Yes	135	Head	Single	2.6	OP+RTx	PPPD	Bone (humerus), lung,	-	41
5	F/68	Bone (tibia)	6	NeoCTx +OP +CTx	No	88	Head	Single	3.5	RTx+CTx	Biopsy	Bone (pelvis)	-	10
6	F/57	Bone (femur)	9	OP+RTx +CTx	No	15 mo prior	Tail	Single	2.7	OP+CTx	DP	Skin (scalp), bone (rib, ilium, sternum, pelvis), brain	18	-
7	F/32	Bone (skull)	4	OP+RTx	No	65	Tail	Single	19	OP	DP	Lung, mesentery, bone (femur)	48	-
8	F/28	Bone (femur)	11.7	NeoCTx +OP+CTx	No	20	Body	Single	4	OP	DP	Bone (pelvis)	11	-
9	F/35	Pulmonary vein	4.6	RTx+OP	Yes	14	Tail	Single	2.6	CTx	Biopsy	Retropitoneal LN, bone (left humerus), lung	29	-
10	M/52	Soft tissue (knee)	8.2	OP+RTx +CTx	No	26	Head	Single	2.5	OP	PPPD	No	-	4
11	M/35	Soft tissue (thigh)	22	OP	No	0	Tail	Multiple	11	OP+CTx	DP	Bone (humerus)	16	-
12	F/60	Uterus	8.5	OP	Yes (vaginal stump)	8	Head, body, tail	Multiple	NA	CTx	Biopsy	No	5	-

F, female; OP, operation; FNCLCC, Fédération Nationale des Centres de Lutte Contre le Cancer; NeoCTx, neoadjuvant chemotherapy; DP, distal pancreatectomy; M, male; RTx, radiation therapy; CTx, adjuvant chemotherapy; T, tumorctomy; WHO, World Health Organization; NA, not available; PPPD, pylorus-preserving pancreaticoduodenectomy; LN, lymph node.

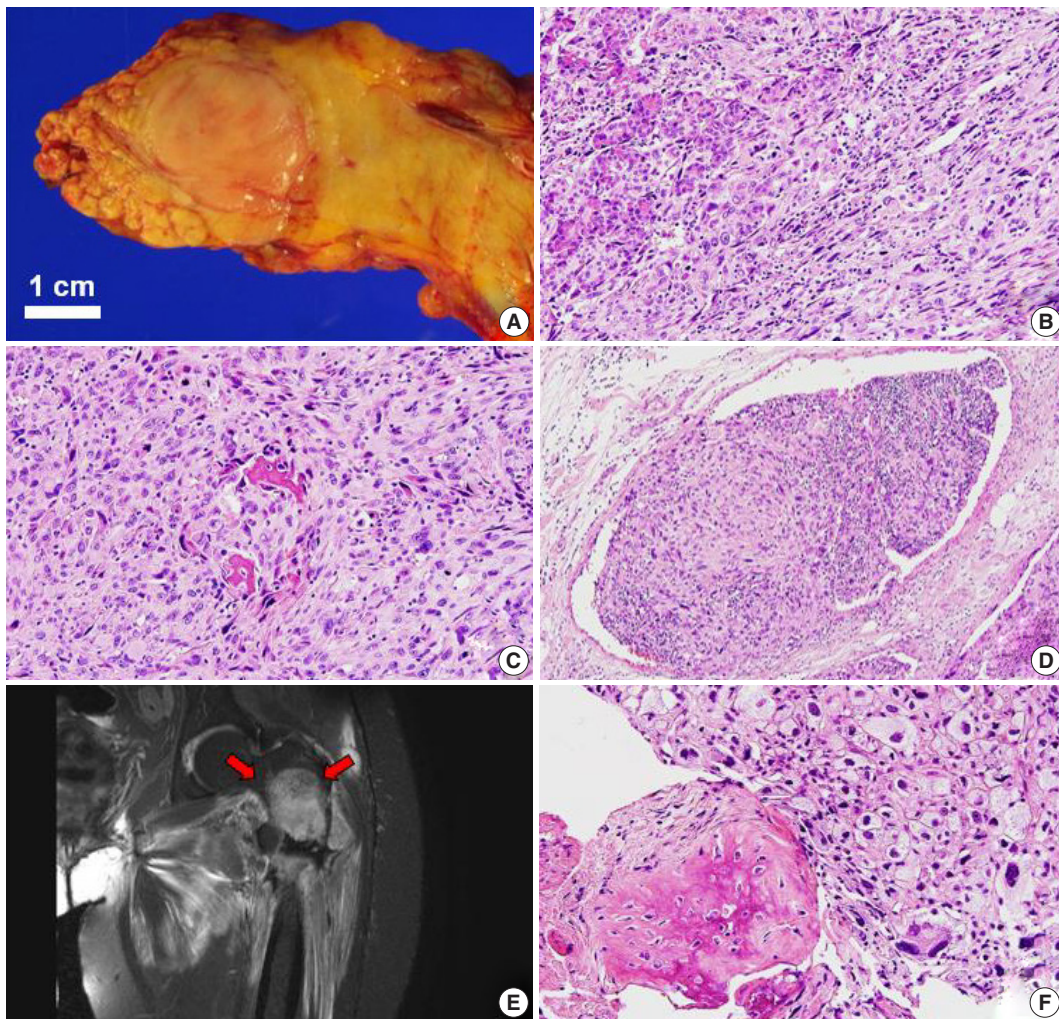


Fig. 1. Primary (A–D) and metastatic (E, F) osteosarcoma. (A) Gross photographs of a distal pancreatectomy specimen bisected along the main pancreatic duct. A well-defined 2.7-cm ovoid solid mass is observed in the tail of the pancreas. Metastatic osteosarcoma to the pancreas shows infiltrative margins (B) and consists of pleomorphic cells and multinucleated giant cells with bone formation and osteoid stroma (C). (D) Vascular invasion is noted. (E) T2-weighted coronal magnetic resonance imaging showing an approximately 9-cm soft tissue mass in the left femur (arrows). (F) The primary lesion of the femur shows similar features to the metastatic pancreatic lesion.

DISCUSSION

Sarcomas preferentially metastasize via the blood rather than the lymphatic system, and lung and bone tissue are the most frequent sites of metastatic sarcoma [17]. Lymph node metastasis is uncommon, but some histologic sarcoma types exhibit high metastasis rates via lymphatic drainage, including rhabdomyosarcoma, angiosarcoma, clear-cell sarcoma, epithelioid sarcoma, and myxoid liposarcoma [18,19]. In our study, the absence of lymph node metastasis in all eight lymph node dissection cases suggests that metastatic sarcoma to the pancreas is more likely to occur via the blood than the lymphatic system. The connective interspaces and cavities such as the peritoneum or pleural

space, in which tumor cells can become entrapped, are also possible routes of metastatic dissemination [18].

Synovial sarcoma metastasizes in approximately 50% of cases, and common metastatic sites are the lung and bone [12]. Unlike other sarcomas, spread to the lymph nodes is not infrequent (3%–23%) [12]. For disseminated disease, chemotherapy based on adriamycin and ifosfamide is usually attempted. Makino et al. [12] suggested that pancreatic metastasis from synovial sarcoma can be successfully treated by surgical resection in cases of solitary pancreatic lesions with no extra-pancreatic metastasis and a more than 3-year interval between diagnosis of the primary tumor and pancreatic metastasis. Only four cases of metastatic synovial sarcoma to the pancreas have been reported in

the literature [5,10,12,20], making our case the fifth. The patient reported here was also treated by surgical resection. Our patient and the two patients described by Makino et al. [12] are

doing well, without recurrence or distant metastasis for 92 months, 40 months, and 30 months after surgical resection, respectively.

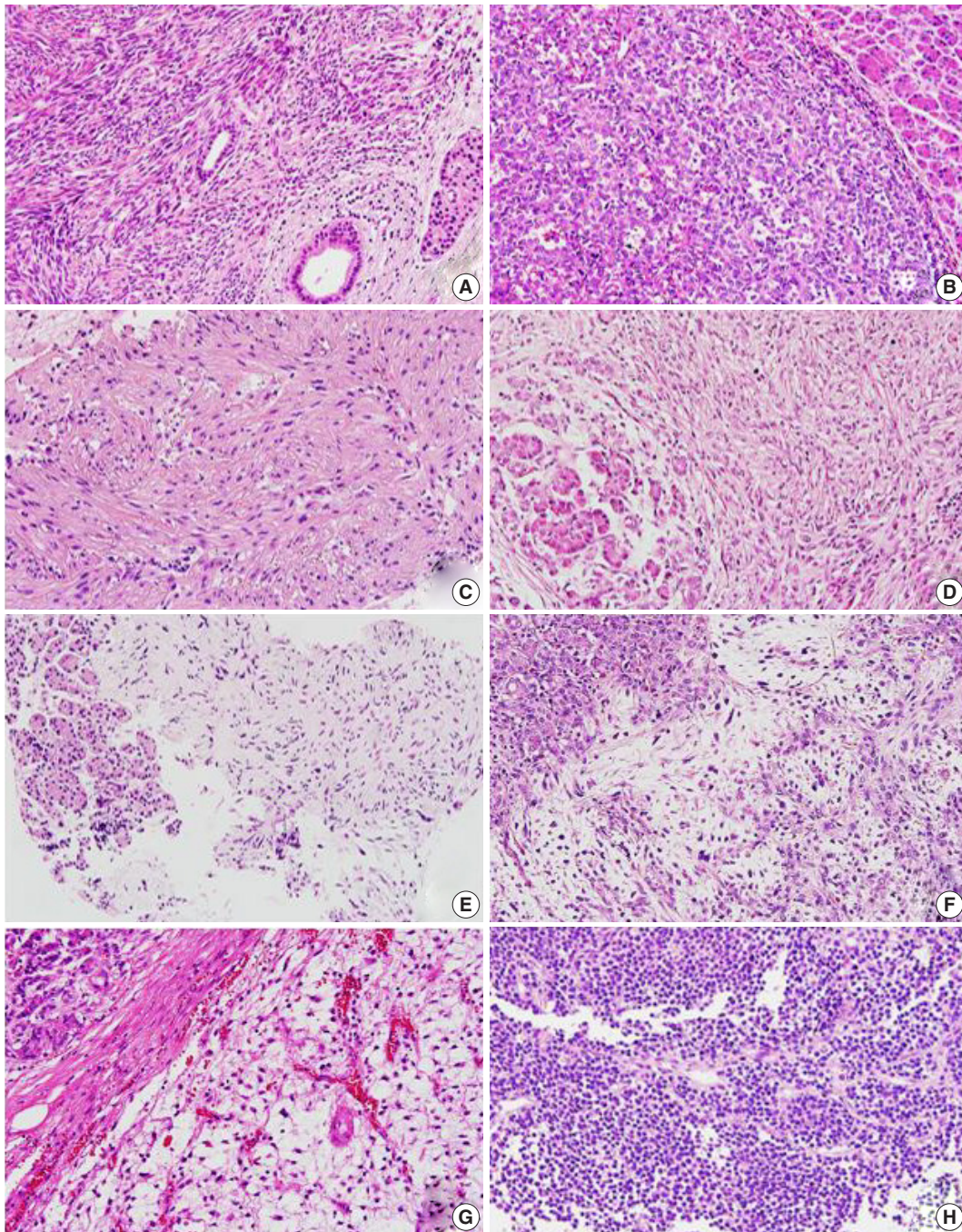


Fig. 2. Metastatic sarcomas to the pancreas. (A) Synovial sarcoma from the lung with cellular fascicles of uniform spindle cells. (B) World Health Organization grade III solitary fibrous tumor/hemangiopericytoma from the brain composed of spindle cells with prominent vascular structure. (C) Undifferentiated pleomorphic sarcoma from the tibia with fascicular arrangement of atypical spindle cells. (D) High-grade spindle-cell sarcoma from the femur. (E) Intimal sarcoma from the pulmonary vein. (F) Myxofibrosarcoma from the knee showing prominent myxoid stroma and elongated, thin-walled blood vessels. (G) Myxoid liposarcoma from the thigh with abundant myxoid stroma, a delicate, arborizing capillary vasculature, and surrounding lipoblasts. (H) Rhabdomyosarcoma, subtype uncertain, from the uterus showing scattered eosinophilic rhabdomyoblasts.

Solitary fibrous tumors/hemangiopericytomas of the central nervous system (CNS) show two distinct histologic phenotypes, a solitary fibrous tumor phenotype and a hemangiopericytoma phenotype [21]. The hemangiopericytoma phenotype has a high recurrence rate (75%–90%) and a high rate of distant metastasis (20%–33%), especially to the liver, lung, and bone [14,21–24]. Both our cases showed the hemangiopericytoma phenotype and were grade III. The metastatic sites of these cases were the lung, bone, breast, and pancreas. A total of 18 cases of metastasis from the brain to the pancreas have been reported to date [14,25]. Interestingly, the interval between diagnosis of the primary tumor and development of pancreas metastasis was long (5.3–24 years, with a median of 10.13 years) [14,25]. After detection of pancreatic metastasis, eight patients died between 2.6–16 years, and seven patients lived for 3.4–25 years.

Outside the CNS, such as in the soft tissue, pleura, and other visceral sites, malignant solitary fibrous tumors showed increased cellularity and mitotic activity (>4 per 10 high-powered fields). Metastatic malignant solitary fibrous tumors to the pancreas have been reported in two cases, one originating in the chest wall [13] and one originating in the kidney [26]. Our case originated in the lung.

Osteosarcoma has a high potential for metastasis [27]. The high incidence of metastasis is related to its strong propensity for early hematogenous spread [15,16,28]. Prolonged survival is possible with treatment including multi-centric chemotherapy and resection of the primary tumor [3,11,15,28]. This result is attributed to the delayed appearance of metastasis and increased metastasis incidence at unusual sites [11]. The common metastasis sites are the lung, bone, pleura, and liver [3,27,29]. Twelve cases of metastatic pancreatic osteosarcoma have been reported [3,6,11,15,16,27–32], making our case the thirteenth. The median interval between primary osteosarcoma diagnosis and development of pancreas metastasis was three years (range, -1.25 to 11 years), including our case, which was the first reported case with a pancreatic metastasis diagnosis prior to primary osteosarcoma diagnosis. Among the eight patients with available follow-up information, four who had undergone surgical resection of the pancreatic metastasis were alive for 7–13 months. Three patients died two weeks, three months, and 18 months after pancreatic metastasis development, respectively [3,28,29,32].

Mesenchymal chondrosarcoma mainly metastasizes to the lungs [33]. Metastasis to the pancreas is extremely rare and has only been reported in six cases, making our case the seventh [1,10,33–36]. The primary site was extra-skeletal soft tissue (thigh, brain, buttock, or femoral vein) in five cases and bone

(skull) in two cases. Among the four patients with available follow-up information, two were alive 6 years and 10 years after surgery for pancreatic metastasis, and two patients died 2 and 4 years after surgery.

Myxoid liposarcoma generally has a favorable prognosis. The round-cell content is a poor prognostic factor in this disease. The most common metastatic site is the abdomen, including the retroperitoneum, abdominal wall, and abdominal cavity, followed by bone [37,38]. Until now, metastasis to the pancreas has not been reported. Our case showed metastasis from the thigh to the bone and the pancreas. Microscopy showed round-cell content of approximately 30% in the primary lesion, but not in the metastatic lesion.

Myxofibrosarcoma was first described in 1977 as a myxoid variant of malignant fibrous histiocytoma and was reclassified as myxofibrosarcoma in 2013 by the WHO [39]. The most common metastatic site is the lung, followed by the pleura, lymph node, bone, and retroperitoneum [40,41]. In this report, a case of myxofibrosarcoma in the knee showed metastasis to the pancreas. Only two cases of pancreatic metastasis of a myxofibrosarcoma have been previously reported, although there are some papers that present cases of metastatic myxofibrosarcoma without describing the specific metastatic sites [40]. Some studies show that adjuvant or neoadjuvant radiation therapy may improve recurrence and metastasis in this indication.

In this study, we present several rare cases of metastatic sarcomas to the pancreas. This is the largest reported case series of pancreatic metastatic sarcomas to date. Metastatic sarcoma comprised 10% of pancreatic metastases, which is high given the overall sarcoma incidence. Furthermore, pancreatic metastasis may manifest as a primary solitary lesion before detection of the primary tumor. Intensive whole-body imaging screening is necessary in sarcoma patients, and metastasis should remain a differential diagnosis in pancreatic tumors with sarcomatoid features. Recently, the efficacy of surgical resection of pancreatic metastases was shown for sarcoma [10,12–16] as well as renal cell carcinoma [4]. Clinicians caring for patients with sarcoma should be aware of the potential for increased survival following surgical resection of the metastasis. This study will contribute to a better understanding of this unusual clinical circumstance and, thus, may lead to improved diagnostic accuracy and treatment.

ORCID

Miseon Lee: <https://orcid.org/0000-0002-6385-7621>

Joon Seon Song: <https://orcid.org/0000-0002-7429-4254>

Seung-Mo Hong: <https://orcid.org/0000-0002-8888-6007>
 Se Jin Jang: <https://orcid.org/0000-0001-8239-4362>
 Jihun Kim: <https://orcid.org/0000-0002-8694-4365>
 Ki Byung Song: <https://orcid.org/0000-0001-5422-5481>
 Jae Hoon Lee: <https://orcid.org/0000-0002-6170-8729>
 Kyung-Ja Cho: <https://orcid.org/0000-0002-4911-7774>

Author Contributions

Conceptualization: KJC.
 Data curation: ML, KJC.
 Formal analysis: ML, KJC.
 Funding acquisition: KJC, SMH.
 Investigation: ML, KJC.
 Methodology: ML, KJC.
 Project administration: ML.
 Resources: JSS, SMH, SJJ, JK, KBS, JHL, KJC.
 Supervision: KJC.
 Validation: ML, KJC.
 Visualization: ML.
 Writing—original draft: ML, KJC.
 Writing—review & editing: ML, KJC.

Conflicts of Interest

J.S.S. and S.J.J., contributing editors of the *Journal of Pathology and Translational Medicine*, were not involved in the editorial evaluation or decision to publish this article. All remaining authors have declared no conflicts of interest.

Funding

No funding to declare.

REFERENCES

1. Chatzipantelis P, Karvouni E, Fragoulidis GP, Voros D, Pafiti A. Clinicopathologic features of two rare cases of mesenchymal metastatic tumors in the pancreas: review of the literature. *Pancreas* 2006; 33: 301-3.
2. Adsay NV, Andea A, Basturk O, Kilinc N, Nassar H, Cheng JD. Secondary tumors of the pancreas: an analysis of a surgical and autopsy database and review of the literature. *Virchows Arch* 2004; 444: 527-35.
3. Bertucci F, Araujo J, Giovannini M. Pancreatic metastasis from osteosarcoma and Ewing sarcoma: literature review. *Scand J Gastroenterol* 2013; 48: 4-8.
4. Sperti C, Moletta L, Patanè G. Metastatic tumors to the pancreas: the role of surgery. *World J Gastrointest Oncol* 2014; 6: 381-92.
5. Krishna SG, Rao BB, Lee JH. Endoscopic sonography and sonographically guided fine-needle aspiration biopsy in the diagnosis of unusual pancreatic metastases from synovial sarcoma. *J Clin Ultrasound* 2014; 42: 180-2.
6. Lasithiotakis K, Petrakis I, Georgiadis G, Paraskakis S, Chalkiadakis G, Chrysos E. Pancreatic resection for metastasis to the pancreas from colon and lung cancer, and osteosarcoma. *JOP* 2010; 11: 593-6.
7. Shinagawa Y, Suzuki T, Hamanaka Y, Nishihara K, Takahasi M. Solitary pancreatic metastasis of malignant fibrous histiocytoma treated by distal pancreatectomy. *Pancreas* 1992; 7: 726-30.
8. Sperti C, Pasquali C, Piccoli A, Pedrazzoli S. Recurrence after resection for ductal adenocarcinoma of the pancreas. *World J Surg* 1997; 21: 195-200.
9. Yeo CJ, Cameron JL, Sohn TA, et al. Six hundred fifty consecutive pancreaticoduodenectomies in the 1990s: pathology, complications, and outcomes. *Ann Surg* 1997; 226: 248-57.
10. Yamamoto H, Watanabe K, Nagata M, et al. Surgical treatment for pancreatic metastasis from soft-tissue sarcoma: report of two cases. *Am J Clin Oncol* 2001; 24: 198-200.
11. Aarvold A, Bann S, Giblin V, Wotherspoon A, Mudan SS. Osteosarcoma metastasising to the duodenum and pancreas. *J Bone Joint Surg Br* 2007; 89: 542-4.
12. Makino Y, Shigekawa M, Kegasawa T, et al. A case report of pancreatic metastasis from synovial sarcoma successfully treated by metastasectomy with adjuvant chemotherapy. *Medicine (Baltimore)* 2016; 95: e4789.
13. Colvin JS, Morris-Stiff G, Cruise M, Purysko A. Pancreatic metastasis from an osseous solitary fibrous tumour. *BMJ Case Rep* 2017; 2017: bcr-2017-220114.
14. Hiraide T, Sakaguchi T, Shibasaki Y, et al. Pancreatic metastases of cerebellar hemangiopericytoma occurring 24 years after initial presentation: report of a case. *Surg Today* 2014; 44: 558-63.
15. Rubin E, Dunham WK, Stanley RJ. Pancreatic metastases in bone sarcomas: CT demonstration. *J Comput Assist Tomogr* 1985; 9: 886-8.
16. Kim SJ, Choi JA, Lee SH, et al. Imaging findings of extrapulmonary metastases of osteosarcoma. *Clin Imaging* 2004; 28: 291-300.
17. Leong SP, Cady B, Jablons DM, et al. Clinical patterns of metastasis. *Cancer Metastasis Rev* 2006; 25: 221-32.
18. Pennacchioli E, Tosti G, Barberis M, et al. Sarcoma spreads primarily through the vascular system: are there biomarkers associated with vascular spread? *Clin Exp Metastasis* 2012; 29: 757-73.
19. Jacobs AJ, Morris CD, Levin AS. Synovial sarcoma is not associated with a higher risk of lymph node metastasis compared with other soft tissue sarcomas. *Clin Orthop Relat Res* 2018; 476: 589-98.
20. Patel S, Martins N, Yantis R, Shepro D, Levey J, Patwardhan R. Endoscopic management of metastatic synovial sarcoma to the pan-

- creas. *Pancreas* 2006; 33: 205-6.
21. Louis DN, Ohgaki H, Wiestler OD, Cavenee WK. WHO classification of tumours of the central nervous system. 4th ed. Lyon: International Agency for Research on Cancer, 2016; 249-54.
 22. Enzinger FM, Smith BH. Hemangiopericytoma: an analysis of 106 cases. *Hum Pathol* 1976; 7: 61-82.
 23. McMaster MJ, Soule EH, Ivins JC. Hemangiopericytoma: a clinicopathologic study and long-term followup of 60 patients. *Cancer* 1975; 36: 2232-44.
 24. Teh BS, Lu HH, Jhala DN, Shahab I, Lynch GR. Pancreatic head mass from metastatic meningeal hemangiopericytoma. *Sarcoma* 2000; 4: 169-72.
 25. Osuga T, Hayashi T, Ishiwatari H, et al. Pancreatic metastasis from a solitary fibrous tumor of the central nervous system. *JOP* 2014; 15: 58-62.
 26. Patel YA, Dhalla S, Olson MT, Lennon AM, Khashab MA, Singh VK. Pancreatic metastasis from a solitary fibrous tumor of the kidney: a rare cause of acute recurrent pancreatitis. *Pancreatology* 2013; 13: 631-3.
 27. Avcu S, Akdeniz H, Arslan H, Toprak N, Unal O. A case of primary vertebral osteosarcoma metastasizing to pancreas. *JOP* 2009; 10: 438-40.
 28. Akpınar B, Obuch J, Fukami N, Pokharel SS. Unusual presentation of a pancreatic cyst resulting from osteosarcoma metastasis. *World J Gastroenterol* 2015; 21: 8452-7.
 29. Jin P, Wang W, Su H, Sheng JQ. Osteosarcoma metastasizing to pancreas confirmed by endoscopic ultrasound-guided fine-needle aspiration. *Endoscopy* 2014; 46 Suppl 1 UCTN: E109-10.
 30. Glass RJ, Eftekhari F, Kleinerman ES, Jaffe N, Nachman J. Osteosarcoma metastatic to the pancreas in young patients. *Clin Radiol* 1996; 51: 293-4.
 31. Khan AS, Crowe DR, Trevino JM, Eloubeidi MA. Multiple metastases to the pancreas from primary maxillary osteosarcoma: diagnosis with EUS-guided FNA. *Gastrointest Endosc* 2011; 73: 1320-2.
 32. Toyama H, Asari S, Goto T, et al. A case of pancreatic metastasis of osteosarcoma resected using laparoscopic spleen preserving distal pancreatectomy. *Gan To Kagaku Ryoho* 2016; 43: 1988-90.
 33. Guo J, Gu Y, Guo L, et al. A case of mesenchymal chondrosarcoma arising from the femoral vein with 8 years of follow-up. *Ann Vasc Surg* 2015; 29: 1455.
 34. Tsukamoto S, Honoki K, Kido A, et al. Chemotherapy improved prognosis of mesenchymal chondrosarcoma with rare metastasis to the pancreas. *Case Rep Oncol Med* 2014; 2014: 249757.
 35. Lightenstein L, Bernstein D. Unusual benign and malignant chondroid tumors of bone. A survey of some mesenchymal cartilage tumors and malignant chondroblastic tumors, including a few multicentric ones, as well as many atypical benign chondroblastomas and chondromyxoid fibromas. *Cancer* 1959; 12: 1142-57.
 36. Komatsu T, Taira S, Matsui O, Takashima T, Note M, Fujita H. A case of ruptured mesenchymal chondrosarcoma of the pancreas. *Radiat Med* 1999; 17: 239-41.
 37. Lin S, Gan Z, Han K, Yao Y, Min D. Metastasis of myxoid liposarcoma to fat-bearing areas: A case report of unusual metastatic sites and a hypothesis. *Oncol Lett* 2015; 10: 2543-6.
 38. Estourgie SH, Nielsen GP, Ott MJ. Metastatic patterns of extremity myxoid liposarcoma and their outcome. *J Surg Oncol* 2002; 80: 89-93.
 39. Fletcher CD, Bridge JA, Hogendoorn P, Mertens F. WHO classification of tumours of soft tissue and bone. 4th ed. Lyon: International Agency For Research on Cancer, 2013; 93-5.
 40. Hambleton C, Noureldine S, Gill F, Moroz K, Kandil E. Myxofibrosarcoma with metastasis to the lungs, pleura, and mediastinum: a case report and review of literature. *Int J Clin Exp Med* 2012; 5: 92-5.
 41. Neagu TP, Sinescu RD, Enache V, Achim SC, Tiglis M, Mirea LE. Metastatic high-grade myxofibrosarcoma: review of a clinical case. *Rom J Morphol Embryol* 2017; 58: 603-9.

A scoring system for the diagnosis of non-alcoholic steatohepatitis from liver biopsy

Kyoungbun Lee^{1,2}, Eun Sun Jung^{1,3}, Eunsil Yu^{1,4}, Yun Kyung Kang^{1,5}, Mee-Yon Cho^{1,6}, Joon Mee Kim^{1,7}, Woo Sung Moon^{1,8}, Jin Sook Jeong^{1,9}, Cheol Keun Park^{1,10}, Jae-Bok Park^{1,11}, Dae Young Kang^{1,12}, Jin Hee Sohn^{1,13}, So-Young Jin^{1,14}

¹Gastrointestinal Pathology Study Group of the Korean Society of Pathologists; ²Department of Pathology, Seoul National University College of Medicine, Seoul; ³Department of Pathology, Seoul St. Mary's Hospital, College of Medicine, The Catholic University of Korea, Seoul; ⁴Department of Pathology, Asan Medical Center, University of Ulsan College of Medicine, Seoul; ⁵Department of Pathology, Inje University Seoul Paik Hospital, Seoul; ⁶Department of Pathology, Yonsei University Wonju College of Medicine, Wonju; ⁷Department of Pathology, Inha University Hospital, Incheon; ⁸Department of Pathology, Jeonbuk National University Medical School, Jeonju; ⁹Departments of Pathology, Dong-A University College of Medicine, Busan; ¹⁰Anatomic Pathology Reference Lab., Seegene Medical Foundation, Seoul; ¹¹Department of Pathology, Daegu Catholic University School of Medicine, Daegu; ¹²Department of Pathology, Chungnam National University Hospital, Chungnam National University School of Medicine, Daejeon; ¹³Department of Pathology, Kangbuk Samsung Hospital, Sungkyunkwan University School of Medicine, Seoul; ¹⁴Department of Pathology, Soon Chun Hyang University Seoul Hospital, Seoul, Korea

Background: Liver biopsy is the essential method to diagnose non-alcoholic steatohepatitis (NASH), but histological features of NASH are too subjective to achieve reproducible diagnoses in early stages of disease. We aimed to identify the key histological features of NASH and devise a scoring model for diagnosis. **Methods:** Thirteen pathologists blindly assessed 12 histological factors and final histological diagnoses ('not-NASH,' 'borderline,' and 'NASH') of 31 liver biopsies that were diagnosed as non-alcoholic fatty liver disease (NAFLD) or NASH before and after consensus. The main histological parameters to diagnose NASH were selected based on histological diagnoses and the diagnostic accuracy and agreement of 12 scoring models were compared for final diagnosis and the NAFLD Activity Score (NAS) system. **Results:** Inter-observer agreement of final diagnosis was fair ($\kappa=0.25$) before consensus and slightly improved after consensus ($\kappa=0.33$). Steatosis at more than 5% was the essential parameter for diagnosis. Major diagnostic factors for diagnosis were fibrosis except 1C grade and presence of ballooned cells. Minor diagnostic factors were lobular inflammation (≥ 2 foci/ $\times 200$ field), microgranuloma, and glycogenated nuclei. All 12 models showed higher inter-observer agreement rates than NAS and post-consensus diagnosis ($\kappa=0.52-0.69$ vs. 0.33). Considering the reproducibility of factors and practicability of the model, summation of the scores of major ($\times 2$) and minor factors may be used for the practical diagnosis of NASH. **Conclusions:** A scoring system for the diagnosis of NAFLD would be helpful as guidelines for pathologists and clinicians by improving the reproducibility of histological diagnosis of NAFLD.

Key Words: Non-alcoholic fatty liver disease; Non-alcoholic steatohepatitis; Biopsy; Consensus

Received: December 27, 2019 **Revised:** March 16, 2020 **Accepted:** March 17, 2020

Corresponding Author: So-Young Jin, MD, Department of Pathology, Soon Chun Hyang University Seoul Hospital, 59 Daesagwan-ro, Yongsan-gu, Seoul 04401, Korea
 Tel: +82-2-709-9424, Fax: +82-2-709-9441, E-mail: jin0924@schmc.ac.kr

Hepatic steatosis has long been regarded as a general morphological change caused by a variety of etiologies, e.g., alcohol, viral hepatitis, drugs or toxins, or metabolic disease. Alcoholic steatohepatitis is a prototype of fatty liver disease but excessive alcohol consumption is regarded as a major challenge to studying the disease. Recently, abnormal hepatic steatosis, irrespective of inducing agents, has been classified as an independent disease that can lead to hepatocellular damage, can progress into chronic liver disease, and increase the incidence of liver

cancer. Non-alcoholic fatty liver disease (NAFLD) is a disease entity characterized by hepatic steatosis without a history of significant alcohol use or other known liver disease. Metabolic syndrome, obesity, hyperlipidemia, nutritional imbalance associated with gastro-intestinal surgery, or parenteral nutrition are risk factors for NAFLD.

NAFLD is part of a hepatic steatosis spectrum that ranges from simple steatosis without clinical abnormality to steatohepatitis with manifestation of clinical symptoms. Clinical assess-

ment, including abnormal liver function tests, radiologic findings, presence of subjective symptoms, other causes of liver disease, or consumption of alcohol or drugs, etc., is critical information for diagnosing NAFLD. A histological assessment with liver biopsy is considered the only means by which to judge simple steatosis and non-alcoholic steatohepatitis (NASH). The degree of steatosis, evidence of hepatocyte injury, and presence of fibrosis, which implies chronic liver injury or the possibility of progression to chronic liver disease, are the major factors that help to discriminate simple steatosis and steatohepatitis. Several grading systems have been published by US and European pathologists since Brunt et al. [1] published the first grading system in 1999 [2-5]. Common morphologic factors include the degree of steatosis, inflammation, ballooning change of hepatocytes indicating cellular damage, and fibrosis reflecting the chronicity of liver disease. These systems play an important role in providing quantitative assessment criteria for NAFLD, but they generally do not provide diagnostic criteria for judging if the disease is so called simple steatosis or NASH [3]. However, clinicians and researchers require pathologists to identify simple steatosis versus NASH for treatment or clinical study.

Classifications for simple steatosis or NASH differ depending on the researcher, and the histomorphological criteria for NAFLD pathological features in liver tissue remains subjective with low reproducibility. Thus, in this study we divided NAFLD into three diagnostic categories: 'not-NASH,' 'borderline,' and 'NASH,' and evaluated diagnostic agreement and proposed a diagnostic scoring system that could increase diagnostic consistency and accuracy.

MATERIALS AND METHODS

Case selection and histological review

Thirteen pathologists reviewed 31 liver biopsies that were clinically and pathologically diagnosed as NAFLD from 10 hospitals (Daegu Catholic University Medical Center, Dong-A University Hospital, Samsung Medical Center, Seoul National University Hospital, Inje University Seoul Paik Hospital, Seoul St. Mary's Hospital, Soon Chun Hyang University Seoul Hospital, Wonju Severance Christian Hospital, Inha University Hospital, Chungnam National University Hospital). The selection criteria were clinically NAFLD (non-alcoholic, serologically negative for viral and autoimmune markers, abnormal levels of liver enzymes such as aspartate aminotransferase and alanine aminotransferase), and aged ≥ 19 years. Cirrhosis cases were excluded. Drug and toxic injuries were excluded. One hematoxylin and eosin and

one Masson's Trichrome-stained slide for each case were prepared anonymously and randomized by a researcher not involved in the study. Pathologists blindly assessed 12 histological parameters and made a final diagnosis of one of three diagnostic categories: 'not-NASH,' 'borderline,' and 'NASH,' in 31 liver biopsies. Twelve histological parameters and detailed scoring criteria were followed as previously reported [6].

Evaluation of diagnostic agreement, selection of histological parameters, and comparison of diagnostic models

The review was blindly conducted twice before and after the consensus meeting. Pre-consensus and post-consensus diagnostic agreements were compared, and selection of diagnostic parameters and modeling were based on the post-consensus results. The gold standard was the diagnosis that accounted for more than half of the participants' agreements after consensus. Final diagnosis agreement rates were assessed by Free-Marginal Multirater Kappa (multirater κ_{free}) [7]. Among the 12 histological parameters, histological parameters that significantly discriminated 'not-NASH,' 'borderline,' and 'NASH' were selected by chi-square test, univariate, and multivariate repeated measures logistic regression analysis. A p-value of $< .05$ was considered statistically significant. All statistical analyses (except kappa analysis) were performed using IBM SPSS statistics ver. 21 (IBM Corp., Armonk, NY, USA). The Kappa value was calculated using an online Kappa Calculator [8]. The cut-off value of the weighted model was determined by the receiver operating characteristic (ROC) curve.

Ethics statement

The Institutional Review Board of Seoul St. Mary's Hospital approved this study with a waiver of informed consent (KIRB-00562_5-001).

RESULTS

Distribution of diagnoses and diagnostic agreement of NAFLD

Diagnostic frequency of all 31 cases before (pre) consensus and after (post) consensus were plotted and shown in Fig. 1. The agreement rate of 'NASH' or 'borderline' in the pre-consensus diagnoses of all 31 cases was 53%–100%, and there was no case in which the major diagnosis was 'not-NASH.' After consensus, five cases were classified as 'not-NASH' (case Nos. 21, 2, 11, 12, and 10) by more than 50% of pathologists and 22 cases were classified as 'borderline' or 'NASH' by more than

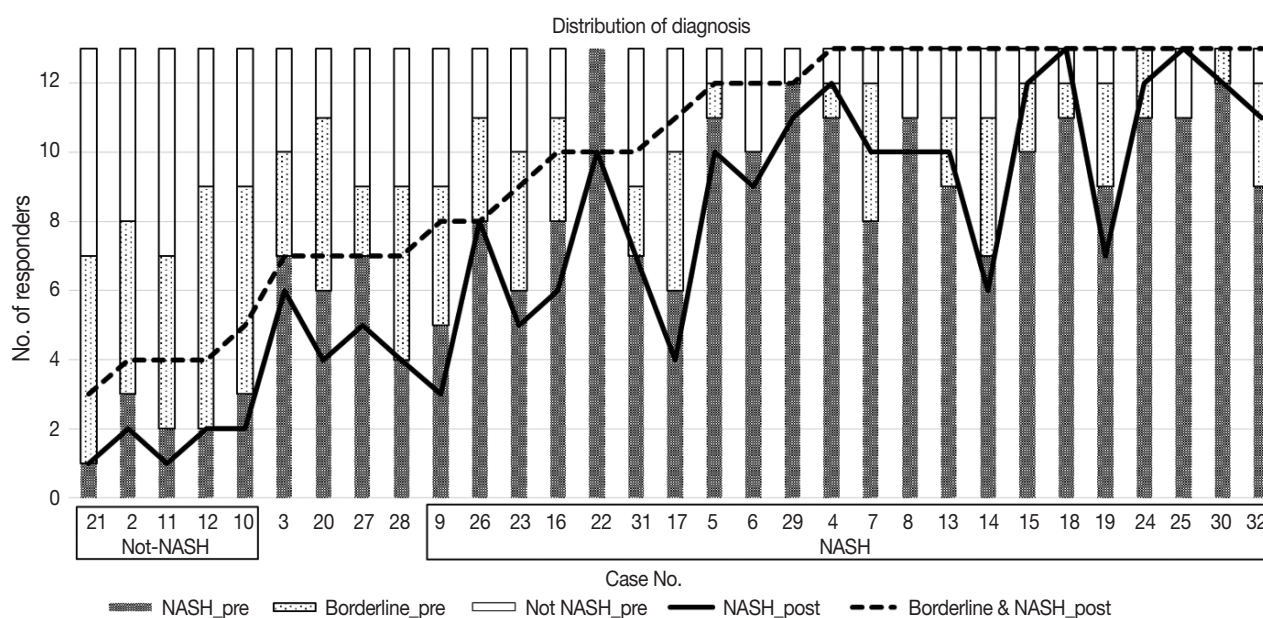


Fig. 1. Distribution of 13 pathologist diagnoses before and after consensus. 'NASH_pre', 'Borderline_pre' and 'Not NASH_pre' are diagnoses before consensus (bar graph), and 'NASH_post' and 'Borderline & NASH_post' are diagnoses after consensus (line graph). The level of 'borderline NASH' decreased in the not-NASH group and increased in the NASH group after consensus. NASH, non-alcoholic steatohepatitis.

50% of pathologists. The remaining four cases (case Nos. 3, 20, 37, and 28) had no dominant diagnosis. Consensus made classification clearer than before consensus. Kappa values for inter-observer agreement for pre-consensus and post-consensus diagnoses are summarized in Table 1. Pre-consensus kappa values were fair grade, and below 0.4 in all categories. Post-consensus kappa values were still fair except in the 'NASH' group (0.41) and were increased in all categories compared to the pre-consensus kappa values. Post-consensus kappa values increased from 0.35 to 0.41 compared to the pre-consensus kappa values in the 'NASH' group ($n = 22$). Agreement rates of NASH after consensus were 60.72%, a slight increase relative to before consensus (overall agreement rate 56.93%). Increase of agreement rates was more pronounced in the 'not-NASH' category, from 33.59% to 49.49%. Histologic pictures of representative cases, 'not-NASH' (case 11), 'borderline' (case 17), and 'NASH' (case 30) after consensus are illustrated in Fig. 2.

Selection of histological parameters for decision modelling

Twelve histological features in 31 cases that were diagnosed by 13 pathologists are summarized in Table 2 by final diagnosis. Significantly different histological parameters among diagnoses (chi-square $p < .05$) were fibrosis, lobular inflammation, microgranuloma, portal inflammation, ballooning change, Mallory body, and glycogenated nuclei. Multivariate logistic regression

Table 1. Inter-observer agreement of diagnosis before and after consensus

	Free-marginal kappa (95% CI)	Overall agreement rates (%)
Pre-consensus		
Total ($n = 31$)	0.25 (0.14 to 0.36)	50.08
NASH ($n = 22$)	0.35 (0.23 to 0.48)	56.93
Not-NASH ($n = 5$)	0.00 (-0.04 to 0.05)	33.59
Post-consensus		
Total ($n = 31$)	0.33 (0.22 to 0.44)	55.38
NASH ($n = 22$)	0.41 (0.27 to 0.55)	60.72
Not-NASH ($n = 5$)	0.24 (0.16 to 0.33)	49.49

CI, confidence interval; NASH, non-alcoholic steatohepatitis.

analysis showed fibrosis (except 1C), ballooning change, and microgranuloma were significant discriminators among the three groups; lobular inflammation, portal inflammation, Mallory body, and glycogenated nuclei were significant discriminators between 'NASH' and 'not-NASH' or 'borderline.' Considering the incidence of parameters, rare parameters, such as portal inflammation and Mallory body, were excluded. Ballooning change and fibrosis (except 1C) were selected as major factors; lobular inflammation, microgranuloma, and glycogenated nuclei were selected as minor factors to construct a diagnostic model.

Decision models and accuracy

Nine models were constructed for quantitative diagnosis and

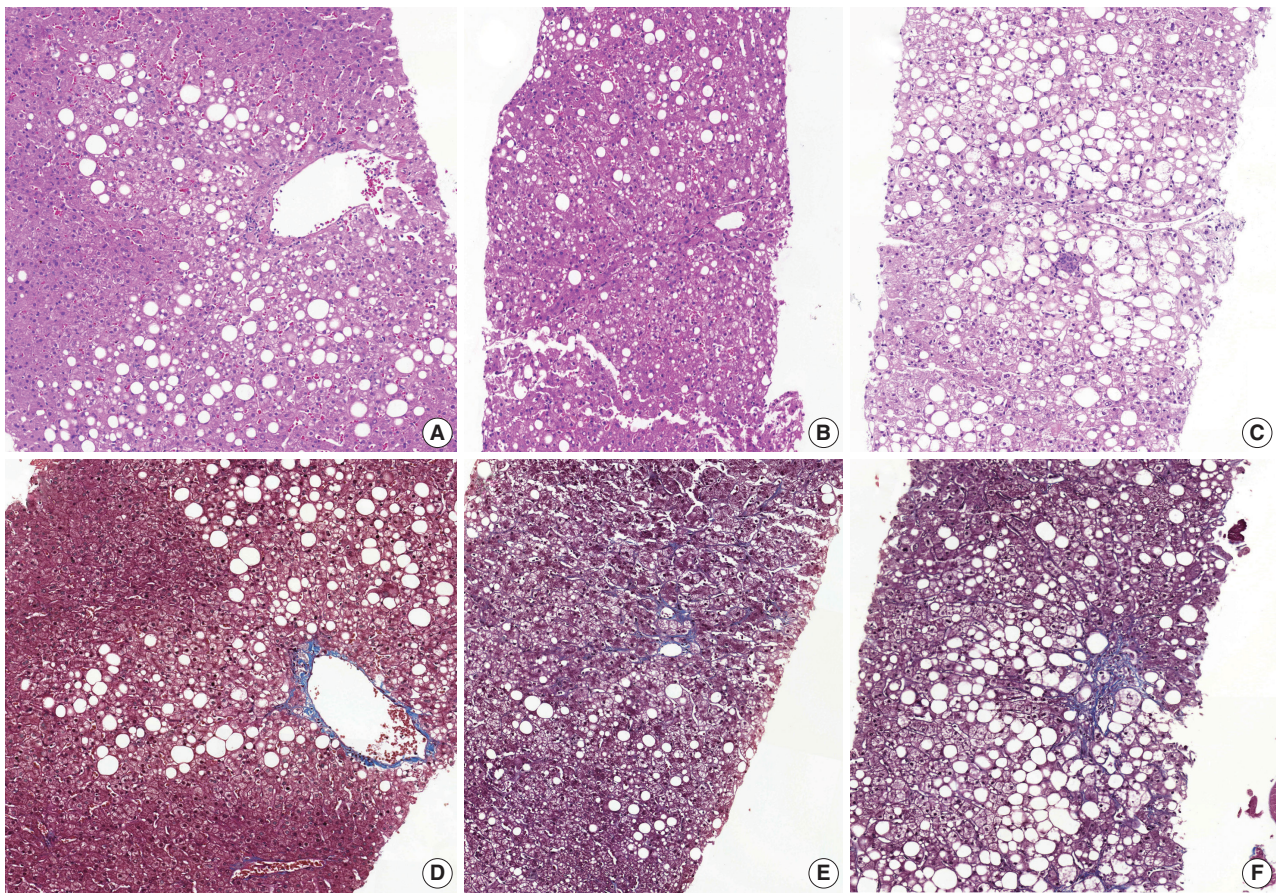


Fig. 2. Representative pictures of 'not-NASH,' 'borderline,' and 'NASH' cases after consensus. (A, D) 'Not-NASH' (case 11) shows steatosis with minimal lobular inflammation, no ballooning and stage 1a fibrosis in Masson-trichrome (MT) staining (B, E). 'Borderline' (case 17) shows steatosis with mild lobular inflammation, rare ballooned cells and stage 1b fibrosis in MT staining. (C, F) 'NASH' (case 20) shows steatosis with moderate lobular inflammation, some ballooned cells and stage 1b fibrosis in MT staining (D-F, MT staining). NASH, non-alcoholic steatohepatitis.

are described in Table 3. Models 1–6 were non-weighted models that depended on the presence of major or minor factors to diagnose, and the severity of factors was not considered (Table 3). Models 7–9 were weighted models which considered the grade of major and minor factors (Table 3). Model 7 used only major factors. Model 8 weighted major factors twice and minor factors were stratified into two groups to reduce the ambiguity of equivocal findings. None to mild grade was scored as 0, and moderate to severe was scored as 1. Model 9 basically adds 9 points to the major factors, which corresponds to the total sum of the minor factors and was the only model that used the degree of steatosis in calculations (Table 3). Table 4 and Fig. 3 summarize the diagnostic accuracy referenced with the post-consensus diagnosis as the gold standard, agreement rates, and area under the curve (AUC) calculated by the ROC curve. Four cases with no consensus diagnosis were excluded. Concordance rates were higher in all scoring models than post-consensus diagnoses ($\kappa = 0.52\text{--}0.69$ vs. 0.33).

Sensitivity, rate of borderline cases, Kappa rates, and overall agreement rates of quantitative models were superior to the NAFLD Activity Score (NAS) system (Table 4). Specificity and false negative rates were similar or higher than the NAS system. Based on the AUC, model 8 showed the best performance (AUC, 0.88) (Fig. 3). Model 9 had lower false-positive and false-negative rates than other models.

Recommendation of decision model

Weighted model 8 and model 9 were the finalists for recommendation. Overall accuracy was better for model 9 than model 8; however, model 9 had higher borderline rates than model 8, and model 8 had a higher AUC curve than model 9. The scoring numbers of model 9 were large, ranging from 0 to 88; therefore, model 8 would be more practical for clinical use. External validation is required to confirm the efficacy of the scoring system for diagnosis.

Table 2. Histological parameters among disease groups

Histological parameter	Frequency of tests				p-value of chi-square test			p-value of logistic regression analysis		
	NASH (n=228)	Borderline (n=78)	Not-NASH (n=97)	p-value	NASH vs. not-NASH	NASH vs. borderline	Borderline vs. not-NASH	NASH vs. not-NASH	NASH vs. borderline	Borderline vs. not-NASH
Steatosis grade										
3: >66%	49	14	24	.094	.038	.272	.487	.374	.444	.059
2: 34%–66%	96	26	25							
1: 5–33%	72	34	40							
0: <5%	11	4	8							
Steatosis location										
1: Zone 1	0	0	0	.096	.027	.078	.287	.155	NA	NA
2: Zone 3	44	17	32							
3: Azonal	111	39	41							
4: Panacinar	73	20	24							
Microvesicular fatty change										
Absent	134	52	63	.354	.297	.218	.812	.024	.353	.755
Present	94	26	34							
Fibrosis										
None	2	13	51	<.001	<.001	<.001	<.001	<.001	<.001	<.001
1A: Mild, zone 3, perisinusoidal	67	36	25							
1B: Moderate, zone 3, perisinusoidal	54	6	1							
1C: Portal/periportal	2	3	5							
2: Perisinusoidal and portal/periportal	64	16	4							
3: Bridging fibrosis	39	4	11							
4: Cirrhosis										
Lobular inflammation										
0: 0/200 ×	0	2	5	<.001	<.001	<.001	0.64	<.001	<.001	.493
1: 1/200 ×	53	53	68							
2: 2–4/200 ×	95	14	12							
3: 5/200 ×	80	9	12							
Microgranuloma										
0: Absent	75	30	54	.001	<.001	.002	.302	<.001	.007	.005
1: Present	153	48	43							
Lipogranuloma										
0: Absent	195	67	78	.467	.025	.936	.339	.133	.943	.407
1: Present	33	11	19							
Portal inflammation										
0: None to minimal	143	64	85	<.001	<.001	.002	.302	<.001	.007	.336
1: Greater than minimal	85	14	12							
Ballooning change										
0: None	14	17	66	<.001	<.001	<.001	<.001	<.001	<.001	<.001
1: Few	17	31	30							
2: Many	157	58	13							
Acidophilic body										
0: None to rare	199	69	91	.220	.082	.785	.209	.410	.723	.380
1: Many	29	9	6							
Mallory body										
0: None to rare	159	74	89	<.001	<.001	<.001	.417	.007	<.001	.271
1: Many	69	4	8							
Glycogenated nuclei										
0: None to rare	100	45	68	<.001	<.001	.035	.088	<.001	.033	.130
1: Many	128	33	29							

NASH, non-alcoholic steatohepatitis; NA, not applicable.

DISCUSSION

NAFLD is a disease spectrum ranging from simple steatosis to steatohepatitis. A major difference between simple steatosis

and steatohepatitis is the presence of cellular injury induced by fat accumulation, which is apparent by the ballooning change of hepatocytes, inflammation, and fibrosis. Many scoring systems have been published by Ludwig since 1980, but the pur-

Table 3. Final histologic criteria for modeling

Criteria	Parameter	Score	Model No.	NASH	Borderline	Not-NASH
Non-weighted method						
Essential requirement	Steatosis >5%, any location		Mo. 1	Major ≥ 1, any minor	No major & minor ≥ 2	No major & minor ≤ 1
Major factors	(1) Any fibrosis except 1C (2) Any ballooning change		Mo. 2	Major ≥ 2, any minor Major ≥ 1 & minor ≥ 2	Major 1 & minor ≤ 1	No major & minor ≤ 1
Minor factors	(1) Lobular inflammation ≥ 2/200 × (2) Many microgranuloma (3) Many glycogenated nuclei		Mo. 3	Major ≥ 2, any minor Major ≥ 1 & minor ≥ 2	Major 1 & minor ≤ 1 No major & minor ≥ 2	No major & minor ≤ 1
			Mo. 4	Major ≥ 2, any minor Major ≥ 1 & minor 3	Major 1 & minor ≤ 2 No major & minor 3	No major & minor ≤ 2
			Mo. 5	Major 2, any minor	Major 1, any minor No major & minor 3	No major & minor ≤ 2
			Mo. 6	Major 2, any minor	Major 1, any minor	No major, any minor
Weighted method 1						
Essential requirement	Steatosis >5%, any location		-	-	-	-
Major factors	(1) Fibrosis except 1C stage	0: None 1: 1A 2: 1B, 2, 3, 4	Mo. 7	= Sum of major score [0–4]		
	(2) Ballooning change	0: None 1: Few 2: Many	Mo. 8	= 2 × Sum of major score + minor [0–11]	1 4-5	0 0-3
Minor factors	(1) Lobular inflammation	0: 0–1/200 × 1: 2 ≥ 2/200 ×	-	-	-	-
	(2) Microgranuloma	0: None to rare 1: Many	-	-	-	-
	(3) Glycogenated nuclei	0: None to rare 1: Many	-	-	-	-
Weighted method 2						
Essential requirement	Steatosis >5%, any location	1: 5%–33% 2: 34%–66% 3: >67%	Mo. 9	= Sum of all scores [0–88]		
Major factors	(1) Fibrosis stage	0: None 9: Stage 1A 10: Stage 1B & 1C 11: Stage 3 12: Stage 4	NAS	= Steatosis + lobular inflammation + ballooning change [0–8]	19–4 3–4	0–3 0–2
	(2) Ballooning change	0: None 9 [1]a: Few 10 [2]a: Many	-	-	-	-
Minor factors	(1) Lobular inflammation	0: 0/200 × 1: <2/200 × 2: 2–4 foci/200 × 3: >4 foci/200 ×	-	-	-	-
	(2) Microgranuloma	0: None to rare 1: Many	-	-	-	-
	(3) Glycogenated nuclei	0: None to rare 1: Many	-	-	-	-

NASH, non-alcoholic steatohepatitis.

^aScore for NAFLD Activity Score (NAS).

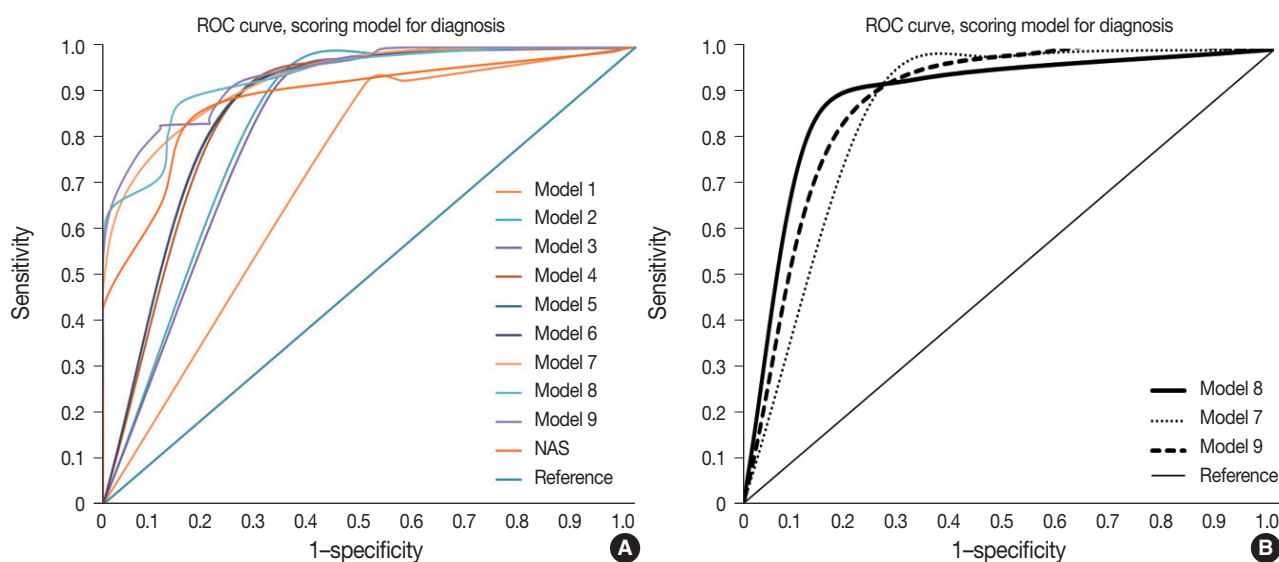


Fig. 3. Receiver operating characteristic (ROC) curve of models. (A) ROC of 10 models. (B) ROC of three weighted models (models 7, 8, and 9).

Table 4. Diagnostic accuracy of diagnostic models

	Sensitivity	Specificity	Borderline rate	False-positive rate	False-negative rate	Free-marginal kappa rate (95% CI)	Overall agreement rate	AUC (ROC)
Model 1	0.92	0.43	0.02	0.11	0.43	0.69 (0.55–0.82)	79.24	0.71
Model 2	0.90	0.43	0.12	0.07	0.31	0.62 (0.46–0.77)	74.48	0.81
Model 3	0.92	0.51	0.11	0.07	0.51	0.59 (0.45–0.74)	72.95	0.81
Model 4	0.93	0.51	0.17	0.06	0.51	0.54 (0.38–0.69)	69.23	0.84
Model 5	0.91	0.51	0.19	0.05	0.51	0.52 (0.37–0.67)	68.20	0.85
Model 6	0.90	0.51	0.01	0.04	0.44	0.52 (0.37–0.66)	67.70	0.85
Model 7	1.00	0.09	0.12	0.06	0.47	0.61 (0.45–0.77)	74.19	0.85
Model 8	0.90	0.68	0.13	0.03	0.57	0.56 (0.40–0.71)	70.55	0.88
Model 9	0.92	0.40	0.21	0.05	0.00	0.60 (0.46–0.74)	73.33	0.86
NAS	0.75	0.49	0.30	0.04	0.41	0.40 (0.28–0.51)	59.84	0.83

CI, confidence interval; AUC (ROC), area under receiver operating characteristic curve; NAS, NAFLD Activity Score.

pose of these systems is to assess the severity of steatohepatitis, not to diagnose [9]. The NAS system is a scoring system using steatosis, ballooning change, and lobular inflammation, but diagnosis should be made before scoring. The reference range for diagnosis is 0–2 for not diagnostic of NASH, 5–8 for diagnostic of NASH, but scores of 3–4 are evenly distributed in not diagnostic, borderline, or positive for NASH groups [2]. Low agreement rates of NASH in histological diagnosis are well known because the evaluation of each diagnostic feature is subjective and has low concordance rates [3,6]. Another limitation of the NAS system as diagnostic criteria is the severity of steatosis that can obscure other grades, such as ballooning change and inflammation.

In the present study, we attempted to construct a scoring system for diagnosis to reduce inter-observer variation based on the 13 pathologists' subjective assessment of 31 liver biopsies.

Concordance rates of subjective assessment were fair before and after consensus, but quantitative scoring increased concordance rates up to a moderate to substantial level in all models ($\kappa = 0.33$ vs. 0.52 – 0.69). Decreased inter-observer variation in a semiquantitative scoring system was reported by the Fatty Liver Inhibition of Progression (FLIP) Pathology Consortium in 2014 [3]. They proposed a NASH diagnostic algorithm and Steatosis, Activity, and Fibrosis score (SAF score) based on the presence of steatosis and grade of ballooning-change and lobular inflammation. Grade 1 or 2 ballooning change, and grade 1 or 2 lobular inflammation were the minimum diagnostic criteria used in the FLIP algorithm [3]. Concordance rates increased from 77% to 97% after using the FLIP algorithm and the kappa value also increased from moderate grade to substantial grade ($\kappa = 0.54$ – 0.66) [3].

The diagnostic components of our study were based on the

key discriminators of post-consensus diagnosis that were selected by multivariate logistic regression analysis and the chi-square test. Ballooning change and lobular inflammation were the same histological factors of other grading systems discriminating NASH from NAFLD. The different component from other grading systems was fibrosis. Generally, many scoring systems for hepatitis and NAFLD use the concepts of grade and stage. Fibrosis is the key feature of liver injury progression and is separately assessed from necroinflammatory activity. Lobular inflammation, portal inflammation, and presence of confluent necrosis are examples of activity. High activity grade means the current status of hepatic injury and stage of fibrosis predict the progression of liver disease. The FLIP algorithm uses ballooning change and lobular inflammation as diagnostic factors but not fibrosis, which is used to assess the severity of NASH [10].

Our study showed that pathologists considered the presence of fibrosis as a major histological feature of NASH. Our study enrolled adult NAFLD cases without other causes of hepatitis, such as virus, alcohol, or autoimmune disease. The pathologists were aware of these conditions beforehand and only assessed the diagnosis of NAFLD according to three categories. As fibrosis with steatosis was presenting as irreversible hepatic injury by steatosis, pathologists easily diagnosed NASH in this situation. Interestingly, grade 1C fibrosis, which is portal fibrosis and is usually observed in pediatric patients, did not affect the diagnosis of 'not-NASH,' 'borderline,' or 'NASH.' As the fibrosis grade increased, the tendency to diagnose NASH increased. The three-tiered scoring system for fibrosis (0, 1A, 1B-4 except 1C) was applied considering practicality, reproducibility of grade 1A, and the smothering effect of a high fibrosis score over other diagnostic factors. Our previous report on the reproducibility of pathologic features of NAFLD mentioned ambiguity between the normal framework of the perivenular area and obvious pericellular collagen deposition [6]. Ballooning change is a mandatory feature of NASH, but inter-observer agreement was not so high (κ -value after consensus = 0.34); therefore, we adopted three levels for fibrosis grade and ballooning change [6] to prevent ambiguous scores affecting NASH diagnosis.

A common feature of our proposed model and the FLIP algorithm is that the amount of fat deposition was dismissed for diagnosis and fat deposition is considered as a minimum requirement of NASH. Grade of steatosis is a major factor in the NAS system [11]. Different features between our proposed model and the FLIP algorithm are (1) presence of the borderline category in the diagnostic group (steatosis vs. NASH in FLIP; 'not-NASH,' 'borderline,' and 'NASH' in our model), (2) cutoff level

of ballooning and lobular inflammation for definite NASH, and (3) adaption of fibrosis as a diagnostic component. In the FLIP criteria, grade 1 ballooning and grade 1 lobular inflammation is the minimum requirement for NASH, but this category might be included as borderline by our model because the cut off value for lobular inflammation in our model was higher than that of the FLIP algorithm/SAF score (2–4 foci/200 × field vs. <2 foci per lobule) [3]. Borderline cases defined by our model might be defined as NASH by the FLIP algorithm. A relatively low NASH criteria by FLIP was reported in a comparative validation study of the NAS and SAF score [12]. Rastogi et al. [12] reported concordance of not-NASH and NASH by the NAS system and SAF algorithm, but 79.4%–94.4% of borderline-NASH diagnosed by NAS were diagnosed as NASH by the SAF algorithm.

Fibrosis is a major predictor for the progression of NAFLD; however, the NAS and FLIP algorithm/SAF score exclude fibrosis in the decision scheme. Exclusion of fibrosis in the score risks missing the fibrotic inactive NAFLD cases. Rastogi and colleagues reported that 76.39% diagnosed by NASH and 78.63% diagnosed by the FLIP algorithm/SAF score, who were not-NASH, showed the presence of fibrosis [12]. Only the fibrosis stage, but no other histological feature, was found to be independently associated with long-term overall mortality, liver transplantation, and liver-related events in a retrospective study of 619 NAFLD patients [13]. Inclusion of fibrosis as a diagnostic criterion may risk narrowing the range of definite NASH; however, considering the low progression rates of simple steatosis without fibrosis and low inter-observer reproducibility of perivenular fibrosis and ballooning change, a borderline category with equivocal features can be a buffering group between not-NASH and definite NASH.

The limitations of our study are that the performance of the model was not verified in external datasets and clinicopathologic analysis was not performed due to the small size of the cohort. Further study including external validation of the model and risk prediction for disease progression of each diagnostic group could provide valuable information.

In summary, a semi-quantitative scoring system increased the diagnostic reproducibility of NASH, and subjective assessment and summation of two major factors ($\times 2$; ballooning and fibrosis, range 0–2) and minor factors (lobular inflammation, glycogenated nuclei, and microgranuloma, range 0–1) are proposed as a practical NASH diagnostic criteria (diagnostic range: 0–3, 'not-NASH'; 4–5, 'borderline'; 6–11, 'NASH').

ORCID

Eun Sun Jung: <https://orcid.org/0000-0002-8451-939X>
 Kyoungbun Lee: <https://orcid.org/0000-0001-8427-3003>
 Eunsil Yu: <https://orcid.org/0000-0001-5474-9744>
 Yun Kyung Kang: <https://orcid.org/0000-0002-2075-4665>
 Mee-Yon Cho: <https://orcid.org/0000-0002-7955-4211>
 Joon Mee Kim: <https://orcid.org/0000-0003-1355-4187>
 Woo Sung Moon: <https://orcid.org/0000-0001-7951-9865>
 Jin Sook Jeong: <https://orcid.org/0000-0001-6474-9772>
 Cheol Keun Park: <https://orcid.org/0000-0001-7689-0386>
 Jae-Bok Park: <https://orcid.org/0000-0002-1841-2316>
 Dae Young Kang: <https://orcid.org/0000-0002-4311-4118>
 Jin Hee Sohn: <https://orcid.org/0000-0002-4735-3853>
 So-Young Jin: <https://orcid.org/0000-0002-9900-8322>

Author Contributions

Conceptualization: SYJ.
 Data curation: ESJ.
 Formal analysis: KL, ESJ.
 Funding acquisition: ESJ, SYJ.
 Investigation: KL, ESJ.
 Methodology: KL, ESJ, EY, SYJ.
 Project administration: SYJ.
 Resources: KL, ESJ, EY, YKK, MYC, JMK, WSM, JSJ, CKP, JBP, DYK, JHS, SYJ.
 Software: KL.
 Supervision: SYJ.
 Validation: KL, SYJ.
 Visualization: KL.
 Writing—original draft: KL.
 Writing—review & editing: KL, SYJ.

Conflicts of Interest

W.S.M. and J.S.J., contributing editors of the *Journal of Pathology and Translational Medicine*, were not involved in the editorial evaluation or decision to publish this article. All remaining authors have declared no conflicts of interest.

Funding

This study was supported by the Academic Research Fund from the Korean Society of Pathologists.

Acknowledgments

We are grateful to all members of the Gastrointestinal Pathology Study Group of the Korean Society of Pathologists, particularly Eunsil Yu for scanning the virtual slides.

REFERENCES

1. Brunt EM, Janney CG, Di Bisceglie AM, Neuschwander-Tetri BA, Bacon BR. Nonalcoholic steatohepatitis: a proposal for grading and staging the histological lesions. *Am J Gastroenterol* 1999; 94: 2467-74.
2. Kleiner DE, Brunt EM, Van Natta M, et al. Design and validation of a histological scoring system for nonalcoholic fatty liver disease. *Hepatology* 2005; 41: 1313-21.
3. Bedossa P, Consortium FP. Utility and appropriateness of the fatty liver inhibition of progression (FLIP) algorithm and steatosis, activity, and fibrosis (SAF) score in the evaluation of biopsies of nonalcoholic fatty liver disease. *Hepatology* 2014; 60: 565-75.
4. Bedossa P, Poitou C, Veyrie N, et al. Histopathological algorithm and scoring system for evaluation of liver lesions in morbidly obese patients. *Hepatology* 2012; 56: 1751-9.
5. Alkhoury N, De Vito R, Alisi A, et al. Development and validation of a new histological score for pediatric non-alcoholic fatty liver disease. *J Hepatol* 2012; 57: 1312-8.
6. Jung ES, Lee K, Yu E, et al. Interobserver agreement on pathologic features of liver biopsy tissue in patients with nonalcoholic fatty liver disease. *J Pathol Transl Med* 2016; 50: 190-6.
7. Randolph JJ. Free-marginal multirater kappa (multirater kfree): an alternative to Fleiss fixed-marginal multirater kappa. In: Joensuu Learning and Learning Symposium; 2005 Oct 14-15; Joensuu, Finland.
8. Randolph JJ. Online kappa calculator [Internet]. Justus Randolph, 2008 [cited 2019 Dec 10]. Available from: <http://justus.randolph.name/kappa>.
9. Ludwig J, Viggiano TR, McGill DB, Oh BJ. Nonalcoholic steatohepatitis: Mayo Clinic experiences with a hitherto unnamed disease. *Mayo Clin Proc* 1980; 55: 434-8.
10. Pournik O, Alavian SM, Ghalichi L, et al. Inter-observer and intra-observer agreement in pathological evaluation of non-alcoholic fatty liver disease suspected liver biopsies. *Hepat Mon* 2014; 14: e15167.
11. Hjelkrem M, Stauch C, Shaw J, Harrison SA. Validation of the non-alcoholic fatty liver disease activity score. *Aliment Pharmacol Ther* 2011; 34: 214-8.
12. Rastogi A, Shasthry SM, Agarwal A, et al. Non-alcoholic fatty liver disease: histological scoring systems: a large cohort single-center, evaluation study. *APMIS* 2017; 125: 962-73.
13. Angulo P, Kleiner DE, Dam-Larsen S, et al. Liver fibrosis, but no other histologic features, is associated with long-term outcomes of patients with nonalcoholic fatty liver disease. *Gastroenterology* 2015; 149: 389-97.

Gene variant profiles and tumor metabolic activity as measured by *FOXM1* expression and glucose uptake in lung adenocarcinoma

Ashley Goodman¹, Waqas Mahmud², Lela Buckingham^{1,2}

¹Rush University College of Health Sciences, Chicago, IL;

²Department of Pathology, Rush University Medical Center, Chicago, IL, USA

Background: Cancer cells displaying aberrant metabolism switch energy production from oxidative phosphorylation to glycolysis. Measure of glucose standardized uptake value (SUV) by positron emission tomography (PET), used for staging of adenocarcinoma in high-risk patients, can reflect cellular use of the glycolysis pathway. The transcription factor, FoxM1 plays a role in regulation of glycolytic genes. Cancer cell transformation is driven by mutations in tumor suppressor genes such as *TP53* and *STK11* and oncogenes such as *KRAS* and *EGFR*. In this study, SUV and *FOXM1* gene expression were compared in the background of selected cancer gene mutations.

Methods: Archival tumor tissue from cases of lung adenocarcinoma were analyzed. SUV was collected from patient records. *FOXM1* gene expression was assessed by quantitative reverse transcriptase polymerase chain reaction (qRT-PCR). Gene mutations were detected by allele-specific PCR and gene sequencing. **Results:** SUV and *FOXM1* gene expression patterns differed in the presence of single and co-existing gene mutations. Gene mutations affected SUV and *FOXM1* differently. *EGFR* mutations were found in tumors with lower *FOXM1* expression but did not affect SUV. Tumors with *TP53* mutations had increased SUV ($p = .029$). *FOXM1* expression was significantly higher in tumors with *STK11* mutations alone ($p < .001$) and in combination with *KRAS* or *TP53* mutations ($p < .001$ and $p = .002$, respectively). **Conclusions:** Cancer gene mutations may affect tumor metabolic activity. These observations support consideration of tumor cell metabolic state in the presence of gene mutations for optimal prognosis and treatment strategy.

Key Words: Lung neoplasms; Forkhead Box protein M1; KRAS protein, human; Treatment outcome

Received: October 9, 2019 **Revised:** January 24, 2020 **Accepted:** February 8, 2020

Corresponding Author: Lela Buckingham, PhD, Department of Pathology, Rush University Medical Center, Chicago, IL 60612, USA
 Tel: +1-312-942-2814, Fax: +1-312-942-7781, E-mail: LelaBAmell@gmail.com

Lung cancer is the leading cause of cancer death in the United States, with the majority of cases falling into the adenocarcinoma (non-small cell lung cancer [NSCLC]) subgroup. There are a large number of somatic mutations that can lead to biological differences among histologically identical tumors in NSCLC patients. This variability partially accounts for the heterogeneity in disease progression and patient outcome seen among the different cases of NSCLC.

Population studies and clinical trials have led to identification of frequently mutated genes and gene products that serve as therapeutic targets [1,2]. Tumor protein P53, *TP53* is the most frequently mutated gene in cancer, encoding a transcription factor that regulates cell cycle arrest and apoptosis. The Kirsten Rat Sarcoma Viral proto-oncogene, *KRAS*, also frequently mutated in cancer cells, is a membrane-associated protein with intrinsic GTPase activity involved in the regulation of cell proliferation. The

epidermal growth factor receptor gene, epidermal growth factor receptor (*EGFR*), encodes a tyrosine kinase membrane receptor identified as a therapeutic target in clinical trials investigating tyrosine kinase inhibitors for treatment of lung cancer. *STK11* encodes a tumor suppressor serine/threonine-protein kinase that controls the activity of AMP-activated protein kinases (AMPK), affecting cell metabolism, cell polarity, apoptosis, and DNA damage response. Current clinical testing includes investigation of these genes along with many others for characterization of tumor mutational status as well as therapeutic strategy. Depending on the testing approach, somatic mutations in one or more cancer genes are frequently detected.

Tumor biochemistry has been proposed as one source of tumor heterogeneity [3]. Aberrant energy metabolism has been well documented, with observations that cancer cells can switch their source of energy production from oxidative phosphorylation to

glycolysis [4,5]. Glucose metabolism in malignant and benign cells is measured using cellular uptake of 18-fluorodeoxyglucose (FDG). FDG is glucose combined with a radionuclide. Malignant cells, growing and metabolizing glucose faster than benign cells, use more of the tracer. Measure of FDG uptake in tumors is expressed in a semiquantitative measure, the standardized uptake value (SUV) which is the ratio of tissue radioactivity concentration (C/T) imaged by positron emission tomography (PET) at a point in time to the injected dose of radioactivity per kilogram of the patient's body weight: $(C/T)/(\text{injection dose [MBq]}/\text{patient's weight [kg]})$.

SUV has been proposed as a factor in determining adjuvant chemotherapy for stage 1A NSCLC [6]. A combination of cytology, computed tomography and PET measurement of SUV has been reported to detect 90% of malignancy in lung pleural effusions [7].

Along with massive glucose utilization, there is also a significant increase in lactate production in tumor cells [8]. The conversion into lactate is performed by the enzyme lactate dehydrogenase (LDHA), which has been shown to have increased activity in breast, gynecological, colorectal and lung cancer. LDHA is partially regulated by the Forkhead Box M1 (*FOX M1*) transcription factor. FoxM1 protein bound to the LDHA promoter increases its expression at the mRNA and protein level. In vivo studies showed silencing FoxM1 expression caused a decrease in LDHA expression with a corresponding decrease in lactate production and glucose utilization [9]. Thus, FoxM1 plays a role in cancer cell metabolism, at least through the transcriptional regulation of LDHA. The study also showed that elevated FoxM1 expression correlated with increased cell growth and metastasis. Increased cell proliferation associated with higher *FOX M1* expression can lead to poorer prognosis [10].

FOX M1 expression is genetically and epigenetically controlled. *FOX M1* transcription is one of several targets of the microRNA, miR-149 [11]. An inverse relationship between miR-149 and *FOX M1* has been reported in colon cancer [12]. FoxM1 protein function is regulated through cell signaling. For FoxM1 protein to become active, it must be phosphorylated at particular sites, a modification mainly achieved through the Ras-Raf-Mek signaling cascade [13]. Thus, FoxM1 could be a downstream target of the Ras oncogenic signaling cascade and Ras is required for FoxM1 activation through phosphorylation. Conversely, FoxM1 may also be necessary for Kras-mediated changes in expression of several different target genes involved in homeostasis, metabolism and tumor growth [14]. Using a mouse model of NSCLC, it was found that the presence of an activating mutation in *KRAS*,

Kras^{G12D}, with simultaneous deletion of *FOX M1*, was sufficient to initiate uncontrolled respiratory epithelial cell proliferation or hyperplasia, but this single stimulus was not enough to progress the hyperplasia into full lung cancer [15]. Therefore, FoxM1 is not necessary for increased cell proliferation of respiratory epithelial cells, but is required for true tumorigenesis. This dependent relationship between Kras and FoxM1 suggests a role for the two genes in increased tumorigenicity and thus affect the overall clinical outcome.

This study assessed the relationship between tumor mutational status and tumor glucose metabolism as measured by standardized glucose uptake volume (SUV) and *FOX M1* gene expression. The results support the consideration of tumor metabolic state in the interpretation of mutation status in NSCLC.

MATERIALS AND METHODS

Patient samples

Analysis of archival tissue in the current study was approved by the Rush University Institutional Review Board (IRB#1212 1202). Participants were deidentified before group statistical analyses. Patient samples consisted of formalin-fixed paraffin-embedded tissue from 301 patients with adenocarcinoma NSCLC (stage I–III) treated at Rush Medical Center through surgical resection and no adjuvant therapy. The study includes cases of adenocarcinoma only.

PET analysis

Tumor metabolic activity was assessed by measure of glucose metabolism (rate of consumption of glucose) through accumulation of FDG. Benign and malignant tumors differ in FDG SUV measured by PET. PET data, measured from tumor tissue prior to surgery, was collected from electronic medical records. When the tumors are imaged by PET, a minimum (PET Min) and maximum (PET Max) density of FDG is reported for the tissue regions scanned. A high (PET Max) and low (PET Min) density was recorded for 301 patients (Table 1). PET Max is considered the maximum SUV of the tissue.

Gene expression analysis

The amount of mRNA expression of the *FOX M1* gene was measured in tumor and non-malignant lung tissue in all patient samples with available corresponding sample material. Hematoxylin and eosin-stained 4-micron sections were reviewed by a pathologist to distinguish tumor and non-malignant tissue for each sample. Tissue was then macro-dissected from the adjacent

Table 1. Patient demographics tumor genetic profile (n=301)

	SUV			Gene expression ^a <i>FOXM1</i> /miR-149	Mutation status, n (%) ^b			
	No.	PET Min	PET Max		<i>EGFR</i>	<i>KRAS</i>	<i>STK11</i>	<i>TP53</i>
Total	301	2.47 ± 1.44	8.85 ± 6.69	3.11 ± 4.69/3.92 ± 9.84	32/267 (12)	105/296 (35)	17/173 (10)	73/173 (42)
Sex								
Female	168	2.33	8.79	1.83/5.94	22/152	61/167	7/99	40/99
Male	133	2.65	8.93	4.38/1.39	9/115	42/123	10/73	32/73
p-value		.077	.867	.055	.661	.675	.150	.652
Age (yr)								
<60	70	2.48	8.99	0.76/3.30	9/53	17/69	4/42	20/42
>60	231	2.47	8.82	17.3/2.25	22/212	85/227	13/126	51/128
p-value		.973	.857	.002	.181	.050	.882	.462
Smoking ^c								
Ever	56	2.16	10.3	-/0.00	2/40	24/53	8/53	34/53
Non-smoker	17	1.87	8.62	-/2.84	3/10	3/17	0/17	5/17
p-value		.527	.529	-	.018	.042	.089	.012

SUV, standardized uptake value; PET, positron emission tomography.

^aExpression normalized to B2M; left-tailed probability of the chi-square distribution; ^bMutated/total resulted; left-tailed probability of the chi-square distribution;

^cSmoking status was not available for all cases.

unstained slide and the RNA extracted using the RecoverAll Total Nucleic Acid Isolation Kit (Ambion/Life Technologies, Austin, TX, USA) according to manufacturer's directions.

Ten microliters of the extracted RNA were converted to cDNA in a reaction mix (Thermo Fisher Scientific, Waltham, MA, USA) containing 5 µL 5× reaction buffer, 2 µL 0.1M DTT, 1 µL each of RNasin (40 units/µL) dNTPs (2.5 mM each) and Moloney virus reverse transcriptase (200 units/µL), yielding 20 µL total volume. Gene expression levels were then measured from the cDNA using TaqMan qRT-PCR. Two microliters of cDNA were mixed with 1.25 µL primer/probe mix (Integrated DNA Technologies, Coralville, IA, USA), 12.5 µL Universal Master Mix with passive reference dye (Roche Diagnostics/Sigma, Mannheim, Germany) brought to a final volume of 25 µL with nuclease-free water. The primers used for *FOXM1* were F: 5'-GATGGC-GAATTGTATCATGGC, R: 5'-GGAGGAAAAGGAGA-ATTGTCAC and probe: 5'-/56-FAM/CAGCGACAG/ZEN/GTTAAGGTTGAGGAGC/3IABkFQ and those used for miR-149 were F: 5'-CGTTGTTCCAGCTGCCCCAGC, R: 5'-GCTCCCAGGCCGCGCC and probe: 5'-/56-FAM/AGACA/ZEN/CGGAGCCAGA/3IABkFQ. In addition to well to well correction through the passive reference dye, the mRNA levels of the housekeeping gene, beta-2 microglobulin (B2M; Integrated DNA Technologies), were concurrently measured in duplicate samples as a cDNA input normalization control. For statistical analysis, target gene expression was normalized to the amount of B2M expression, to compensate for variability in the amount of tissue used and the input cDNA of each sample.

Mutation status

KRAS mutation status was measured from column purified, diluted tissue DNA using the Therascreen PCR method (Qiagen, Hilden, Germany) according to manufacturer's directions. Further variant information was collected from a clinical next-generation sequencing panel of 500 genes (Foundation Medicine, Cambridge, MA, USA).

Statistics

Statistical analysis was performed using SPSS software ver. 18.0 (SPSS Inc., Chicago, IL, USA). Association between gene expression and tumor mutation status was analyzed using the independent T-test. Nonparametric data were analyzed by the Mann-Whitney U test. Association of dichotomized gene expression and mutation status with patient outcome (time to recurrence [TTR] and overall survival [OS]) was analyzed for significance using Kaplan-Meier survival curves.

Ethics statement

All procedures performed in the current study were approved by the Rush University Institutional Review Board (IRB#1212 1202, approved date 3/22/18) with a waiver of individual consent in accordance with the Common Rule (45CFR46, December 13, 2001) and any other governing regulations or subparts. The Institutional Federalwide Assurance Number is FWA000 00482 in accordance with the 1964 Helsinki declaration and its later amendments.

RESULTS

Patient demographics and PET activity

FDG uptake reflects active glucose metabolism in tumor cells but is not constant across tumor tissue. PET Min and PET Max define the low and high metabolic activity of cells, respectively, for each tumor. PET Max is a measure of the maximum metabolic activity of the tumor. Nucleic acid was successfully extracted from 301 archival tissue samples for analysis (Table 1). Tested patients had an average age of 66.8 years (range, 40 to 92 years), were 44% male, and 77% ever smokers. Tumor PET activity was similar in demographic groups, except for marginally increased PET Min in tumors from male patients. It is noted that younger and older patients are not evenly represented in the patient group: 77% of patients were older than 60 years. PET Max (maximum SUV) was not significantly different by sex.

Mutation status

Mutation status was assessed by allele-specific PCR, Sanger sequencing and/or next-generation sequencing of tumor tissue (Table 1). *EGFR* mutations were present in 12% of cases. Fourteen percent of female patient tumors had *EGFR* mutations compared to 8% of male patient tumors. Exon 19 deletions ($n = 15$) and L858R point mutations ($n = 5$) accounted for the majority of *EGFR* variants in this patient group.

KRAS mutations present in 35% of cases were equally represented by sex (36% vs. 34% in females and males, respectively). Of the 105 *KRAS* mutations, the most common variants were G12C ($n = 42$) and G12D ($n = 22$), and G12V ($n = 20$). *TP53* is the most mutated gene in cancer and was the most frequently mutated gene in this patient group. *TP53* mutation frequency was 42%, about equally represented in male (40%) and female (44%) patients. The spectrum of *TP53* mutations fell mostly

within the DNA binding domain of the protein.

Chi-square analysis revealed significantly increased mutation frequency in smokers compared to non-smokers for *KRAS* ($p = .042$) and *TP53* ($p = .012$). The reverse was true for *EGFR*, where 30% of non-smokers had *EGFR* mutated tumors, compared to 5% of those in smokers ($p = .018$). Older patients had increased *KRAS* mutations ($p = .042$).

Metabolic activity as measured by SUV vs. gene mutation status

Maximal SUV was assessed in tumor tissue. There was no significant difference in SUV with *KRAS* nor *EGFR* mutation compared to no mutation ($p = .443$) nor with any *TP53* nor *STK11* mutations ($p = .114$ and $p = .191$, respectively) (Fig. 1). Mutation status for all genes were grouped as “mutated” vs. “not mutated.” Similar grouping was done for *STK11* due to the low number of *STK11* mutant cases.

Median SUV did not differ significantly among the most fre-

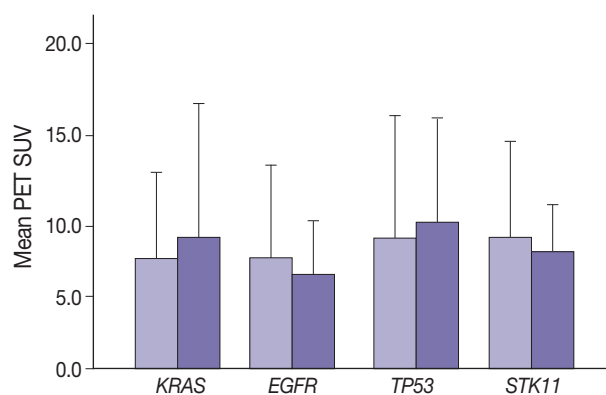


Fig. 1. Maximum positron emission tomography (PET) standardized uptake value (SUV) in the presence of mutations (darker bars) in *KRAS* ($p = .089$) (A), *EGFR* ($p = .443$) (B), *TP53* ($p = .114$) (C), and *STK11* ($p = .191$) (D).

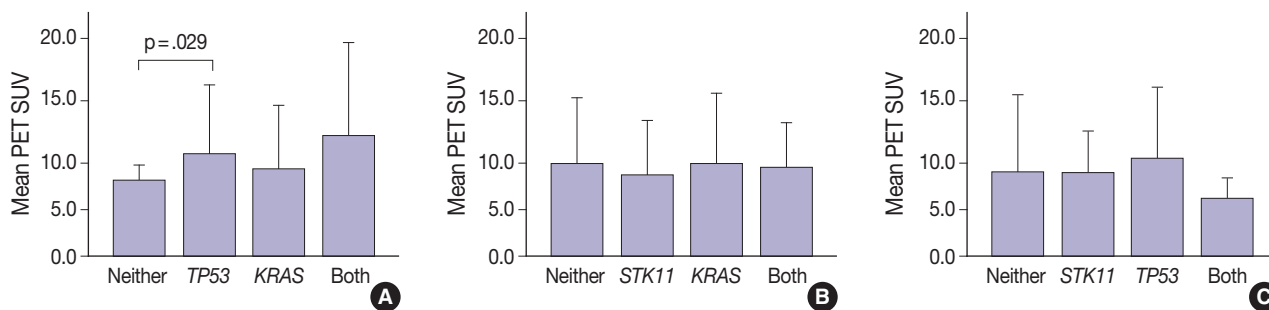


Fig. 2. Metabolic activity as measured by positron emission tomography (PET) standardized uptake value (SUV) in the presence of multiple mutations. Tumors with *TP53* and *KRAS* mutations together had higher SUV ($p = .029$ vs. no mutations) (A). No significant differences in SUV were observed in tumors with *KRAS* with and without *STK11* mutations (B). Tumors with *STK11* and *TP53* mutations had marginally decreased SUV ($p = .141$ vs. *TP53* only) (C).

quent *KRAS* mutations. For 170 wild-type, 31 G12C, 22 G12D, 19 G12V, and 14 other *KRAS* mutations, median SUV ranged from 6.4 (G12D) to 8.4 (G12V). Median SUV in the absence of any *KRAS* was 7.4.

Thirty-one tumors displayed mutations in more than one oncogene. Tumor metabolic activity measured by PET was compared in the presence of these mutation profiles ($n = 168$) (Fig. 2). Tumors with co-existing *KRAS* and *TP53* mutations showed higher metabolic activity ($p = .029$) (Fig. 2A). The presence of single *KRAS* and *STK11* mutations vs. combinations showed no significant relationship to metabolic activity (Fig. 2B). FDG uptake was lower in the presence of *STK11* mutations when *TP53* mutations were present, but not significantly so (Fig. 2C).

Metabolic activity as measured by FOXM1 gene expression

The role of *FOXM1* in glycolysis along with its tumor suppressor potential led to assessing its association with tumor metabolic activity. *FOXM1* is epigenetically regulated, in part, by miRNA, specifically miR-149, the expression of which was also measured. The amount of *FOXM1* and miR-149 expression in the tumor samples was assessed by quantitative reverse transcriptase PCR normalized to B2M expression. There was significantly higher *FOXM1* expression in tumor tissue from older patients accompanied by half the miR-149 expression (chi-square $p = .002$) (Table 1).

Compared to non-malignant tissue, *FOXM1* transcription is increased in tumor cells. To confirm this, mRNA was isolated from adjacent non-malignant lung tissue to estimate endogenous *FOXM1* expression before the oncogenic transformation. Only two of the 34 normal tissue samples tested were positive for *FOXM1* expression (5.9%) indicating that expression differences were not likely due to differences in endogenous levels of gene expression between patients, but *FOXM1* was specifically induced in and unique to the tumor cells (*FOXM1*/B2M% 8.65 tumor vs. 1.67 normal; $p < .001$).

Because miR-149 negatively regulates *FOXM1*, an inverse expression pattern between the two genes might be expected. *FOXM1* expression was inversely proportional to miR-149 expression, 13.6 *FOXM1*/B2M% with no detectable miR-149 expression versus 4.6 with miR-149 expression. If both gene activities were dichotomized (expressed/not expressed), cross-tabulation showed more cases of *FOXM1* expressed when miR-149 was not detected, consistent with an inverse relationship which was also observed in dichotomized data for both genes (expressed/not expressed).

FOXM1 expression in the tumor samples was compared to

metabolic activity as measured by SUV from FDG-PET imaging. SUV (minimal and maximal) were higher with any *FOXM1* expression compared to no detectable *FOXM1* (avg. maximum SUV, 8.90 vs. 6.8 [$p = .425$]; avg. minimal SUV, 2.62 vs. 2.02 [$p = .069$] with and without *FOXM1*, respectively).

FOXM1 gene expression and mutation status

Marginally lower *FOXM1* expression was observed in the presence of any *EGFR* mutations (Fig. 3), regardless of the mutation. No difference was observed in *FOXM1* expression with *KRAS* nor *TP53* mutated. There was significantly higher *FOXM1* expression when *STK11* was mutated than with no mutations ($p < .001$).

Comparing *FOXM1* expression and the different *KRAS* mutant subtypes, the G12V mutants had the highest median *FOXM1* expression (2.8; range, 1.0 to 2.1), higher than the levels seen with wild-type *KRAS* (3.5; range, 0.0 to 9.0). G12C mutants had the lowest *FOXM1* expression with a median of 0.16 (range, 0.0 to 10.5).

FOXM1 expression patterns in the presence of multiple mutations were dissimilar to patterns seen with SUV for *KRAS* and *TP53* mutations (compare Figs. 2 and 4). Tumors with *KRAS* and *TP53* mutations had increased *FOXM1* expression compared to no mutations or either mutation alone (Fig. 4A). In contrast, the presence of *STK11* with *KRAS* mutations resulted in significantly higher levels of *FOXM1* expression than with no mutation ($p < .001$) (Fig. 4B). A significant increase was seen in combination with *TP53* versus no mutation and versus *TP53* alone ($p = .002$ and $p < .001$, respectively) (Fig. 4C).

Patient outcome studies

To assess predictive value of metabolic state combined with

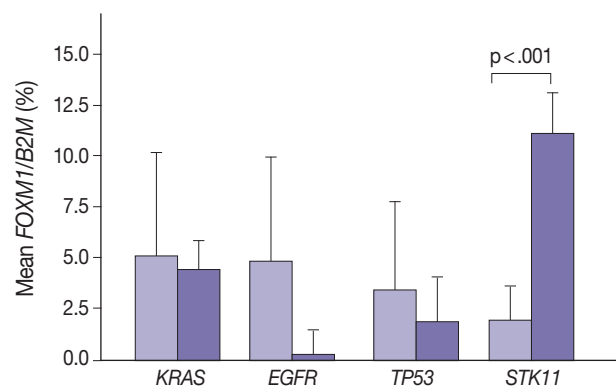


Fig. 3. Tumor *FOXM1* expression in the presence of mutations in *EGFR*, *TP53*, and *STK11* mutations. Cases were classified only on the basis of the indicated mutation.

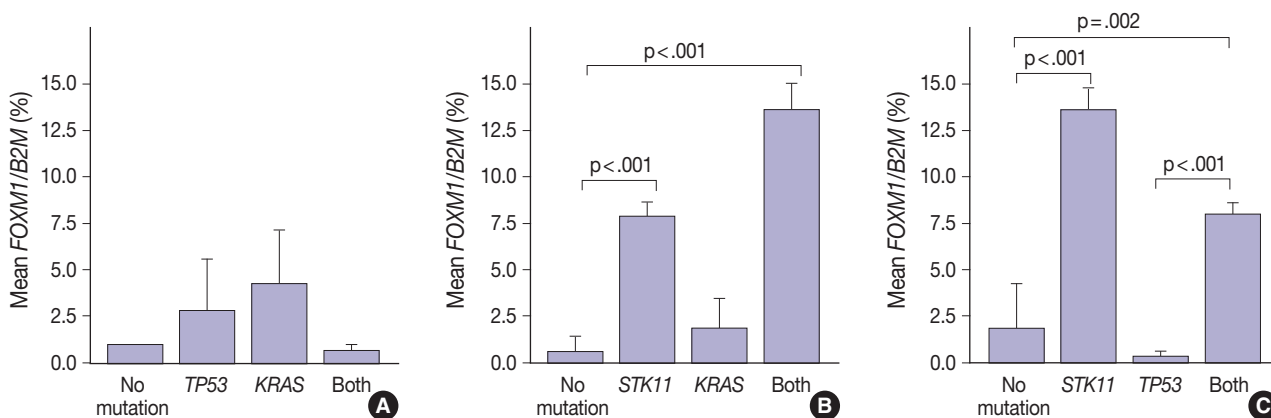


Fig. 4. *FOXM1* expression patterns in tumors in the presence of multiple mutations. Tumors with *TP53* and *KRAS* mutations alone or together had higher *FOXM1* expression than those with neither mutation (A). Unlike standardized uptake value, tumors with *STK11* mutations showed significantly higher *FOXM1* expression with or without *KRAS* mutations (B) or *TP53* mutations (C).

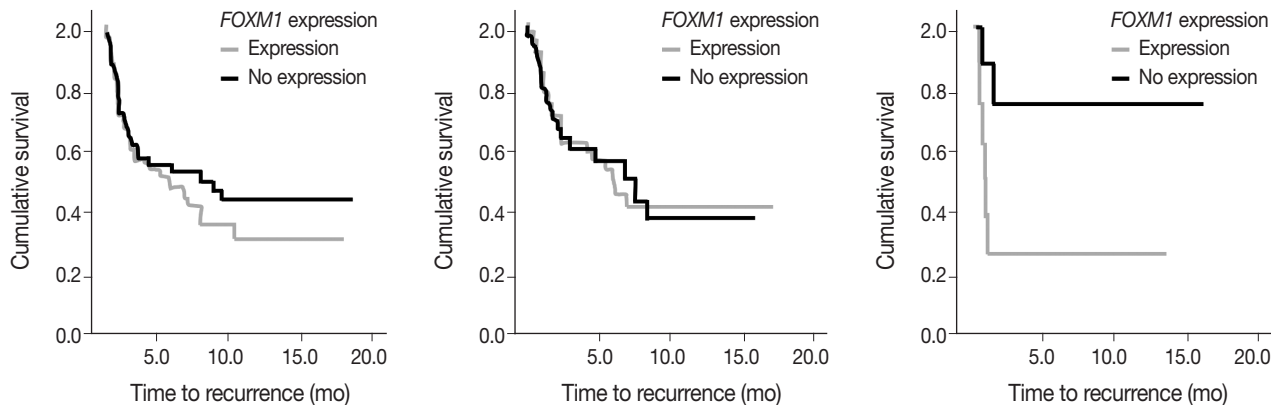


Fig. 5. *FOXM1* expression versus TTR in all cases ($n=104$; $p=0.253$; left), *KRAS* unmutated cases ($n=67$, $p=.274$, center), and *KRAS* mutated cases ($n=16$, $p=.033$, right).

mutational status, *FOXM1* expression (any expression vs. no expression) in the tumor samples was compared to TTR and OS in early-stage surgically treated patients. There was no significant difference in OS and marginal decrease in TTR when *FOXM1* was expressed versus not expressed. In cases with *KRAS* mutations, however, a significantly shortened TTR was observed when *FOXM1* was expressed (24 months vs. median not reached, respectively; $p=.033$) (Fig. 5).

DISCUSSION

Identification of somatic variants in tumors is essential in the prognosis and treatment strategy for lung adenocarcinoma. Tumor mutational and glycolytic status can vary in predicting treatment efficacy. The current study examined the relationship between tumor metabolic activity as measured by glucose uptake, gene expression in the glycolysis pathway and mutational status,

with potential consequences on outcome.

Frequencies of the selected mutations in this patient group: *TP53* (42% of cases), *KRAS* (35% of cases), *EGFR* (12% of cases), and *STK11* (10% of cases) reflected reported frequencies of these variants in lung cancer [16]. Co-existing mutations (among the four genes tested) was observed in 10% of cases. In previous studies, the presence of co-existing mutations such as *TP53* and *EGFR* mutations in NSCLC were associated with inferior survival [2]. Others have observed that survival with chemotherapy was longer for patients without *TP53* and *KRAS* mutations compared with patients with *KRAS*, *TP53* mutations, or double mutant tumors [1,17].

Glucose metabolism and the glycolysis pathway are dysregulated in lung cancer. This is a complex issue, with numerous factors involved, including tumor stage, co-morbidities, age, performance status, and tumor mutational state. Metabolic activity may not predict the presence of mutations in cancer genes, such

as *EGFR* [18,19]. Consistent with these reports, no significant relationship between *EGFR* mutation status and SUV was observed in the current study. SUV was increased, however, with co-existing *TP53* and *KRAS* mutations ($p = .029$) (Fig. 2). *STK11* or any *KRAS* alone were also not related to tumor metabolic status as measured by maximum SUV. Significant differences in SUV in the presence of co-existing mutations were not observed. There was marginally decreased maximum SUV in tumors with co-existing *KRAS* + *STK11* mutations ($p = .141$).

In contrast, there was significantly increased glycolytic activity as measured by levels of *FOXM1* expression in the presence of mutated *STK11* ($p < .001$). Furthermore, tumors with co-existing *TP53* or *KRAS* + *STK11* mutations showed significantly increased *FOXM1* expression ($p = .002$ and $p < .001$, respectively). *FOXM1* is downregulated by *TP53* through the *FOXO3* transcription factor to slow DNA repair functions in cells with DNA damage. FoxO3 and FoxM1 transcription factors are also implicated in cancer initiation through metabolic programs [20].

Reported higher levels of *FOXM1* expression in oral cancer tumors with *TP53* mutations than with wild-type *TP53* were not observed here with lung adenocarcinoma [21]. One explanation for this difference is the effect of co-existing mutations, such as *STK11*. *STK11* serine/threonine-protein kinase (also called LKB1) controls the activity of AMPK, to dampen cell metabolism. Human bronchial epithelial cells carrying mutated *KRAS* together with downregulated *STK11* produced squamous cell carcinoma and adenosquamous cell carcinoma when injected into nude mice [15]. Furthermore, *Stk11*-deficient lung tumors showed primary resistance to treatments that are effective to *Kras*^{G12D} mutants [16,17]. These results show the potential heterogeneity in outcome of gene inactivation in NSCLC. Differences in PET and *FOXM1* response in *STK11* + *KRAS* mutant tumors complicate coordination of tumor progression with metabolic adaptation by gene (*STK11* and *KRAS*) inactivation. FoxM1 protein is activated by *Kras* which is one of its downstream effectors. *STK11* may also down-regulate *Kras* activity.

Adding to the complexity are differences in SUV and *FOXM1* expression levels in the presence of the *KRAS* mutant subtypes suggesting that the mutant proteins produced could behave differently within the tumor cells and act through different pathways (causing differences in the progression and/or severity of the disease). The particular point mutation can change the overall stoichiometry of the encoded protein altering the proteins native interactions and normal effects on the cell. These mutation subtypes also interact differently with *FOXM1*, leading to varying levels of expression and activation.

Expression of the *FOXM1* transcription factor gene is highly correlated with the glycolytic pathway. Its expression was observed to be significantly higher in tumor tissue than in non-malignant tissue. PET SUV (also correlated with malignancy) trended lower when *FOXM1* was not expressed than with any *FOXM1* expression. Furthermore, *FOXM1* expression is under epigenetic control, in part, as a target of miR-149. In this study minimum and maximum SUV trended lower when *FOXM1* was not expressed than with any *FOXM1* expression.

FOXM1 expression on its own did not have a significant effect on patient survival ($p = .875$) nor tumor recurrence ($p = .274$), but did have a significant negative effect on TTR in patients who also expressed mutant *KRAS*. The effect of *FOXM1* expression on tumor recurrence in cases with *KRAS* mutations (Fig. 5), suggests that *FOXM1* expression may have a minor effect on the tumor phenotype, but could still be a viable prognostic factor, especially in the presence of other cancer gene mutations [22]. The phosphatidylinositol 3-kinase pathway signals growth and survival and helps drive the glycolytic phenotype of cancer cells by increasing cellular glucose uptake and glycolysis [23]. HNSCC patients with high levels of *FOXM1* expression in the presence of *TP53* mutations have been observed to have poor survival outcomes [21]. The presence of *FOXM1* expression could indicate a higher chance of tumor recurrence, which can then be used by a provider when deciding on the intensity of the course of treatment [24,25].

These observations are limited to the four genes investigated in this study. The effects of co-existing mutations suggest that cancer cells with high tumor mutational burden (coding somatic mutations/Mb of tumor DNA) may have further differences in metabolic characteristics. Tumor mutational burden also affects immune characteristics of tumors which contribute to recurrence and survival following treatment. Further studies with more comprehensive mutational analysis would address this question.

With the effects of mutation state on *FOXM1* expression, further studies on outcome were performed comparing *FOXM1* expression and outcome. *STK11* mutations were significantly related to increased *FOXM1* expression; however, numbers were not sufficient for analysis. Although measurement of *FOXM1* gene expression is not currently a practical method for tumor assessment, its comparison to PET activity shows a degree of complexity in metabolic activity in tumor cells with and without mutations. The effect of *KRAS* mutations on outcome with and without *FOXM1* expression suggests that both metabolic and mutational status affect tumor characteristics, and predicted patient outcome.

ORCID

Waqas Mahmud: <https://orcid.org/0000-0002-2773-1749>

Lela Buckingham: <https://orcid.org/0000-0002-2735-0946>

Author Contributions

Conceptualization: AG, LB, WM.

Data curation: AG, LB, WM.

Formal analysis: AG, LB, WM.

Funding acquisition: LB.

Investigation: AG, LB, WM.

Methodology: AG, LB, WM.

Project administration: LB.

Resources: LB, WM.

Software: AG, LB, WM.

Supervision: LB.

Validation: WM.

Visualization: AG, LB, WM.

Writing—original draft: AG.

Writing—review & editing: WM, LB.

Conflicts of Interest

The authors declare that they have no potential conflicts of interest.

Funding

This work was supported departmental funds (Rush University Medical Center, Department of Pathology and College of Health Sciences).

REFERENCES

1. Tomasini P, Mascaux C, Jao K, et al. Effect of coexisting *KRAS* and *TP53* mutations in patients treated with chemotherapy for non-small-cell lung cancer. *Clin Lung Cancer* 2019; 20: e338-45.
2. Aggarwal C, Davis CW, Mick R, et al. Influence of *TP53* mutation on survival in patients with advanced *EGFR*-mutant non-small-cell lung cancer. *JCO Precis Oncol* 2018 Aug 31 [Epub]. <https://doi.org/10.1200/PO.18.00107>.
3. Ding M, Li F, Wang B, Chi G, Liu H. A comprehensive analysis of WGCNA and serum metabolomics manifests the lung cancer-associated disordered glucose metabolism. *J Cell Biochem* 2019; 120: 10855-63.
4. Cairns RA, Harris IS, Mak TW. Regulation of cancer cell metabolism. *Nat Rev Cancer* 2011; 11: 85-95.
5. Soga T. Cancer metabolism: key players in metabolic reprogramming. *Cancer Sci* 2013; 104: 275-81.
6. Park HL, Yoo IR, Boo SH, et al. Does FDG PET/CT have a role in determining adjuvant chemotherapy in surgical margin-negative stage IA non-small cell lung cancer patients? *J Cancer Res Clin Oncol* 2019; 145: 1021-6.
7. Brun C, Gay P, Cottier M, et al. Comparison of cytology, chest computed and positron emission tomography findings in malignant pleural effusion from lung cancer. *J Thorac Dis* 2018; 10: 6903-11.
8. Vander Heiden MG, Cantley LC, Thompson CB. Understanding the Warburg effect: the metabolic requirements of cell proliferation. *Science* 2009; 324: 1029-33.
9. Cui J, Shi M, Xie D, et al. *FOXM1* promotes the warburg effect and pancreatic cancer progression via transactivation of LDHA expression. *Clin Cancer Res* 2014; 20: 2595-606.
10. Liao GB, Li XZ, Zeng S, et al. Regulation of the master regulator *FOXM1* in cancer. *Cell Commun Signal* 2018; 16: 57.
11. He Y, Yu D, Zhu L, Zhong S, Zhao J, Tang J. miR-149 in human cancer: a systemic review. *J Cancer* 2018; 9: 375-88.
12. Xu K, Liu X, Mao X, et al. MicroRNA-149 suppresses colorectal cancer cell migration and invasion by directly targeting forkhead box transcription factor *FOXM1*. *Cell Physiol Biochem* 2015; 35: 499-515.
13. Wierstra I, Alves J. *FOXM1*, a typical proliferation-associated transcription factor. *Biol Chem* 2007; 388: 1257-74.
14. Wang IC, Ustiyani V, Zhang Y, Cai Y, Kalin TV, Kalinichenko VV. Foxm1 transcription factor is required for the initiation of lung tumorigenesis by oncogenic *Kras*(G12D). *Oncogene* 2014; 33: 5391-6.
15. Wang IC, Snyder J, Zhang Y, et al. Foxm1 mediates cross talk between *Kras*/mitogen-activated protein kinase and canonical Wnt pathways during development of respiratory epithelium. *Mol Cell Biol* 2012; 32: 3838-50.
16. Catalogue of Somatic Mutations in Cancer (COSMIC) [Internet]. Hinxton: Wellcome Sanger Institute; 2020 [cited 2020 Feb 2]. Available from: <https://cancer.sanger.ac.uk/cosmic>.
17. Arbour KC, Jordan E, Kim HR, et al. Effects of co-occurring genomic alterations on outcomes in patients with *KRAS*-mutant non-small cell lung cancer. *Clin Cancer Res* 2018; 24: 334-40.
18. Zhu L, Yin G, Chen W, et al. Correlation between *EGFR* mutation status and F(18) -fluorodeoxyglucose positron emission tomography-computed tomography image features in lung adenocarcinoma. *Thorac Cancer* 2019; 10: 659-64.
19. Kim HS, Mendiratta S, Kim J, et al. Systematic identification of molecular subtype-selective vulnerabilities in non-small-cell lung cancer. *Cell* 2013; 155: 552-66.
20. Saavedra-Garcia P, Nichols K, Mahmud Z, Fan LY, Lam EW. Unravelling the role of fatty acid metabolism in cancer through the *FOXO3*-*FOXM1* axis. *Mol Cell Endocrinol* 2018; 462: 82-92.

21. Tanaka N, Zhao M, Tang L, et al. Gain-of-function mutant p53 promotes the oncogenic potential of head and neck squamous cell carcinoma cells by targeting the transcription factors FOXO3a and FOXM1. *Oncogene* 2018; 37: 1279-92.
22. Shimamura T, Chen Z, Soucheray M, et al. Efficacy of BET bromodomain inhibition in Kras-mutant non-small cell lung cancer. *Clin Cancer Res* 2013; 19: 6183-92.
23. Kompier LC, Lurkin I, van der Aa MN, van Rhijn BW, van der Kwast TH, Zwarthoff EC. *FGFR3*, *HRAS*, *KRAS*, *NRAS* and *PIK-3CA* mutations in bladder cancer and their potential as biomarkers for surveillance and therapy. *PLoS One* 2010; 5: e13821.
24. He SY, Shen HW, Xu L, et al. *FOXM1* promotes tumor cell invasion and correlates with poor prognosis in early-stage cervical cancer. *Gynecol Oncol* 2012; 127: 601-10.
25. Wang IC, Meliton L, Ren X, et al. Deletion of Forkhead Box M1 transcription factor from respiratory epithelial cells inhibits pulmonary tumorigenesis. *PLoS One* 2009; 4: e6609.

Continuous quality improvement program and its results of Korean Society for Cytopathology

Yoo-Duk Choi^{1,2}, Hoon-Kyu Oh^{1,3}, Su-Jin Kim^{1,4}, Kyung-Hee Kim^{1,5}, Yun-Kyung Lee^{1,6}, Bo-Sung Kim^{1,7}, Eun-Jeong Jang^{1,8}, Yoon-Jung Choi^{1,9}, Eun-Kyung Han^{1,10}, Dong-Hoon Kim^{1,11}, Younghee Choi^{1,12}, Chan-Kwon Jung^{1,13}, Sung-Nam Kim^{1,14}, Kyueng-Wan Min^{1,15}, Seok-Jin Yoon^{1,16}, Hun-Kyung Lee^{1,17}, Kyung Un Choi^{1,18}, Hye Kyoung Yoon^{1,19}

¹The Committee of Quality Improvement of Korean Society for Cytopathology, Seoul; ²Department of Pathology, Chonnam National University Medical School, Gwangju; ³Department of Pathology, Daegu Catholic University School of Medicine, Daegu; ⁴Department of Pathology, Seegene Medical Foundation, Busan; ⁵Department of Pathology, Chungnam National University School of Medicine, Daejeon; ⁶Department of Pathology and Translational Genomics, Samsung Medical Center, Sungkyunkwan University School of Medicine, Seoul; ⁷Department of Pathology, National Medical Center, Seoul; ⁸Department of Pathology, Fatima Hospital, Daegu; ⁹Department of Pathology, National Health Insurance Service, Ilsan Hospital, Goyang; ¹⁰Department of Pathology, Seoul Clinical Laboratories, Seoul; ¹¹Department of Pathology, Kangbuk Samsung Hospital, Sungkyunkwan University School of Medicine, Seoul; ¹²Department of Pathology, Hallym University Dongtan Sacred Heart Hospital, Hwaseong; ¹³Department of Hospital Pathology, College of Medicine, The Catholic University of Korea, Seoul; ¹⁴Department of Pathology, Sure Quest Lab, Yongin; ¹⁵Department of Pathology, Hanyang University Guri Hospital, Hanyang University College of Medicine, Guri; ¹⁶Department of pathology, Dankook University Hospital, Cheonan; ¹⁷Department of Pathology, Ewha Laboratory of Medicine, Seoul; ¹⁸Department of Pathology, Pusan National University Hospital, Busan; ¹⁹Department of Pathology, Busan Paik Hospital, Inje University, Busan, Korea

Background: Since 1995, the Korean Society for Cytopathology has overseen the Continuous Quality Improvement program for cytopathology laboratories. The Committee of Quality Improvement has carried out an annual survey of cytology data for each laboratory and set standards for proficiency tests. **Methods:** Evaluations were conducted four times per year from 2008 to 2018 and comprised statistics regarding cytology diagnoses of previous years, proficiency tests using cytology slides provided by the committee, assessment of adequacy of gynecology (GYN) cytology slides, and submission of cytology slides for proficiency tests. **Results:** A total of 206 institutes participated in 2017, and the results were as follows. The number of cytology tests increased from year to year. The ratio of liquid-based cytology in GYN gradually decreased, as most of the GYN cytology had been performed at commercial laboratories. The distribution of GYN diagnoses demonstrated nearly 3.0% as atypical squamous cells. The rate for squamous cell carcinoma was less than 0.02%. The atypical squamous cell/squamous intraepithelial lesion ratio was about 3:1 and showed an upward trend. The major discordant rate of cytology-histology in GYN cytology was less than 1%. The proficiency test maintained a major discordant rate less than 2%. The rate of inappropriate specimens for GYN cytology slides gradually decreased. **Conclusions:** The Continuous Quality Improvement program should be included in quality assurance programs. Moreover, these data can contribute to development of national cancer examination guidelines and facilitate cancer prevention and treatment.

Key Words: Cytology; Quality; Statistics; Proficiency

Received: December 27, 2019 **Revised:** February 16, 2020 **Accepted:** February 22, 2020

Corresponding Author: Hoon-Kyu Oh, MD, PhD, Department of Pathology, Daegu Catholic University School of Medicine, 33 Duryugongwon-ro 17-gil, Namgu, Daegu 42472, Korea
 Tel: +82-53-650-4156, Fax: +82-53-650-3456, E-mail: ap510@cu.ac.kr

The Committee of Quality Improvement of the Korean Society for Cytopathology (CQIKSC) was organized in 1992 for quality control management in advancement of cytopathology. In the initial period, the Committee distributed quality assurance slides to participating institutions, assessed diagnostic accuracy based on the received results, and issued quality assurance certification to those who qualified. Since 2004, the Committee has

collected internal quality assurance data for the previous year from each institution at the first of the four quality assurance evaluation rounds per year and evaluated diagnostic accuracy from the second to fourth rounds. In 2008, the Committee compiled and reported the quality assurance status for the cytopathology field until 2007 in *Korean Journal of Cytopathology* [1].

This study seeks to explore future quality assurance in cyto-

pathology while simultaneously evaluating past work by compiling and reporting the results of cytopathologic quality assurance situations and activities.

MATERIALS AND METHODS

This study was based on data collected from 2008 to 2018 by institutions participating in cytopathologic quality assurance. Data collected included: (1) previous years' statistics of internal quality control (data from 2007 to 2017), including degree of concordance between gynecology (GYN) cytology and histology correlation; (2) proficiency test of cytology slides provided by the CQIKSC; (3) assessment of adequacy of GYN cytology slides; and (4) cytology slides submitted for proficiency tests. For this study, the institutions were categorized into three groups: university hospitals, general hospitals, and commercial laboratories [2].

Statistics of internal quality control

The first quality assurance implementation of the year was to collect internal quality control data of the previous year, including GYN, non-GYN, fine needle aspirations (FNA) cytology statistics, test methods, diagnosis-specific frequencies (under the Bethesda assessment criteria for GYN cytology), statistics on concordance between GYN cytology and histology correlation, personnel situations of cytopathologists, and initial microscopic specimen assessments. GYN cytology methods were investigated using conventional smear method or liquid-based

cytology (LBC). Concordance between GYN cytology and histology was analyzed based on the criteria defined by the CQIKSC. Briefly, the results were categorized into category O, concordant; category A, discordant but minimal clinical impact; category B, discordant with minor clinical impact; and category C, discordant with major clinical impact.

Proficiency test for cytology slides provided by the CQIKSC (external quality control)

The slides for proficiency tests were provided every year by institutions participating in quality assurance. The slides were randomly sent to the institutions according to an ordered series, and each institution returned their diagnostic results along with an evaluation of the adequacy of the slides received. Any slides that were deemed inadequate were reexamined by the CQIKSC and reevaluated for appropriateness as quality assurance slides. From 2008 to 2012, virtual slide or image file-based proficiency tests were also conducted once a year. However, since 2013, only the slide-based proficiency test has been implemented annually (Table 1).

For proficiency tests, a total of five slides was sent to each institution, consisting of two GYN slides, one non-GYN slide (body fluid or urine), and two respiratory sample or FNA slides. The diagnoses received by each institution within a set period were compared by CQIKSC. With respect to the diagnostic form, the cervical smear test was evaluated based on the Bethesda system [3], and the thyroid gland FNA test was based on the Bethesda

Table 1. Changes in quality improvement items from 2007 to 2017

	First	Second	Third	Fourth
2007	Total C. statistics Diagnostic-specific frequency of GYN C. Concordance between GYN C. and H.	Proficiency test (3 slides)	Proficiency test (3 slides)	Proficiency test (3 slides)
2008	Total C. statistics Diagnostic-specific frequency of GYN C. Concordance between GYN C. and H.	Proficiency test (5 slides)	Proficiency test (virtual slide)	-
2009	Total C. statistics Diagnostic-specific frequency of GYN C. Concordance between GYN C. and H.	Proficiency test (5 slides)	Proficiency Test (5 image files)	Slide submission Image submission
2010	Total C. statistics Diagnostic-specific frequency of GYN C. Concordance between GYN C. and H. Describe the discordant GYN cases	Proficiency test (5 image files)	Proficiency test (5 slides)	Slide submission Image submission
2011–12	Total C. statistics Diagnostic-specific frequency of GYN C. Concordance between GYN C. and H. Describe the discordant GYN cases	Proficiency test (5 slides)	Proficiency test (4 image files)	Slide submission (6 slides)
2013–17	Total C. statistics Diagnostic-specific frequency of GYN C. Concordance between GYN C. and H. Describe the discordant GYN cases	Proficiency test (5 slides)	Assessment of adequacy for GYN 5 slides	Slide submission (6 slides)

GYN, gynecology; C., cytology; H., histology.

system for reporting thyroid cytopathology [4]. The CQIKSC defined the diagnostic forms of respiratory sample, body fluid, and FNA for organs other than the thyroid gland. In addition, the Committee set up the evaluation criteria for diagnostic concordance for GYN, non-GYN, and FNA tests, classifying them into category O, concordant; category A, discordant but minimal clinical impact; category B, discordant with minor clinical impact; and category C, discordant with major clinical impact. Institutions that were categorized into C for any slide were scheduled to receive one reevaluation. If still categorized into C in the reevaluation, the institution did not receive the quality assurance certification for the corresponding round and was required to undergo cytopathologic training. Repeated category C also indicated failure in the cytopathology area of the proficiency evaluation of the Quality Assurance of Pathology Division at the Korean Society of Pathologists.

Assessment of adequacy of gynecologic cytology slides

Since 2013, GYN slide adequacy has been evaluated in the Cytology Quality Improvement program once a year. Institutions evaluate the adequacy of five consecutive gynecologic slides prepared on a given random day and send the slides and reports to CQIKSC, which then assesses the adequacy of the GYN sample. Using this method, each institution was evaluated to ensure that the adequacy of samples had been properly reported.

Cytology slide submission for diagnostic accuracy evaluation

Every year, institutions participating in quality assurance submitted to the CQIKSC two GYN slides, two non-GYN slides, and two FNA slides for proficiency tests. The submitted slides were limited to cases of histologically confirmed diagnoses. CQIKSC members reviewed the slides to ensure that they were appropriate and useful as quality assurance data before using them as quality control slides.

Statistics

The distribution of GYN diagnostic categories according to year was conducted using the score test for trend in IBM SPSS Statistics software ver. 23.0 (IBM Corp., Armonk, NY, USA). A *p*-value of < 0.05 was considered statistically significant.

Ethics statement

This study was approved by the Institutional Review Board of Daegu Catholic University Medical Center (IRB No. CR-18-162), and informed consent was waived due to the retrospective nature of the study.

RESULTS

The number of institutions participating in the Continuous Quality Improvement program of the Korean Society of Cytopathology (KSC) has gradually increased from 196 in 2007 to 206 in 2017. The results of diagnostic accuracy and sample adequacy evaluation have been reflected in the proficiency assessment of the cytopathology area within the proficiency evaluation program, Pathology Division, Korean Society of Pathologists' Quality Assurance Committee.

Statistics of cytopathology cases

The total number of cytology results exceeded 6.1 in 2008, 7.7 million in 2011, 8.4 million in 2014, and 9.3 million in 2017. The number of GYN cytology results in 2008 was 4.34 million; in 2011, 5.63 million; in 2013, 6.18 million; and in 2017, 7.51 million. In 2013, of the number of total cytology results, the number of GYN cytology was 6.18 million, which accounted for 80.3%; non-GYN cytology, 1.06 million, 13.8%; and FNA cytology, 450,000, 5.9%. In 2017, of the number of total cytology, the number of GYN cytology was 7.51 million, accounting for 80.3%; non-GYN cytology, 1.54 million, 16.5%; and FNA cytology, about 300,000, 3.2%. Of the number of non-GYN cytology results, the number of respiratory cytology samples, including sputum, accounted for the largest number, followed by urine and then body fluid. In relation to the FNA, thyroid gland FNA was the highest at 68.4%. In 2013, the number of GYN LBC was 1.65 million, or 26.8% of the total GYN cytology results. In 2017, 1.99 million LBC were performed, accounting for 21.3% of the number of total cytology results. Of them, the number of GYN LBC was 1.52 million, 20.3% of the total GYN cytology results, and the number of non-GYN LBC was 340,000, 22.3% of the total non-GYN cytology results. The total number of FNA tests implemented as LBC was 120,000, accounting for 40.4% of all FNA tests (Table 2).

Statistics of GYN cytology

In 2010, of the number of GYN cytology results, 61.1% were implemented by commercial laboratories; this frequency increase in 2011 to 73.2%; in 2014 to 77.1%; in 2015 to 77.9%; and in 2017 to 79.2%. Of all GYN cytology results, in 2009, 95.9% were negative; 2.2% were atypical squamous cells of undetermined significance (ASC-US); 0.2% were atypical squamous cells cannot exclude high-grade squamous lesions (ASC-H); 0.9% were low-grade squamous intraepithelial le-

sions (LSIL); 0.4% were high-grade squamous intraepithelial lesions (HSIL); 0.12% were squamous cell carcinomas (SQCC); and 0.02% were atypical glandular cells (AGC). In 2017, 95.1% were negative; 3.3% were ASC-US; 0.2% were ASC-H; 0.7% were LSIL; 0.2% were HSIL; 0.02% were SQCC; and 0.06% were AGC. The atypical squamous cell/squamous intraepithelial lesion (ASC/SIL) ratio was 3.00 in 2013 and gradually increased to 3.82 in 2017 ($p = .011$). The ASC/SIL ratio of commercial laboratories increased from 3.68 in 2013 to 4.95 in 2017 ($p = .004$). The ASC/SIL ratio of university hospitals increased from 1.70 in 2013 to 1.95 in 2017 ($p = .042$) (Table 3). With respect to concordance between GYN cytology and histology evaluated by each institution, in the year 2009, category O accounted for 78.3%; category A for 11.6%; category B for 8.6%; and category C for 1.4%. In 2013, category O was 86.3%; while categories A, B, and C were 8.9%, 4.0%, and 0.8%, respectively. In 2017, category O was 84.8%; and categories A, B, and C were 11.0, 3.7%, and 0.5%.

External proficiency test

The external proficiency tests for GYN cytology samples pro-

Table 2. Total cytology cases according to category and method in 2017

	GYN	Non-GYN	FNA
Total	7,510,563	1,539,926	297,885
CS	5,984,869 (79.7)	1,196,103 (77.6)	177,679 (59.6)
LBC	1,525,694 (20.3)	343,823 (22.4)	120,206 (40.4)

Values are presented as number (%).

GYN, gynecology; FNA, fine needle aspiration; CS, conventional smear; LBC, liquid based cytology.

Table 3. Changes of abnormal gynecologic cytology diagnostic criteria according to laboratory category from 2012 to 2017

Year	Laboratory category	No. of ASCs	ASC rate (%)	No. of SILs	SIL rate (%)	ASC/SIL ratio	No. of carcinomas
2012	UH	27,143	3.13	15,960	1.84	1.70	1,323
	GH	19,460	3.17	7,627	1.24	2.55	571
	CL	124,219	2.99	33,737	0.81	3.68	953
	Total	170,822	3.03	57,324	1.02	2.98	2,847
2014	UH	29,624	3.41	17,034	1.96	1.74	1,299
	GH	19,703	2.90	7,631	1.12	2.58	658
	CL	183,076	3.50	43,511	0.83	4.21	887
	Total	232,403	3.42	68,176	1.00	3.41	2,844
2016	UH	31,944	3.65	17,771	2.03	1.80	1,276
	GH	18,867	2.95	6,958	1.09	2.71	419
	CL	219,749	3.77	49,407	0.85	4.45	843
	Total	270,560	3.68	74,136	1.01	3.65	2,538
2017	UH	41,371	3.82	21,173	1.96	1.95	1,188
	GH	14,489	3.04	5,616	1.18	2.58	210
	CL	204,737	3.44	41,374	0.70	4.95	622
	Total	260,597	3.47	68,163	0.91	3.82	2,020

ASC, atypical squamous cell; SIL, squamous intraepithelial lesion; UH, university hospital; GH, general hospital; CL, commercial laboratories.

vided by CQIKSC were analyzed based on category. As a result, in 2014, category O represented 81.0% of the results; category A, 12.4%; category B, 5.1%; and category C, 1.5%. In 2017, category O comprised 78.1%; category A, 13.2%; category B, 6.5%; and category C, 2.2%. With respect to diagnostic consistency between non-GYN cytology of respiratory, urine, and body fluid samples, in 2014, category O was 91.1%; category A, 5.5%; category B, 2.4%; and category C, 1.0%. In 2017, category O was 88.0%; category A, 8.7%; category B, 2.5%; and category C, 0.8%. The FNA cytology in 2014 showed category O, 99.0%; category A, 0.5%; category B, 0.5%; and category C, 0.0%. In 2017, these values changed to category O, 95.8%; category A, 2.1%; category B, 1.3%; and category C, 0.8% (Fig. 1).

GYN cytology specimen adequacy evaluation

In 2013, inadequate results for GYN cytology specimens were found in eight of the 77 participating university hospitals (10.4%), eight of 77 participating general hospitals (10.4%), and one of the 35 included commercial laboratories (2.9%). In 2017, two of 79 university hospitals (2.5%) and two of 74 general hospitals (2.7%) were inadequate. The total number of inadequate results decreased from 2013, but increased to three among the 30 commercial laboratories (10.0%). However, in the samples with an unsatisfactory institution-specific diagnostic ratio among all GYN diagnoses in 2017, university hospitals had a proportion of 0.39%; general hospitals, 1.9%; and commercial laboratories, as low as 0.07%.

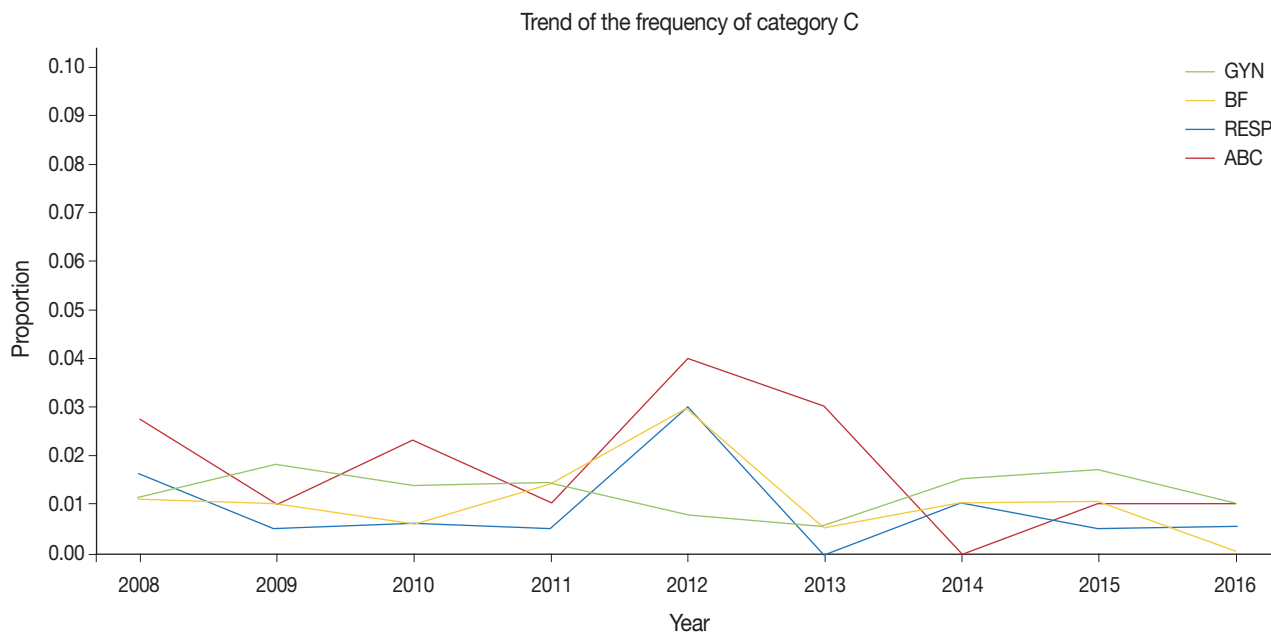


Fig. 1. Trend of frequency of category C in diagnostic accuracy evaluation (external quality control). GYN, gynecology; BF, body fluid; RESP, respiratory; ABC, aspiration cytology.

Quality assurance slide submission evaluation

Slides were submitted to the CQIKSC in the final round each year to be reviewed by quality assurance committee members in the following year for suitability as quality assurance slides. Slides that had been judged to be appropriate were used for proficiency test 2 years later. Of the 1,035 slides submitted in 2016, 473 were utilized for proficiency tests in 2018. In 2013, inappropriate slides from university or general hospitals accounted for 39.2% of the total not used for testing, and that at commercial laboratories was 60.0%; these numbers declined to 24.6% and 41.0% in 2016, respectively

DISCUSSION

The number of institutions participating in the Continuous Quality Improvement program managed by the CQIKSC has increased each year to include most of the institutions that practice cytopathology nationwide. The Continuous Quality Improvement program includes the degree of inconsistency between cytologic statistics and diagnostic accuracy, sample appropriateness, and quality assurance slide submission evaluation.

The cytopathologic quality assurance checklist was independently initiated by the KSC. However, in 2007, it was moved into the cytopathologic area of the checklist for the “pathology division’s quality control” implemented by the Korean Society of Pathologists. Nevertheless, modification, improvement, and

evaluation of any details are performed by CQIKSC. The checklist addresses quality assurance in cytopathologic laboratories, personnel management, operating manuals, test equipment, test methods, reporting systems, environment, safety measures, etc.

In the initial period after the LBC method was introduced in GYN cytology, the number and ratio of LBC tended to increase continuously; however, the ratio decreased to 21.4% in 2017 from 26.8% in 2013. However, the total number of GYN LBC slightly decreased to 1.52 million in 2017 from 1.65 million in 2013. It seems that the ratio of total GYN samples submitted to commercial laboratories continuously increased, as most national cancer screening GYN samples are referred to these entities. LBC is not being used for the national cancer screening project. LBC, however, was found to account for a larger portion of the FNA test compared to GYN cytology or non-GYN cytology in 2017. It seems that LBC is largely introduced in FNA tests for the thyroid gland [5,6]. Nonetheless, further general investigation on the issue is necessary.

Regarding the statistics on gynecologic cytology, the ratio of SQCC decreased from 0.12% in 2009 to 0.02% in 2017. AGC accounted for 0.02% in 2009 and increased to 0.06% in 2017. Compared to 2009, the number of total tests surged in 2017, while the ratio of inappropriate results remained relatively constant. These results are correlated with the positive effects of increased frequency of regular screening under the national cancer prevention project and declining cancer incidence with socio-

economic improvement. This supports the view that domestic cervical SQCC incidence reduces cancer registration results. The data are also consistent with an increasing incidence of adenocarcinoma [7].

Given that the purpose of GYN cytology is primarily to detect SQCC in the early stage, the initial lesion, ASC (ASC-US and ASC-H), is most important. Many institutions have aimed to maintain the ASC diagnosis and ASC/SIL ratios within appropriate levels, which means that SIL lesions reflect low inter-observer variation and are more objective than ASC for maintaining ASC objectivity [8-11]. In the initial period after 2009, the ASC/SIL ratio was maintained at 2.00 or under but increased to 3.00 in 2013 and then further to 3.82 in 2017. Commercial laboratory ASC/SIL rate (2013, 3.68; 2017, 4.95) is growing more than that of university hospitals (2013, 1.70; 2017, 1.95). Compared with university hospitals commercial laboratories rarely implement simultaneous biopsy, resulting in relatively high ASC and low SIL ratios. This finding will require further review.

The histologic diagnostic accuracy of each institution's GYN cytology was not significant. Most pathology departments lacked the necessary resources such as personnel and computer systems, making it difficult to perform and maintain statistical processes for diagnostic consistency. Moreover, there were no criteria on whether tissue sample subject comparison was based on punch biopsy, cone biopsy, or hysterectomy. There was no mention on the time difference between cytology and histology. The criteria for assessment of diagnostic accuracy about GYN cytology were different according to time, limiting comparison of category ratios over years. For quality improvement of each institution, a previous GYN cytology slide review seems a good method, in addition to cytology and histology correlation diagnostic consistency analysis. Reviewing 10% of slides under ASC and reviewing high-risk groups is recommended [12].

With respect to the external proficiency test, most of the institutions showed a lower diagnostic accuracy rate of GYN cytology compared with non-GYN or FNA cytology. This is likely because, compared with other samples, GYN cytology and diagnosis structure are more complicated and difficult. Some other countries divide the diagnostic codes of GYN cytology into three categories of inadequate sample, negative or reactive lesion, and epithelial cell abnormal lesion. Minor differences within a category are defined as minor discrepancies and differences between categories as major discrepancies to determine false positivity and false negativity. In this situation, it seems necessary to improve the discrepancy grade system as defined by the CQIKSC.

The sample adequacy evaluation that has been implemented

since 2013 is related to the diagnosis rate of inadequate samples. The percentage of inadequate samples in university hospitals decreased in 2017, compared with 2013, while the percentage in commercial laboratories increased. Regarding the finding that commercial laboratories had a very low percentage of unsatisfactory diagnosis in GYN cytology compared to university and general hospitals, an important factor could be that commercial laboratories are pushed to maintain higher thresholds for 'inappropriate/inadequate samples' because they rather not offend the referring clinicians by implying that they had not done well in collecting the samples.

The most urgent and necessary aspect observed while organizing the quality control results was that, if participating institutions utilized a common program for internal and external quality assurance, they would efficiently make use of the quality assurance results. If a quality assurance program compatible for each institution is developed by the Society or Committee and provided to institutions for quality control data organization, it would be very helpful for future advancement of cytopathology. In addition to such a system, other programs that need to be developed include quality assurance on the human papillomavirus test and quality assurance on automatic screening equipment for GYN cytology.

The KSC, in cooperation with the CQI program, has developed a computer program and plan to utilize it beginning in 2018. This more advanced and efficient quality improvement program is expected to play an advanced role in determining the foundation for cancer prevention and treatment. The KSC quality improvement program has continuously developed since 1995, comprising about 206 participating institutions. Four evaluations are implemented each year. Since 2008, factual surveys in cytopathology have been integrated into the "pathology division's quality control" program. However, inspection is currently ongoing. With the national cancer prevention project expansion, an increasing number of GYN cytology tests are being implemented by commercial laboratories. Although the number of LBC increased in various areas, its proportion in GYN cytology tended to gradually decrease. In GYN cytology, the proportion of SQCC diagnoses is decreasing, whereas the proportion of AGC is rising. Compared with university or general hospitals, commercial laboratories tend to show a lower rate of unsatisfactory diagnoses in GYN cytology with a higher ASC/SIL frequency. External diagnostic accuracy remains high. It seems that more advanced and higher-quality upgrades would be achieved when the computerized cytopathologic quality assurance program launches in 2018. The researchers also hope for expedited devel-

opment of quality assurance programs on human papillomavirus and automatic screening equipment for GYN cytology.

ORCID

Yoo-Duk Choi: <https://orcid.org/0000-0002-4385-1759>
 Hoon-Kyu Oh: <https://orcid.org/0000-0001-8793-1948>
 Su-Jin Kim: <https://orcid.org/0000-0001-5954-5281>
 Kyung-Hee Kim: <https://orcid.org/0000-0003-0214-0296>
 Yun-Kyung Lee: <https://orcid.org/0000-0001-6821-8653>
 Bo-Sung Kim: <https://orcid.org/0000-0002-2344-7230>
 Eun-Jeong Jang: <https://orcid.org/0000-0003-1482-5022>
 Yoon-Jung Choi: <https://orcid.org/0000-0002-5701-8864>
 Eun-Kyung Han: <https://orcid.org/0000-0002-7521-5095>
 Dong-Hoon Kim: <https://orcid.org/0000-0001-5722-6703>
 Younghee Choi: <https://orcid.org/0000-0002-3882-4000>
 Chan-Kwon Jung: <https://orcid.org/0000-0001-6843-3708>
 Sung-Nam Kim: <https://orcid.org/0000-0001-9235-7805>
 Kyueng-Whan Min: <https://orcid.org/0000-0002-4757-9211>
 Seok-Jin Yoon: <https://orcid.org/0000-0001-5879-1392>
 Hun-Kyung Lee: <https://orcid.org/0000-0002-9802-5235>
 Kyung Un Choi: <https://orcid.org/0000-0002-3848-1781>
 Hye Kyoung Yoon: <https://orcid.org/0000-0003-0714-8537>

Author Contributions

Conceptualization: YDC.

Data curation: KHK, YKL, EKH, YC, CKJ, KWM, SJY, HKL, KUC.

Formal analysis: SJK, BSK, DHK, SNK.

Investigation: HKO, EJJ, YJC.

Methodology: YDC, YJC.

Project administration: HKO, HKY.

Supervision: HKO, YJC, HKY.

Validation: YDC, HKO, YJC.

Visualization: HKO, DHK, CKJ.

Writing—original draft: YDC.

Writing—review & editing: YDC, HKO, HKY.

Conflicts of Interest

C.K.J., the editor-in-chief of the *Journal of Pathology and Translational Medicine*, were not involved in the editorial evaluation or decision to publish this article. All remaining authors have declared no conflicts of interest.

Funding

This research was supported by the Korean Society for Cytopathology Grant No. 2017-01.

REFERENCES

1. Lee HK, Kim SN, Khang SK, Kang CS, Yoon HK. Quality control program and its results of Korean Society for Cytopathologists. *Korean J Cytopathol* 2008; 19: 65-71.
2. Oh EJ, Jung CK, Kim DH, et al. Current cytology practices in Korea: a nationwide survey by the Korean Society for Cytopathology. *J Pathol Transl Med* 2017; 51: 579-87.
3. Solomon D, Davey D, Kurman R, et al. The 2001 Bethesda System: terminology for reporting results of cervical cytology. *JAMA* 2002; 287: 2114-9.
4. Cibas ES, Ali SZ. The Bethesda System for Reporting Thyroid Cytopathology. *Thyroid* 2009; 19: 1159-65.
5. Fadda G, Rossi ED. Liquid-based cytology in fine-needle aspiration biopsies of the thyroid gland. *Acta Cytol* 2011; 55: 389-400.
6. Chong Y, Ji SJ, Kang CS, Lee EJ. Can liquid-based preparation substitute for conventional smear in thyroid fine-needle aspiration? A systematic review based on meta-analysis. *Endocr Connect* 2017; 6: 817-29.
7. Kim Y, Jun JK, Choi KS, Lee HY, Park EC. Overview of the National Cancer screening programme and the cancer screening status in Korea. *Asian Pac J Cancer Prev* 2011; 12: 725-30.
8. Confortini M, Carozzi F, Dalla Palma P, et al. Interlaboratory reproducibility of atypical squamous cells of undetermined significance report: a national survey. *Cytopathology* 2003; 14: 263-8.
9. Davey DD, Neal MH, Wilbur DC, Colgan TJ, Styer PE, Mody DR. Bethesda 2001 implementation and reporting rates: 2003 practices of participants in the College of American Pathologists Interlaboratory Comparison Program in Cervicovaginal Cytology. *Arch Pathol Lab Med* 2004; 128: 1224-9.
10. Nascimento AF, Cibas ES. The ASC/SIL ratio for cytopathologists as a quality control measure: a follow-up study. *Am J Clin Pathol* 2007; 128: 653-6.
11. Renshaw AA, Deschênes M, Auger M. ASC/SIL ratio for cytotechnologists: a surrogate marker of screening sensitivity. *Am J Clin Pathol* 2009; 131: 776-81.
12. Krieger P, Naryshkin S. Random rescreening of cytologic smears: a practical and effective component of quality assurance programs in both large and small cytology laboratories. *Acta Cytol* 1994; 38: 291-8.

Morphologic variant of follicular lymphoma reminiscent of hyaline-vascular Castleman disease

Jiwon Koh¹, Yoon Kyung Jeon^{1,2}

¹Department of Pathology, Seoul National University Hospital, Seoul; ²Department of Pathology, Seoul National University College of Medicine, Seoul, Korea

Follicular lymphoma (FL) with hyaline-vascular Castleman disease (FL-HVCD)-like features is a rare morphologic variant, with fewer than 20 cases in the literature. Herein, we report a case of FL-HVCD in a 37-year-old female who presented with isolated neck lymph node enlargement. The excised lymph node showed features reminiscent of HVCD, including regressed germinal centers (GCs) surrounded by onion skin-like mantle zones, lollipop lesions composed of hyalinized blood vessels penetrating into regressed GCs, and hyalinized interfollicular stroma. In addition, focal areas of abnormally conglomerated GCs composed of homogeneous, small centrocytes with strong BCL2, CD10, and BCL6 expression were observed, indicating partial involvement of the FL. Several other lymphoid follicles showed features of in situ follicular neoplasia. Based on the observations, a diagnosis of FL-HVCD was made. Although FL-HVCD is very rare, the possibility of this variant should be considered in cases resembling CD. Identification of abnormal, neoplastic follicles and ancillary immunostaining are helpful for proper diagnosis.

Key Words: Malignant lymphoma; Follicular lymphoma; Hyaline-vascular Castleman disease; In situ follicular neoplasia

Received: November 13, 2019 **Revised:** December 9, 2019 **Accepted:** December 17, 2019

Corresponding Author: Yoon Kyung Jeon, MD, PhD, Department of Pathology, Seoul National University Hospital, Seoul National University College of Medicine, 101 Daehak-ro, Jongno-gu, Seoul 03080, Korea

Tel: +82-2-740-8323, Fax: +82-2-743-5530, E-mail: ykjeon@snu.ac.kr

Follicular lymphoma (FL) is an indolent B-cell lymphoma and the second most common non-Hodgkin lymphoma (NHL) in the western world [1]. FL is the third most common form of B-cell NHL in Korea, accounting for 7.1% of all malignant lymphomas [2]. Several morphological variants of FL exist, including marginal zone variant, floral variant, and sclerosing variant [3-5]. Although typical cases of FL lead to straightforward diagnosis, the morphological variants are sometimes very challenging, rendering proper diagnosis difficult for pathologists. Herein, we describe a case of FL with hyaline-vascular Castleman disease (FL-HVCD)-like features, an extremely rare morphological variant.

CASE REPORT

A 37-year-old female presented with a palpable right neck mass that had been found one month prior. She denied having any previous medical problems, except anemia. On review of systems, she denied fever, unintentional weight loss, or night

sweats. Enlargement of the right cervical lymph node (LN) was found on physical examination, and complete blood count revealed decreased hemoglobin level (10.5 g/dL); white blood cell and platelet counts were within normal limits. Neck ultrasonography showed a 3.5-cm-sized mass in the right neck (Fig. 1A), and computed tomography scan confirmed a well-enhanced LN along with smaller LNs in the right cervical level II area (Fig. 1B). On ¹⁸F-positron emission tomography scan, an enlarged LN in the right level II area was found with maximal standardized uptake value of 4.0; no other hypermetabolic lesions were found, except for the mild physiologic uptake at bilateral tonsils and oropharynx (Fig. 1C). Overall, the clinical impression was consistent with benign lymphoproliferative disease or localized lymphoma.

The patient underwent needle biopsy of the right cervical LN. Microscopic examination revealed a small fragment of LN tissue showing relatively preserved nodular LN structure. BCL2 was diffusely positive with more intense staining within the germinal center (GC); GC areas were also positive for CD20,

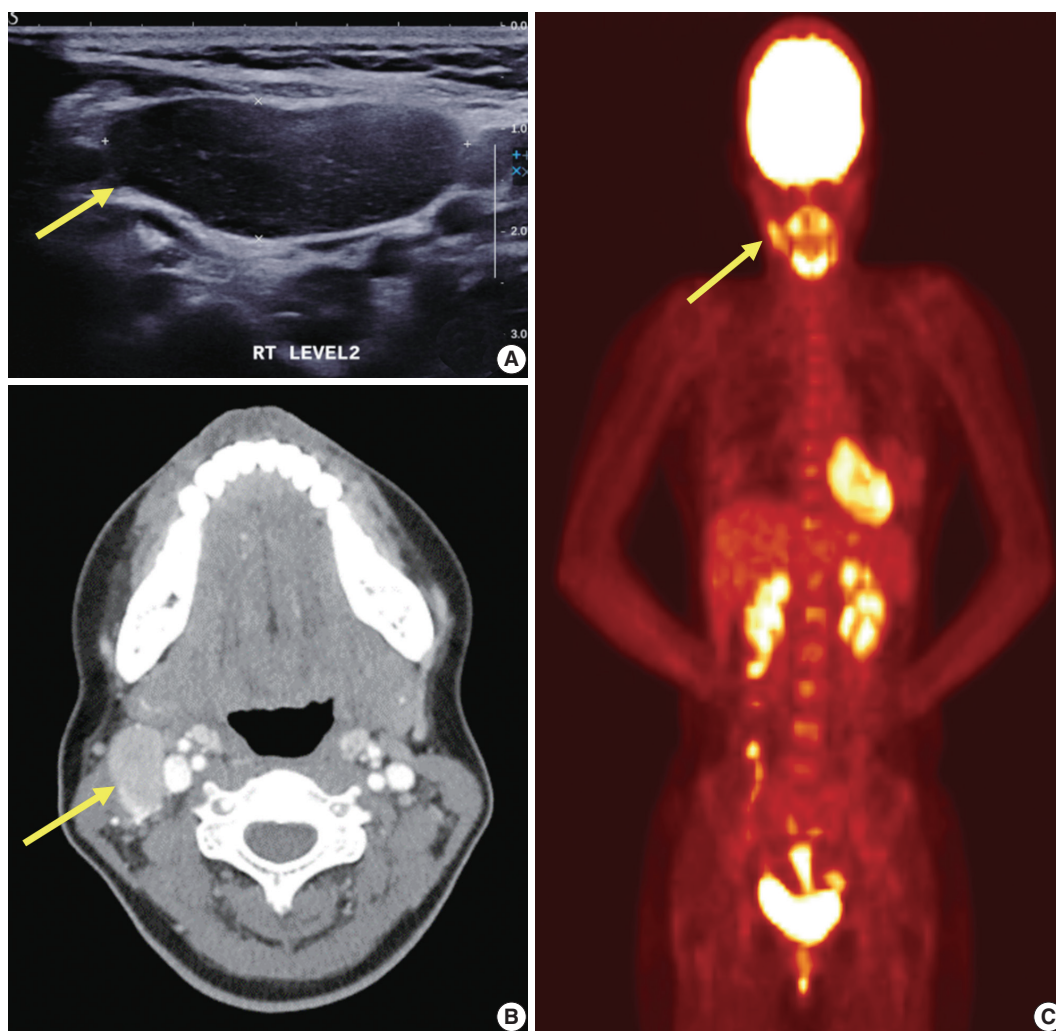


Fig. 1. Imaging work-up of the patient at presentation. (A) Neck ultrasonography shows a hypoechoic mass (arrow). (B) Neck computed tomography shows a well-enhanced ovoid mass at level II area (arrow). (C) ^{18}F -positron emission tomography scan shows hypermetabolic lesion in the right neck (arrow) and no other hypermetabolic lesions.

BCL6, and CD10 with low Ki-67 proliferation index. Possibilities of both in situ follicular neoplasia (ISFN) and partially biopsied FL was considered, and complete excision of the LN was recommended.

On microscopic examination, the excised neck LN was composed of numerous regressed GCs surrounded by expanded mantle zones (Fig. 2A, B), often showing concentric distribution of small lymphocytes (onion skin pattern) (Fig. 2C) and follicles separated by hyalinized interfollicular stroma. In addition, hyalinized blood vessels penetrating into regressed GCs, forming a typical “lollipop” appearance, were observed (Fig. 2D). Although predominant histological features of the excised LN were suggestive of HVCD, several conglomerated follicles with GCs composed of small, monotonous, and centrocyte-like lymphocytes were found on careful examination (Fig. 3A, B).

As shown in Fig. 3B, BCL2-positive, BCL6-positive, and CD10-positive B-cells were identified within the abnormally conglomerated GCs. The presence of neoplastic follicles showing structural abnormality and aberrant immunophenotype indicated FL (in the form of partial nodal involvement). In addition, some follicles with relatively preserved structure and polarity also harbored BCL2-positive, BCL6-positive, and CD10-positive B-cells (Fig. 3C), which is consistent with ISFN. Neoplastic cells were also present within typical HVCD-looking regressed follicles, as shown in Fig. 2E. Final pathologic diagnosis of FL grade 1 was made, with additional remarks stating that HVCD-like features were noted. Subsequent bone marrow examination confirmed no evidence of lymphoma involvement; therefore, the patient was finally diagnosed with FL grade 1, Ann Arbor stage I, and no further treatment was initiated.

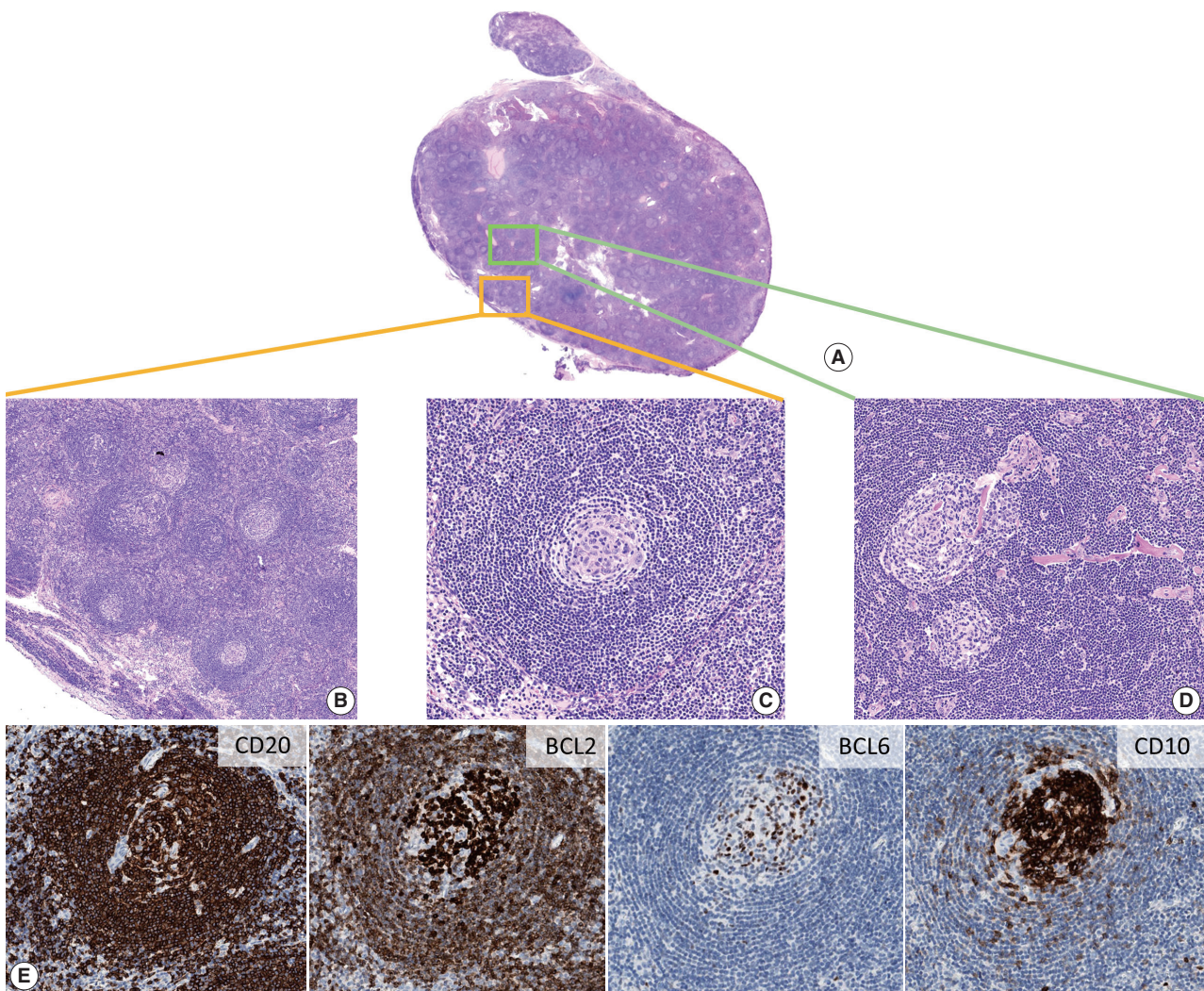


Fig. 2. Excised lymph node reminiscent of hyaline-vascular Castleman disease (HVCD). Vaguely nodular pattern is noted on low power (A), where regressed lymphoid follicles (B) with expanded onion skin-like mantle zones (C) are observed. (D) Hyalinized blood vessels within follicles are frequently noted. (E) Immunostaining shows the presence of BCL2-positive, BCL6-positive, and CD10-positive cells within the regressed follicles.

Ethics statement

The Institutional Review Board of Seoul National University Hospital (SNUH) approved this study (No. H-1911-032-107) and waived the need for written informed consent from the patient.

DISCUSSION

The incidence of FL in Korea is increasing over time; compared with the 2005–2006 statistics [6], the proportion of FL has increased 2.5-fold from 2015–2016, becoming the third most common form of B-cell NHL in Korea, following diffuse large B-cell lymphoma and extranodal marginal zone B-cell

lymphoma of mucosa-associated lymphoid tissue [2]. Due to the overall increase in incidence, pathologists are more likely to encounter FL variants in daily practice; therefore, awareness of rare morphological variants is important for accurate identification and diagnosis.

FL-HVCD was first described in 1994 [7], and only 11 cases have been reported in the English literature to date [8–12]. Pina-Oviedo et al. [12] reviewed and reported clinicopathological findings of these cases. All previously reported patients were older than the patient in the present study, and median age at diagnosis was 63 years (range, 41 to 77 years). The patients presented with a wide range of symptoms from asymptomatic, incidentally found lesion to generalized lymphadenopathy. Eight

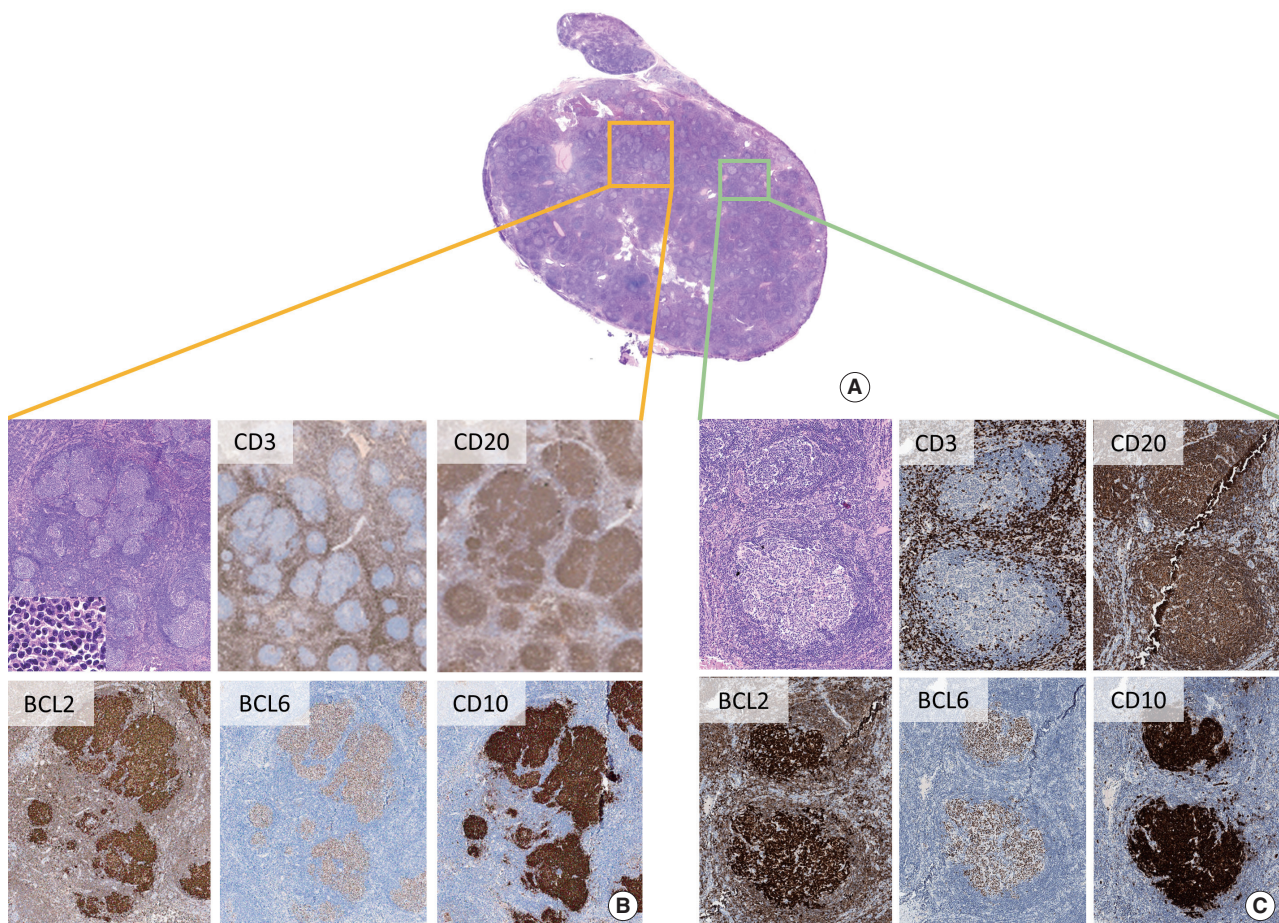


Fig. 3. Features of follicular lymphoma. Upon careful examination, abnormally conglomerated follicles are identified (A, B), and presence of BCL2-positive, BCL6-positive, and CD10-positive neoplastic B-cells is noted (B), confirming follicular lymphoma. (C) In addition, cells having an aberrant BCL2-positive, BCL6-positive, and CD10-positive immunophenotype within otherwise normal-looking follicles are observed, indicating involvement of in situ follicular neoplasia (ISFN).

of 11 patients received either chemotherapy or radiation therapy, and recurrence or death from the disease has not been reported to date. Morphologically, cases were reported to have several HVCD features including hyalinized blood vessels penetrating regressed GCs, increased vascularity in interfollicular stroma, and onion skin-like mantle zones, complicating differential diagnosis. However, all cases harbored at least one focal area showing conventional FL histology.

The current case differs from previously reported FL-HVCD cases in several aspects. First, the patient had localized disease, presenting with an incidentally found, isolated neck mass with no evidence of systemic lymphadenopathy. In addition, the patient was 37 years old, which is relatively young for FL to be included in the differential diagnosis, considering the median age of FL patients at presentation is approximately 60 years. These two factors complicated the diagnostic process: considering both clinical features and histopathologic characteristics of the

patient, unicentric HVCD was the most likely diagnosis. However, identification of abnormally conglomerated follicles that contained densely packed centrocytes was critical for suspicion of a neoplastic process. The immunostaining of CD20, BCL2, BCL6, and CD10 showed conglomerated follicles replaced with BCL2-positive neoplastic GC-type B-cells, resulting in diagnosis of FL-HVCD.

Due to the rare incidence, FL-HVCD is one of the most under-recognized variants of FL. Furthermore, the underlying etiologic mechanism of this disease is obscure. Hypothetically, FL-HVCD is a coincidence in which FL involves an LN that previously underwent CD-like changes [12]. Furthermore, because FL cells are dependent on follicular dendritic cells for survival [13,14] and are important for the pathogenesis of HVCD [15], there might be a pathogenic link between FL and HVCD. To further clarify this condition, long-term follow-up of FL-HVCD patients may provide additional information.

Distinction of FL-HVCD from CD is critically important, mostly due to therapeutic perspective. Though alleged to be indolent, FLs are a lymphoid malignancy, warranting systemic staging work-up upon diagnosis. Patients with symptomatic or advanced stage should be advised to receive therapeutic intervention [16]. Therefore, possibility of FL-HVCD should be considered a differential diagnosis when a specimen shows typical HVCD features.

In summary, we report a case of FL-HVCD. Acknowledgment of rare FL variants and thorough microscopic examination to identify at least a focal area suggestive of neoplastic follicles are helpful for accurate diagnosis of FL-HVCD.

ORCID

Jiwon Koh: <https://orcid.org/0000-0002-7687-6477>

Yoon Kyung Jeon: <https://orcid.org/0000-0001-8466-9681>

Author Contributions

Conceptualization: YKJ.

Data curation: JK, YKJ.

Formal analysis: JK, YKJ.

Investigation: JK, YKJ.

Visualization: JK.

Writing—original draft: JK, YKJ.

Writing—review & editing: JK, YKJ.

Conflicts of Interest

The authors declare that they have no potential conflicts of interest.

Funding

No funding to declare.

REFERENCES

- Harris NL, Swerdlow SH, Jaffe ES, et al. Follicular lymphoma. In: Swerdlow SH, Campo E, Harris NL, et al., eds. WHO classification of tumours of haematopoietic and lymphoid tissues. 4th ed. Lyon: IARC Press, 2008; 220-6.
- Jung HR, Huh J, Ko YH, et al. Classification of malignant lymphoma subtypes in Korean patients: a report of the 4th nationwide study. *J Hematopathol* 2019; 12: 173-81.
- Goodlad JR, Batstone PJ, Hamilton D, Hollowood K. Follicular lymphoma with marginal zone differentiation: cytogenetic findings in support of a high-risk variant of follicular lymphoma. *Histopathology* 2003; 42: 292-8.
- Goates JJ, Kamel OW, LeBrun DP, Benharroch D, Dorfman RF. Floral variant of follicular lymphoma. Immunological and molecular studies support a neoplastic process. *Am J Surg Pathol* 1994; 18: 37-47.
- Kojima M, Matsumoto M, Miyazawa Y, Shimizu K, Itoh H, Masawa N. Follicular lymphoma with prominent sclerosis ("sclerosing variant of follicular lymphoma") exhibiting a mesenteric bulky mass resembling inflammatory pseudotumor: report of three cases. *Pathol Oncol Res* 2007; 13: 74-7.
- Kim JM, Ko YH, Lee SS, et al. WHO classification of malignant lymphomas in Korea: report of the third nationwide study. *Korean J Pathol* 2011; 45: 254-60.
- Warnke RA, Weiss LM, Chan JK, Cleary ML, Dorfman RF. Tumors of the lymph nodes and spleen. In: Rosai J, Sobin LH, eds. *Atlas of tumor pathology*. 3rd series. Washington, DC: Armed Forces Institute of Pathology, 1994; 85.
- Nozawa Y, Hirao M, Kamimura K, Hara Y, Abe M. Unusual case of follicular lymphoma with hyaline-vascular follicles. *Pathol Int* 2002; 52: 794-5.
- Kojima M, Sakurai S, Isoda A, Tsukamoto N, Masawa N, Nakamura N. Follicular lymphoma resembling with hyaline-vascular type of Castleman's disease: the morphological and immunohistochemical findings of two cases. *Cancer Ther* 2009; 7: 109-12.
- Siddiqi IN, Brynes RK, Wang E. B-cell lymphoma with hyaline vascular Castleman disease-like features: a clinicopathologic study. *Am J Clin Pathol* 2011; 135: 901-14.
- Pina-Oviedo S, Wang W, Vicknair E, Manning JT Jr, Medeiros LJ. Follicular lymphoma with hyaline-vascular Castleman disease-like follicles and CD20 positive follicular dendritic cells. *Pathology* 2017; 49: 544-7.
- Pina-Oviedo S, Miranda RN, Lin P, Manning JT, Medeiros LJ. Follicular lymphoma with hyaline-vascular Castleman-like features: analysis of 6 cases and review of the literature. *Hum Pathol* 2017; 68: 136-46.
- Kagami Y, Jung J, Choi YS, et al. Establishment of a follicular lymphoma cell line (FLK-1) dependent on follicular dendritic cell-like cell line HK. *Leukemia* 2001; 15: 148-56.
- Takata K, Sato Y, Nakamura N, et al. Duodenal and nodal follicular lymphomas are distinct: the former lacks activation-induced cytidine deaminase and follicular dendritic cells despite ongoing somatic hypermutations. *Mod Pathol* 2009; 22: 940-9.
- Chang KC, Wang YC, Hung LY, et al. Monoclonality and cytogenetic abnormalities in hyaline vascular Castleman disease. *Mod Pathol* 2014; 27: 823-31.
- Freedman A. Follicular lymphoma: 2015 update on diagnosis and management. *Am J Hematol* 2015; 90: 1171-8.

Gastric IgG4-related disease presenting as a mass lesion and masquerading as a gastrointestinal stromal tumor

Banumathi Ramakrishna¹, Rohan Yewale², Kavita Vijayakumar¹, Patta Radhakrishna³, Balakrishnan Siddartha Ramakrishna²

Departments of ¹Pathology, ²Medical Gastroenterology, and ³Surgical Gastroenterology, SRM Institutes for Medical Science, Vadapalani, India

IgG4-related disease of the stomach is a rare disorder, and only a few cases have been reported. We present two cases that were identified over a 2-month period in our center. Two male patients aged 52 and 48 years presented with mass lesion in the stomach, which were clinically thought to be gastrointestinal stromal tumor, and they underwent excision of the lesion. Microscopic examination revealed marked fibrosis, which was storiform in one case, associated with diffuse lymphoplasmacytic infiltration and an increase in IgG4-positive plasma cells on immunohistochemistry. Serum IgG4 level was markedly elevated. Although rare, IgG4-related disease should be considered in the differential diagnosis of gastric submucosal mass lesions.

Key Words: IgG4-related disease; Stomach; Autoimmune diseases; Gastrointestinal stromal tumors

Received: December 4, 2019 **Revised:** February 5, 2020 **Accepted:** February 10, 2020

Corresponding Author: Banumathi Ramakrishna, MBBS, MD, Department of Pathology, SRM Institutes for Medical Science, 1 Jawaharlal Nehru Road, Vadapalani, Chennai 600026, India

Tel: +91-44-20002001, Fax: +91-44-49211455, E-mail: banu_ramakrishna@hotmail.com

IgG4-related disease (IgG4-RD) is a newly-recognized, immune-mediated fibroinflammatory disorder that most commonly affects the pancreas [1]. It can also involve other organs such as the bile duct, liver, gallbladder, salivary glands, lacrimal glands, retroperitoneum, and lymph nodes, although involvement of the gastrointestinal tract is very rare [2,3]. The disorder can present as diffuse wall thickening or as polyp or mass-like lesion [2]. Histologically, this disease is characterized by storiform fibrosis, diffuse lymphoplasmacytic infiltrates, obliterative or non-obliterative phlebitis, increase in IgG4-positive plasma cells on immunostaining, and often with elevated serum IgG4 level [1,3,4]. We report two cases of IgG4-RD of the stomach that presented as a mass lesion, were identified over a two-month period, and were clinically suspected to be gastrointestinal stromal tumor (GIST) and surgically excised.

CASE REPORT

Case 1

A 42-year-old male patient was admitted to our hospital with a diagnosis of acute pyelonephritis. Computed tomography

(CT) of the kidney, ureter, and bladder revealed an incidental mass lesion in the posterior wall of the stomach. Upper gastrointestinal endoscopy revealed submucosal lesions in the esophagus and stomach that were clinically suspected to be GIST. The patient underwent endoscopic ultrasound-guided fine-needle aspiration biopsy of the esophageal lesion and endoscopic mucosal biopsy of the stomach, both of which were inconclusive. The patient also underwent wedge resection of the gastric lesion. Histopathological examination revealed a wedge of the gastric wall with a globular submucosal lesion measuring 6.5×6.0×4.0 cm. The cut surface had a greyish white appearance with foci of calcification. Microscopically, there was marked fibrous expansion of the submucosa with collagenization extending through the muscularis propria to the subserosa, diffuse infiltrates of predominantly plasma cells arranged in cords and clusters admixed with lymphocytes and eosinophils, and several lymphoid follicles with reactive germinal centers (Fig. 1A, B). Small foci of calcification were also present. The muscle coat was disorganized and had muscular hypertrophy in foci. There was no storiform fibrosis or evidence of obliterative or non-obliterative phlebitis. Based on these characteristics, a possible diagnosis of IgG4-RD was suggested.

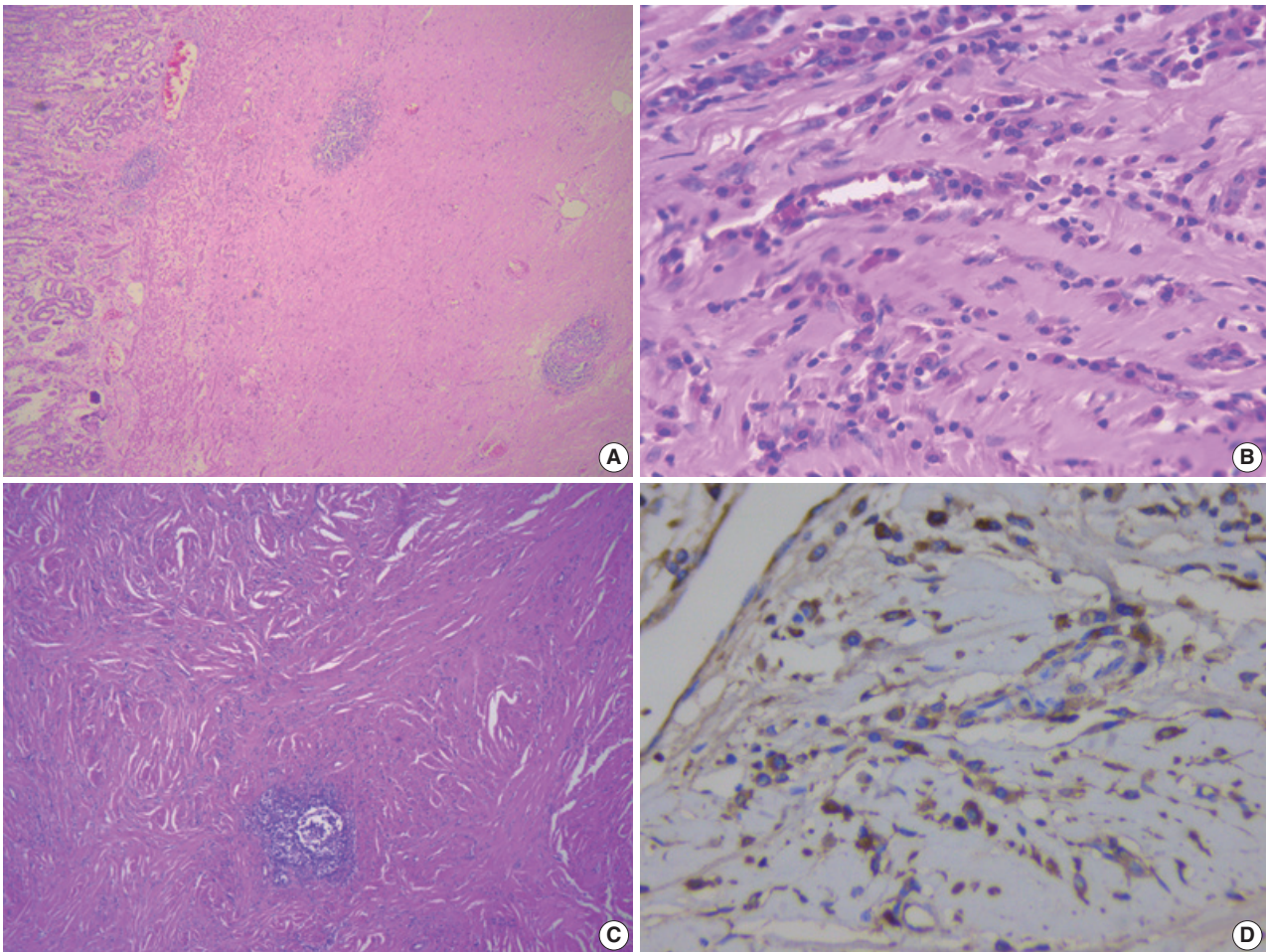


Fig. 1. (A) Gastric wall with marked submucosal fibrosis and prominent lymphoid follicles. (B) Diffuse plasma cell rich inflammation. (C) Storiform fibrosis with diffuse inflammation and a lymphoid follicle. (D) Many immunoreactive IgG4-positive plasma cells.

IgG4 immunohistochemistry (IHC) and serum IgG4 level were assessed. The IgG4 IHC showed 35–40 immunoreactive plasma cells per high power field (hpf), and serum IgG4 level was elevated (4.36 g/L). These tests confirmed the diagnosis of IgG4-RD. Subsequent serum levels after 3 and 4 months were 2.71g/L and 2.53 g/L, respectively. The patient was treated with steroids and azathioprine. He experienced postsurgery complications that required revision of the gastric anastomosis. During follow-up, his prognosis while receiving medical treatment has been good.

Case 2

The second patient was a 58-year-old male found to have erosive gastritis and a submucosal swelling in the body of the stomach in December 2017, while undergoing upper gastrointestinal endoscopy for investigation of dyspepsia. CT examination showed a well-defined, 3 × 2.9 cm, round, homogeneous, en-

hancing soft tissue lesion in the distal body of the stomach along the lesser curvature, which was suspected to be GIST or leiomyoma. He was advised to undergo follow-up and elective surgery. His gastric symptoms worsened over the next 10 months, and he underwent excision of the gastric submucosal lesion in October 2018. Histopathological examination revealed a well-circumscribed globular mass measuring 4 × 3.3 × 3.5 cm, and whorling was seen on the cut surface. Microscopically, the lesion was composed of extensively fibrotic and sclerotic stroma with a storiform pattern of fibrosis in foci (Fig. 1C). Discrete, cords and clusters of plasma cells admixed with lymphocytes, a few eosinophils and a few scattered lymphoid aggregates and follicles were present. Perivascular aggregates of plasma cells were also present. There was no evidence of obliterative or non-obliterative phlebitis. Bundles of smooth muscle were identified at the periphery on one aspect. The possibility of IgG4-RD of the stomach was suggested, and IgG4 IHC and serum estima-

tion were recommended. The IgG4 IHC revealed 20–30 immuno-reactive plasma cells/hpf (Fig. 1D). Serum IgG4 was elevated at 3.11g/L, well above the 1.35 g/L cut-off for diagnosis of IgG4-RD. The patient did not return for follow-up.

Ethics statement

The authors certify that they obtained patient consent for publication, and the study was approved by the Institutional Review Board of Sri Ramaswamy Memorial Institutes for Medical Science, Chennai, India (IEC NO: SIMS IEC/other/18/2019).

DISCUSSION

IgG4-RD is an immune-mediated fibroinflammatory lesion, first described in patients with sclerosing cholangitis associated with autoimmune pancreatitis type 1 [5]. Later, it was identified in other organs including the liver, bile ducts, salivary glands, retroperitoneum, lymph nodes, and lungs. It is characterized by

diffuse or partial enlargement of the organ and histologically as dense lymphoplasmacytic infiltration with an increase in IgG4 plasma cells on immunostaining, a storiform pattern of fibrosis and obliterative or non-obliterative phlebitis, and an increase in serum IgG4 level.

IgG4-RD of the gastrointestinal tract is very rare and can present as diffuse wall thickening or as polyp or mass-like lesion [2,3]. Even though obliterative phlebitis was not present in these two cases, the presence of dense fibrosis, which was storiform in one case, and dense lymphoplasmacytic infiltration with lymphoid aggregates and follicles, presenting as a submucosal mass-like lesion, suggested the possibility of IgG4-RD, which was confirmed by IHC and elevated serum IgG4 level. The presence of at least two histological features is required for confident diagnosis of IgG4-RD; in most cases, dense lymphoplasmacytic infiltrate and diffuse/storiform fibrosis are seen. Additional clinical, serological (serum level > 135 mg/dL or 1.35 g/L), or radiological evidence is required to confirm IgG4-RD [1].

Table 1. Clinicopathological features of IgG4-related disease manifesting as gastric lesions

Case No.	Age (yr)	Sex	Endoscopic finding/ Clinical diagnosis	Location	Size (mm)	Histopathology/IHC	Serum IgG4 levels	Treatment	Study
1	48	F	Mass/GIST/NET	Mid body	36 × 22	SF, LP, OP, IgG4 + 210/hpf, IgG4/IgG ratio about 85%	NA	WR	Woo et al. [3]
2	62	F	Mass/gastric cancer	Antrum	80 × 30	SF, LP, OP, IgG4 + ve lymphoplasmacytes >50/hpf	Elevated	DG	Bulanov et al. [6]
3	59	F	Mass/GIST	NA	33 × 14	Abundant LP, SF, lymphoid follicles, IgG4 >50/hpf	Normal	WR	Kim et al. [7]
4	56	F	Mass/GIST	NA	21 × 15	Abundant LP, SF, calcification, IgG4 >50/hpf	Normal	WR	Kim et al. [7]
5	60	F	Nodule/NA	Fundus	10 × 15	Fibrosis, dense LP, IgG4 >80/hpf	Normal	WR	Chetty et al. [8]
6	45	M	Multiple nodules/NA	Antrum	Up to 22	LP, many eosinophils, IgG4/IgG ratio 0.84	NA	DG	Chetty et al. [8]
7	56	M	Nodule/NA	Body	8	SF, LP, IgG4-40-102/hpf IgG4/IgG ratio 80%–90%	NA	ESR	Na et al. [9]
8	58	M	Nodule/AIP	Fundus and body	14	Dense LP, extensive IgG and IgG4 + staining	Normal	Steroid	Baez et al. [10]
9	55	F	Nodule/GIST	Body	20	Dense hyalinization, LP, IgG4/IgG ratio 41%	Normal	ESR	Zhang et al. [11]
10	75	F	Polyp/GIST	Body	56 × 50	Fibrosis, LP, many eosinophils, IgG4-39/hpf	Normal	WR	Rollins et al. [12]
11	44	M	Mass/GIST	Body	20 × 18	Fibrosis, LP, IgG4 + ve lymphoplasmacytes	Normal	ESR	Otsuka et al. [13]
12	27	F	Mass/GIST/NET	Fundus	40	Dense fibrosis, LP, IgG4/IgG ratio 25.3%	Normal	WR	Cheong et al. [14]
13	29	F	Mass/GIST	Body	20 × 15	Fibrosis, LP, IgG4 + ve plasma cells 150/hpf	NA	WR	Skorus et al. [15]
14	43	M	Mass/GIST	Antrum	70 × 50	Dense LP, IgG4 + plasma cells 35-40/hpf	Elevated	WR + Steroids	Present case 1
15	58	M	Mass/GIST	Distal body	45 × 40	LP, SP, IgG4 + ve plasma cells 20-30/hpf	Elevated	WR	Present case 2

IHC, immunohistochemistry; GIST, gastrointestinal stromal tumor; NET, neuroendocrine tumor; SF, storiform fibrosis; LP, lymphoplasmacytic infiltrate; OP, obliterative phlebitis; hpf, high power field; NA, not available; WR, wedge resection; DG, distal gastrectomy; ESR, endoscopic submucosal resection; AIP, autoimmune pancreatitis.

The cut-off point for the presence of IgG4 plasma cells in tissues varies and can range from > 30 plasma cells/hpf to > 50/hpf, which is highly specific [1,5]. In biopsy specimens, more than 10 IgG4 plasma cells/hpf were reported in one study [16]. However, the cut-off points vary depending on organ system. Some studies have suggested that IgG4⁺/IgG⁺ plasma cell ratio > 0.4 is a marker of IgG4-RD in the presence of classic histopathological features and with a compatible clinical features [1,17].

IgG4-RD can involve multiple organs or any sites in the body synchronously or metachronously [18]. Patients can present with non-specific symptoms and swelling or mass-like lesion. Patients with biliary or pancreatic lesion can present with jaundice, weight loss, and vague abdominal pain. The disease can be an incidental finding during radiological examination and can be mistaken for malignancy, as there are no specific radiological features characteristic of this disease [18,19]. Most cases of gastric IgG4-RD have been reported in middle-aged patients, and both men and women are affected [3,6]. Both patients in this report were middle-aged men.

IgG4-RD of the stomach was first described in 2004 by Shinji et al. [20], presenting as a gastric ulcer. Because it is difficult to diagnose clinically, especially in isolated cases, most of the reported patients have undergone surgery. Because this disease involves a submucosal lesion in the stomach, these cases are often misdiagnosed as GIST [3,7,18,19] and are difficult to diagnose on endoscopic forceps biopsy, similar to our cases. Gastric lesions that have been mistaken for GIST or gastric cancer have been reported in the literature (Table 1) [3,6-15]. IgG4-RD of the stomach that involved the regional lymph nodes has also been reported [6].

Although steroids are the first therapeutic option for treating IgG4-RD, it is difficult to diagnose gastric IgG4-RD without histopathological examination. Almost all cases have been reported after surgical resection. Therefore, this disease should be considered in the differential diagnosis of gastric submucosal mass lesion.

To conclude, we present two cases of IgG4-RD of the stomach that presented as a mass lesion and were clinically suspected to be GIST. The diagnosis was made only after histopathological examination of resection specimens. This highlights the importance of considering this disease in differential diagnosis to avoid surgical resection.

ORCID

Banumathi Ramakrishna:

<https://orcid.org/0000-0001-5635-1633>

Balakrishnan Siddhartha Ramakrishna:

<https://orcid.org/0000-0001-5090-9501>

Author Contributions

Conceptualization: BR.

Data curation: BR, RY.

Investigation: BR, KV, PR, RY, BSR.

Visualization: BR.

Writing—original draft: BR.

Writing—review and editing: BR, RY, BSR.

Conflicts of Interest

The authors declare that they have no potential conflicts of interest.

Funding

No funding to declare.

REFERENCES

- Deshpande V, Zen Y, Chan JK, et al. Consensus statement on the pathology of IgG4-related disease. *Mod Pathol* 2012; 25: 1181-92.
- Koizumi S, Kamisawa T, Kuruma S, et al. Immunoglobulin G4-related gastrointestinal diseases, are they immunoglobulin G4-related diseases? *World J Gastroenterol* 2013; 19: 5769-74.
- Woo CG, Yook JH, Kim AY, Kim J. IgG4-related disease presented as a mural mass in the stomach. *J Pathol Transl Med* 2016; 50: 67-70.
- Stone JH, Zen Y, Deshpande V. IgG4-related disease. *N Engl J Med* 2012; 366: 539-51.
- Kamisawa T, Funata N, Hayashi Y, et al. A new clinicopathological entity of IgG4-related autoimmune disease. *J Gastroenterol* 2003; 38: 982-4.
- Bulanov D, Arabadzhieva E, Bonev S, et al. A rare case of IgG4-related disease: a gastric mass, associated with regional lymphadenopathy. *BMC Surg* 2016; 16: 37.
- Kim DH, Kim J, Park DH, et al. Immunoglobulin G4-related inflammatory pseudotumor of the stomach. *Gastrointest Endosc* 2012; 76: 451-2.
- Chetty R, Serra S, Gauchotte G, Markl B, Agaimy A. Sclerosing nodular lesions of the gastrointestinal tract containing large numbers of IgG4 plasma cells. *Pathology* 2011; 43: 31-5.
- Na KY, Sung JY, Jang JY, et al. Gastric nodular lesion caused by IgG4-related disease. *Pathol Int* 2012; 62: 716-8.
- Baez JC, Hamilton MJ, Bellizzi A, Mortelé KJ. Gastric involvement in autoimmune pancreatitis: MDCT and histopathologic features. *JOP* 2010; 11: 610-3.

11. Zhang H, Jin Z, Ding S. Gastric calcifying fibrous tumor: a case of suspected immunoglobulin G4-related gastric disease. *Saudi J Gastroenterol* 2015; 21: 423-6.
12. Rollins KE, Mehta SP, O'Donovan M, Safranek PM. Gastric IgG4-related autoimmune fibrosclerosing pseudotumour: a novel location. *ISRN Gastroenterol* 2011; 2011: 873087.
13. Otsuka R, Kano M, Hayashi H, et al. Probable IgG4-related sclerosing disease presenting as a gastric submucosal tumor with an intense tracer uptake on PET/CT: a case report. *Surg Case Rep* 2016; 2: 33.
14. Cheong HR, Lee BE, Song GA, Kim GH, An SG, Lim W. Immunoglobulin G4-related inflammatory pseudotumor presenting as a solitary mass in the stomach. *Clin Endosc* 2016; 49: 197-201.
15. Skorus U, Kenig J, Mastalerz K. IgG4-related disease manifesting as an isolated gastric lesion- a literature review. *Pol Przegl Chir* 2018; 90: 41-5.
16. Chari ST. Diagnosis of autoimmune pancreatitis using its five cardinal features: introducing the Mayo Clinic's HISORt criteria. *J Gastroenterol* 2007; 42 Suppl 18: 39-41.
17. Miyabe K, Zen Y, Cornell LD, et al. Gastrointestinal and extra-intestinal manifestations of IgG4-related disease. *Gastroenterology* 2018; 155: 990-1003.
18. Seo HS, Jung YJ, Park CH, Song KY, Jung ES. IgG4-related disease in the stomach which was confused with gastrointestinal stromal tumor (GIST): two case reports and review of the literature. *J Gastric Cancer* 2018; 18: 99-107.
19. Inoue D, Yoneda N, Yoshida K, et al. Imaging and pathological features of gastric lesion of immunoglobulin G4-related disease: A case report and review of the recent literature. *Mod Rheumatol* 2019; 29: 377-82.
20. Shinji A, Sano K, Hamano H, et al. Autoimmune pancreatitis is closely associated with gastric ulcer presenting with abundant IgG4-bearing plasma cell infiltration. *Gastrointest Endosc* 2004; 59: 506-11.

Noninvasive encapsulated papillary RAS-like thyroid tumor (NEPRAS) or encapsulated papillary thyroid carcinoma (PTC)

Pedro Wesley Rosario

Endocrinology Service, Santa Casa de Belo Horizonte, Minas Gerais, Brazil

In a recent case study, Ohba et al. [1] suggested that presence of papillae in absence of other criteria of malignancy and exuberant nuclear alterations (nuclear score 3 [2]) may not be sufficient for diagnosis of papillary thyroid carcinoma (PTC) and proposed the name “noninvasive encapsulated papillary RAS-like thyroid tumor” (NEPRAS) to encompass the borderline nature of the diagnosis [1].

CASE REPORT

Based on the diagnostic proposal of Ohba et al. [1], we revised our cases of tumors > 1 cm previously diagnosed as PTC and that were encapsulated/well-delimited (thick, thin, or partial capsule or well-circumscribed with a clear demarcation from adjacent thyroid tissue) and noninvasive (absence of capsular or vascular invasion) (n = 185). A total of 129 cases met all criteria for noninvasive follicular thyroid neoplasm with papillary like nuclear features (NIFTP) [3], and 11 were excluded due to the presence of papillae [4]. These and an additional 35 cases were initially considered encapsulated PTC, and nine were diagnosed as poorly differentiated carcinoma or an aggressive PTC subtype. Among the 11 cases not considered NIFTP due to the presence of papillae, eight had exuberant nuclear alterations (nuclear score 3 [2]). The three reported here had a nuclear score of 2 and would be reclassified from encapsulated PTC to NEPRAS [1]. Ultimately, we analyzed 43 cases of noninvasive encapsulated PTC and three of NEPRAS. None of the tumors carried the *BRAF*^{V600E}

mutation, which was the only mutation investigated. Thus, the three cases diagnosed as NEPRAS met all criteria presented in Table 1. The characteristics of the patients are shown in Table 2.

None of these cases exhibited metastasis at presentation, were treated with radioiodine, or were maintained under TSH suppression. Excellent response to initial therapy was achieved in all three cases. No recurrence was detected after 36, 48, and 60 months of follow-up. Because of the small number of NEPRAS cases (n = 3), we did not perform statistical comparison between NIFTP and noninvasive encapsulated PTC, analyzing only patients with lymph node metastases at presentation and/or recurrence.

Ethics statement

The study was approved by the research ethics committee of Santa Casa de Belo Horizonte (No. 21968013.8.0000.5138). Informed consent was obtained from all individual participants included in the study.

DISCUSSION

Well-delimited or encapsulated thyroid neoplasms without vascular or capsular invasion or necrosis, with low mitotic index

Table 1. Criteria for diagnosing “noninvasive encapsulated papillary RAS-like thyroid tumor”

Criteria
Presence of papillae
Encapsulation or clear demarcation
No vascular or capsular invasion
<30% solid/trabecular/insular growth pattern
No tumor necrosis or high mitotic activity [2]
Nuclear score 2 [2]
Lack of <i>BRAF</i> ^{V600E} mutation

Received: January 22, 2020 Revised: February 4, 2020
 Accepted: February 5, 2020

Corresponding Author: Pedro Wesley Rosario, MD, PhD
 Santa Casa de Belo Horizonte, Rua Domingos Vieira, 590, Santa Efigênia. CEP 30150-240, Belo Horizonte, MG, Brasil
 Tel: +55-31-32388819, Fax: +55-31-32388980, E-mail: pedrowsrosario@gmail.com

Table 2. Characteristics of three patients with NEPRAS

Sex	Age (yr)	Presentation	Tumor size (cm)	Nuclear score [2]	Papillae (%)	Associated thyroid pathology	Initial therapy	TNM/AJCC
F	35	Atoxic uninodular disease, US: hypoechoic solid nodule 4.5 cm ^a , FNA: Bethesda IV	4	2	<1	Normal extranodular hyroid parenchyma	Total thyroidectomy	T2NxM0/stage I
F	43	Atoxic multinodular disease; US: hypoechoic solid nodule 2.5 cm ^a , two nodules 0.6 and 0.5 cm; FNA: Bethesda III	2.2	2	1	Benign nodular disease	Lobectomy	T2N0M0/stage I
M	48	Atoxic uninodular disease, US: hypoechoic solid nodule 4 cm ^a , FNA: Bethesda IV	3.5	2	1	Normal extranodular thyroid parenchyma	Lobectomy	T2NxM0/stage I

NEPRAS, noninvasive encapsulated papillary RAS-like thyroid tumor; AJCC, American Joint Committee on Cancer; F, female; US, ultrasonography; FNA, fine-needle aspiration; M, male.

^aWithout suspicious findings for malignancy (irregular margins, microcalcification, taller-than-wide shape).

and < 30% solid/trabecular/insular growth patterns, and with nuclear alterations characteristic of PTC (nuclear score 2 or 3 [2]) are diagnosed as NIFTP or encapsulated PTC depending on the presence (PTC) or absence (NIFTP) of papillae [2]. NIFTP is a borderline tumor that requires no additional surgical complementation, adjuvant therapy with radioiodine, TSH suppression, or monitoring with serum thyroglobulin and neck ultrasound after complete resection [5]. In contrast, encapsulated PTC is a malignant tumor that must be staged. Even when restricted to the thyroid, surgical complementation, radioiodine ablation, long-term follow-up, and TSH suppression may be necessary depending on tumor size and patient age.

Although the present study comprises only case reports, the patients supported the observations of Ohba et al. [1] that lesions that do not exhibit other malignancy criteria or exuberant nuclear alterations despite the presence of papillae may be reclassified from malignant (encapsulated PTC) to borderline (NEPRAS). This proposal would result in changes of patient management, with the same implications as those seen for the change from noninvasive encapsulated follicular variant of PTC to NIFTP [2].

ORCID

Pedro Wesley Rosario:

<https://orcid.org/0000-0002-5190-382X>

Conflicts of Interest

The authors declare that they have no potential conflicts of interest.

Funding

No funding to declare.

REFERENCES

- Ohba K, Mitsutake N, Matsuse M, et al. Encapsulated papillary thyroid tumor with delicate nuclear changes and a KRAS mutation as a possible novel subtype of borderline tumor. *J Pathol Transl Med* 2019; 53: 136-41.
- Nikiforov YE, Baloch ZW, Hodak SP, et al. Change in diagnostic criteria for noninvasive follicular thyroid neoplasm with papillary-like nuclear features. *JAMA Oncol* 2018; 4: 1125-6.
- Rosario PW, Mourao GF, Nunes MB, Nunes MS, Calsolari MR. Noninvasive follicular thyroid neoplasm with papillary-like nuclear features. *Endocr Relat Cancer* 2016; 23: 893-7.
- Rosario PW. Diagnostic criterion of noninvasive follicular thyroid neoplasm with papillary-like nuclear features (NIFTP): absence of papillae. *Hum Pathol* 2019; 83: 225.
- Haugen BR, Sawka AM, Alexander EK, et al. American Thyroid Association Guidelines on the Management of Thyroid Nodules and Differentiated Thyroid Cancer Task Force review and recommendation on the proposed renaming of encapsulated follicular variant papillary thyroid carcinoma without invasion to noninvasive follicular thyroid neoplasm with papillary-like nuclear features. *Thyroid* 2017; 27: 481-3.

